universität
wien

DISSERTATION

Titel der Dissertation

In vivo role of high-affinity immunoglobulin E receptors on
dendritic cells

angestrebter akademischer Grad

Doktor/in der Naturwissenschaften (Dr. rer. nat.)

Verfasserin / Verfasser:	Mag.ᵃ Eva Mitterhumer
Matrikel-Nummer:	9820440
Dissertationsgebiet (lt. Studienblatt):	441 Genetik - Mikrobiologie
Betreuerin / Betreuer:	Univ.-Prof. Dr. Dieter Maurer

Wien, am 25. Juni 2009

Abstract

Type 1 allergy, in particular allergic asthma, is a severe inflammatory disease of high socioeconomic importance. Pathophysiologically, type 1 allergic responses consist of an early (EAR) and a late-phase allergic reaction (LAR). The short-lived EAR is initiated by allergen-dependent crosslinking of mast cell-expressed high-affinity IgE receptors (FcεRI). The LAR, in contrast, persists for hours to days and is independent of mast cell activation but depends on tissue infiltration with allergen-specific Th2 lymphocytes, dendritic cells (DCs), and eosinophils. Eosinophils release soluble mediators of tissue damage and, thus, are the main effector cells of LARs. In human allergic asthma, LAR-associated inflammation is the main cause for ventilatory insufficiency. Frequent occurrence of severe LARs can promote chronic asthma and irreversible fibrotic lung remodelling. As the consequence, the LAR, even more the EAR, is the main reason of morbidity and mortality in human type 1 allergy.

Besides its presence on mast cells, FcεRI is also expressed on human antigen-presenting cells such as DCs in various tissues like the lung. In vitro studies demonstrated that IgE bound to FcεRI on DCs increases antigen uptake, processing and peptide presentation to CD4$^+$ T helper (Th) lymphocytes. Accordingly, it can be speculated that DC-expressed FcεRI contributes to the induction and the severity of LARs in vivo. However, the in vivo relevance of FcεRI on DCs remained enigmatic due to the lack of suitable animal models. Mice, for instance, express FcεRI on mast cells and basophils but, unlike humans, lack FcεRI expression on any type of their antigen-presenting cells.

In order to study the in vivo role of DC-expressed FcεRI for T cell activation and its contribution to allergic inflammation, we generated transgenic mice which display a "human-like" expression pattern of FcεRI. These α-DC TG mice express the IgE binding α-chain of human FcεRI and green fluorescent protein under the control of the murine DC-specific CD11c promoter. α-DC TG mice allowed us to demonstrate that FcεRI on DCs is an efficient inducer of Th2

cell development and a critical amplifier of the Th2-dependent LAR in the lung. In the presence of allergen and IgE, the FcεRI⁺ DCs instructed naïve T cells to differentiate into Th2 cells leading to augmented allergen-specific Th2 responses in vivo. Eosinophils, the main inflammatory effector cells in the LAR, were attracted into the lungs as dependent on IgE and the expression of FcεRI by DCs. This recruitment was mediated by the enhanced expression of eosinophil chemoattractants in the lungs of α-DC TG mice. Thus, FcεRI on DCs initiates the cascade of those immunologic events which result in cell-dependent late-phase allergic tissue inflammation.

Zusammenfassung

Die Typ 1 Allergie, im Besonderen allergisches Asthma, ist eine schwerwiegende entzündliche Erkrankung von großer sozioökonomischer Bedeutung. Pathophysiologisch gesehen, setzt sich die Typ 1 allergische Reaktion aus einer Früh- (early-phase allergic reaction, EAR) und einer Spätphasenkomponente (late-phase allergic reaction, LAR) zusammen. Die nur kurz andauernde EAR wird durch die Allergen-abhängige Vernetzung des auf Mastzellen exprimierten hochaffinen IgE Rezeptors (FcεRI) initiiert. Im Gegensatz dazu besteht die LAR für Stunden bis zu Tagen und ist nicht von Mastzellaktivierung abhängig, beruht jedoch auf der Infiltration des Gewebes mit Allergen-spezifischen Th2 Lymphozyten, dendritischen Zellen (DZ) und eosinophilen Granulozyten. Eosinophile Granulozyten setzen lösliche Mediatoren zur Schädigung des Gewebes frei und sind demzufolge die Haupteffektorzellen der LAR. Beim allergischen Asthma des Menschen ist die LAR-assoziierte Inflammation die Hauptursache für die krankheitstypische Atmungsinsuffizienz. Häufiges Auftreten von schweren LARs kann zur irreversiblen fibrotischen Remodellierung der Lungenstruktur und damit zu persistierender restriktiver Lungenfunktionsschädigung führen. Folglich ist die LAR mehr noch als die EAR die Hauptursache für Morbidität und Mortalität der Typ 1 Allergie beim Menschen.

Neben seiner Präsenz auf Mastzellen ist FcεRI auch auf humanen Antigen-präsentierenden Zellen wie auf DZ in verschieden Geweben wie der Lunge exprimert. In vitro Studien zeigten, dass IgE, gebunden an FcεRI auf DZ, die Antigenaufnahme, Prozessierung und Peptidpräsentation an CD4$^+$ Helfer T(Th)-Zellen erhöht. Dementsprechend kann man vermuten, dass dem auf DZ exprimierten FcεRI eine Bedeutung in der Induktion und der Regulation des Schweregrads der Th2 Zell-abhängigen LAR in vivo zukommt. Die in vivo Relevanz des von DZ exprimierten FcεRI blieb jedoch aufgrund des Fehlens von geeigneten Tiermodellen unklar. Mäuse exprimieren FcεRI auf Mastzellen und basophilen Granulozyten, aber anders als im Menschen, fehlt ihnen die

FcεRI-Expression auf Antigen-präsentierenden Zellen.

Um die in vivo Rolle des von DZ exprimierten FcεRI für die T-Zell-Aktivierung und seine Rolle in der allergischen Entzündung zu untersuchen, entwickelten wir ein transgenes Mausmodell, welches das „humane" Expressionsmuster von FcεRI simuliert. Diese α-DC TG Maus exprimiert die IgE-bindende α-Kette des humanen FcεRI und ein grün fluoreszierendes Protein unter dem für murine DZs spezifischen CD11c Promotor. Mit Hilfe dieser α-DC TG Mäuse konnten wir zeigen, dass FcεRI auf DZs ein effizienter Auslöser einer Th2 Zellentwicklung und ein entscheidender Verstärker der Th2-abhängigen allergischen Entzündung ist. In Anwesenheit eines Allergens und IgE, instruierten FcεRI$^+$ DCs naive Th Zellen in Th2 Zellen zu differenzieren, was in einer verstärkten Allergen-spezifischen Th2 Antwort in vivo resultierte. Eosinophile Granulozyten, die Haupteffektorzellen der LAR, wurden IgE- und FcεRI-abhängig in die Lunge rekrutiert. Diese Rekrutierung wurde durch die vermehrte Expression von Chemoattraktantien für eosinophile Granulozyten in den Lungen von α-DC TG Mäusen vermittelt. Demzufolge schließen wir, dass FcεRI auf DZs die Kaskade von immunologischen Prozessen initiiert, welche die Spätphase der allergischen Gewebsentzündung bewirken.

6

Index

List of Abbreviations

Ab	antibody
AD	atopic dermatitis
Ag	antigen
APC	(1) antigen-presenting cell
	(2) allophycocyanin
biot	biotinylated
BSA	bovine serum albumine
CHO	Chinese hamster ovary
$CaCl_2$	calcium chloride
CD	cluster of differentiation
CD40L	CD40 ligand
CFSE	Carboxyfluorescein succinimidyl ester
DC	dendritic cell
DDC	interstitial (dermal) DCs
DMF	dimethylformamide
DTH	delayed-type hypersensitivity reactions
EAR	early-phase of allergic reaction
EC_{50}	effective concentration$_{50}$
eGFP	enhanced green fluorescent protein
ELISA	enzyme-linked immunosorbent assay
eos	eosinophil
EtOH	ethanol
Fab	antigen-binding fragment
FACS	fluorescence-activated cell sorting
Fc	Fragment, crystalline; receptor binding site
FcεRI	high-affinity IgE receptor
FcεRIα	alpha-chain of the high-affinity IgE receptor
FcεRIβ	beta-chain of the high-affinity IgE receptor
FcεRIγ	gamma-chain of the high-affinity IgE receptor

10

FcεRII	low affinity IgE-receptor
FcγR	receptors for IgG
ER	endoplasmic reticulum
FCS	fetal calf serum
FITC	fluoresceinisothiocyanate
GAB2	growth-factor receptor-bound protein 2 –associated binding protein 2
h	hour(s)
HEPES	(N-[2-hydroxyethyl]piperazin-N´-[2-ethane sulfonic acid])
HRP	horseradish peroxidase
IFN	interferon
IFNAR	IFN-α receptor
IFNAR 1/2	subunit ½ of IFN-α receptor
Ig	immunoglobulin
IL	interleukin
IL-12Rβ2	IL-12 receptor β2-chain
IMDM	Iscove´s modified Dulbecco´s medium
i.p.	intraperitoneal
IRES	internal ribosome entry site
IRF	interferon regulatory factor
ISRE	IFN-stimulated response element
ITAM	immunoreceptor tyrosine-based activation motif
iTreg	induced regulatory T cell
i.v.	intravenously
LAR	late-phase of allergic reaction
LAT	linker for activation of T cells
LN	lymph node
MΦ	macrophage
mAb(s)	monoclonal antibody (-ies)
MACS	magnet-activated cell sorting
MFI	mean fluorescence intensity
MHC	major histocompatibility complex

min	minute(s)
mg	milligram
ml	milliliter
mM	millimolar
NP	4-Hydroxy-3-nitrophenylacetyl
nTreg	naturally occurring regulatory T cell
ON	over night
Ova	ovalbumin
PBS	phosphate-buffered saline
$_p$CD11c	CD11c promoter
PE	phycoerythrin
PerCP	peridinin chlorophyll protein
pH	negative decadic logarithm of hydrogen ion concentration ([H+])
PI3K	phosphatidylinositol 3-kinase
PTK	protein tyrosine kinase
RAG1	recombination-activating gene 1
RAG2	recombination-activating gene 2
RLV	Rauscher leukemia virus
RSS	recombination signal sequence
RT	room temperature
SA	streptavidin
sec	second (s)
TAP	transporter associated with antigen presentation
TCR	T cell receptor
TG	transgenic
ThN cell	naïve Th cell
TNF	tumor necrosis factor
Treg	regulatory T cell
µg	microgram
µl	microliter
µm	micrometer

°C	degrees Celsius
v/v	volume per volume
WT	wildtype
w/v	weight per volume

1. Introduction

1.1. Immunoglobulin E - IgE

1.1.1. Structure of Immunoglobulin E

As a result of the seminal studies of Ishizaka, Bennich and Johansson, Humphrey and Stanworth, immunoglobulin E was officially implemented in 1968 at the meeting of the "World Health Organization Immunoglobulin Reference Laboratory" (1). Immunoglobulin E has a molecular weight of 190 kD (2). IgE shares the same structural domains with the other immunoglobulin isotypes. The IgE molecule consists of two identical heavy (H) chains and two identical light (L) chains connected by disulfide bounds. The heavy ε-chain contains one extra domain compared to other immunoglobulins like IgG (2). Each heavy and light chain consists of constant (C) and variable (V) regions. The constant regions ($C\varepsilon1$ - $C\varepsilon4$ and C_L) are identical in all IgE antibodies whereas the variable regions (V_H and V_L) differ depending on the IgE-producing B cell clone. The expression of a unique IgE molecule requires somatic recombination, also known as V(D)J recombination (Fig. 1.1). During V(D)J recombination, genes encoding the variable region are brought randomly chosen into contiguity from dispersed variable (V), diversity (D) and joining (J) elements (3). V, D and J segments are found in the V_H region whereas the V_L region lacks D gene segments. Each gene segment contains a recombination signal sequence (RSS) which is recognized by recombination-activating gene 1 (RAG1) and recombination-activating gene 2 (RAG2). These two enzymes, as a complex, cleave the double-stranded DNA between the V, D or J sequence and the appropriate RSS, intervening DNA is removed and the V, D or J regions joined. During this DNA rearrangement process one of each V, D (when existing) and J segments are combined to form a V(D)J exon. The C region lies downstream

the V(D)J exon. During RNA splicing the V(D)J exon and the C region exons are combined forming mRNA ready to be translated (4).

The Cε3 and Cε4 domain are homologues and share the same quaternary structure with the Cγ2 and Cγ3 of the immunoglobulin G concluding that the Cε2 domains are additional (1).

Furthermore, the immunoglobulin E can be divided into Fab (Fragment, antigen-binding) and Fc (Fragment, crystalline) fragments (Fig. 1.2). The Fab fragment is located at the amino-terminal end of the antibody and is responsible for antigen-binding. The Fab fragment is composed of one variable and one constant region of each heavy and light chain (2). The Fc fragment is located at the carboxy-terminal end. Fc-IgE binds to cell surface receptors like the high-affinity (FcεRI) and the low-affinity IgE receptor (FcεRII) to initiate its biological activity. The Fc fragment is composed of the remaining three constant regions of the two heavy chains (2).
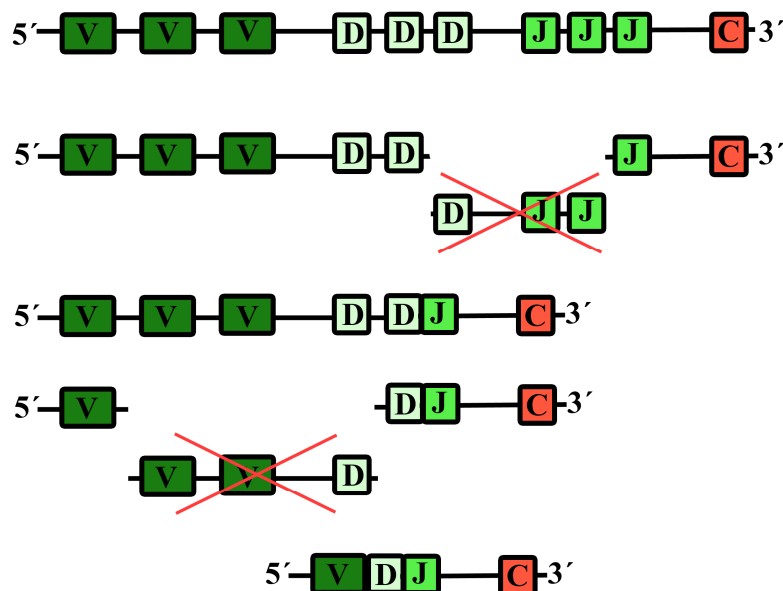
Fig. 1.1. Simplified scheme of V(D)J recombination. During DNA rearrangement one V, one D and one J segment are combined. Segments are recombined by RAG1 and RAG2. The C region lies downstream the V(D)J exon.

16
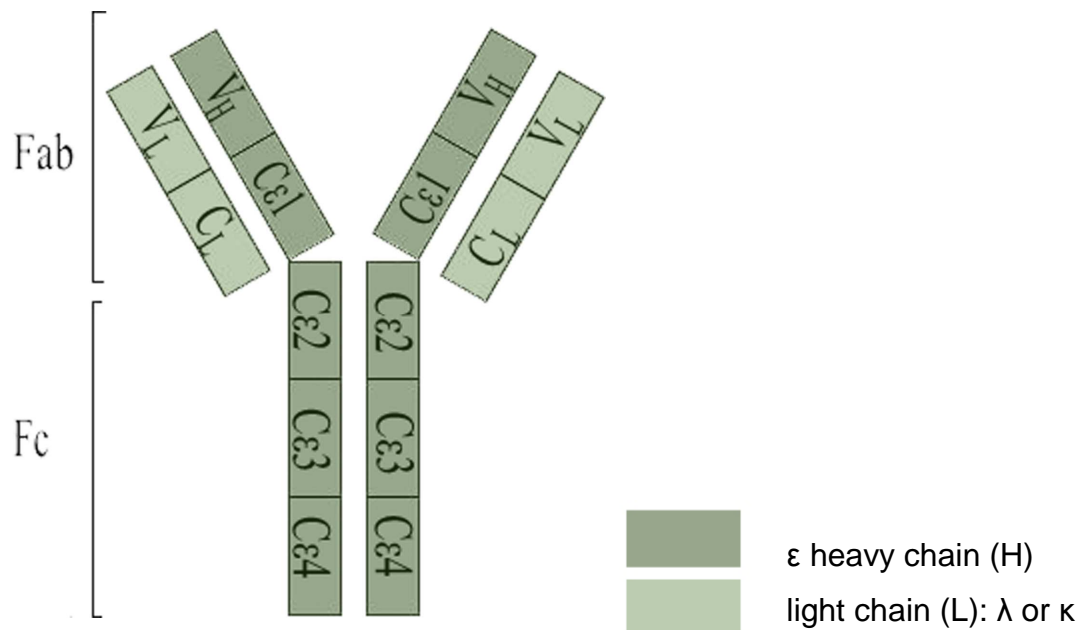
Fig. 1.2. Structure of immunoglobulin E. IgE consists of two identical heavy (H) chains and two identical light (L) chains. The ε heavy chain is composed of four constant regions (Cε1 - Cε4) and one variable region (V_H). The light chain is composed of one constant (C_L) and one variable (V_L) region. The immunoglobulin E binds antigen through the amino-terminal end (Fab) and can bind on Fc receptors through its carboxy-terminal region (Fc); modified from (1)

1.1.2. Physiology of Immunoglobulin E

Initially IgE was thought to play a role in pathogen defense only, but due to the observation of increasing IgE levels in patients suffering from allergy, it has emerged, that IgE plays a crucial role in the development of hypersensitivity reactions (1).

In contrast to other immunoglobulin classes, the concentration of IgE in the serum of healthy individuals is very low (30-100 ng/ml compared to 10 mg/ml of IgG) (2). In atopic diseases and allergies, the IgE serum concentration can be dramatically increased (1, 5). IgE has a half-life of two to three days when free

in serum. The half-life of IgE increases up to several weeks when IgE is cell-bound (2, 6).

Following sensitization to certain antigens under certain conditions, Th2 cells are primed and secrete Th2 cytokines including IL-4 and IL-13 (Fig.1.3). These cytokines induce a class switch from µ (IgM) to ε (IgE) heavy chain usage and subsequent IgE production and secretion by B cells (1).

Crosslinking of IgE bound to FcεRI on mast cells by allergen leads to mast cell activation and to the early-phase of the allergic reaction (EAR). This includes mast cell degranulation and subsequent release of histamine and other inflammatory mediators (1). Clinically, the EAR manifests as rhinoconjunctivitis, urticaria, acute asthma attacks or in the worst case, anaphylaxis (7). Hours after the initial allergen encounter the late-phase of allergic reaction (LAR) gradually develops. This inflammatory reaction requires the chemokine- and cytokine-induced recruitment of leukocytes like Th2 lymphocytes, dendritic cells (DCs), and eosinophils to the site of allergen exposure (1). Allergen-specific T cells are activated and proliferate in situ. Several lines of evidence show that the LAR is strictly dependent on Th2 cells. Th2 cells secrete cytokines like IL-4, IL-5 and IL-13 thereby activating effector cells like eosinophils, which can mediate tissue damage and mucus production during chronic inflammation (Fig. 1.3).

In the lung, the LAR includes oedema and erythema of airways, increased mucus production, airway obstruction, long-lasting ventilatory insufficiency and if untreated, fibrotic lung remodeling (7). The repeated occurrence of LARs contributes to chronic allergic symptoms.
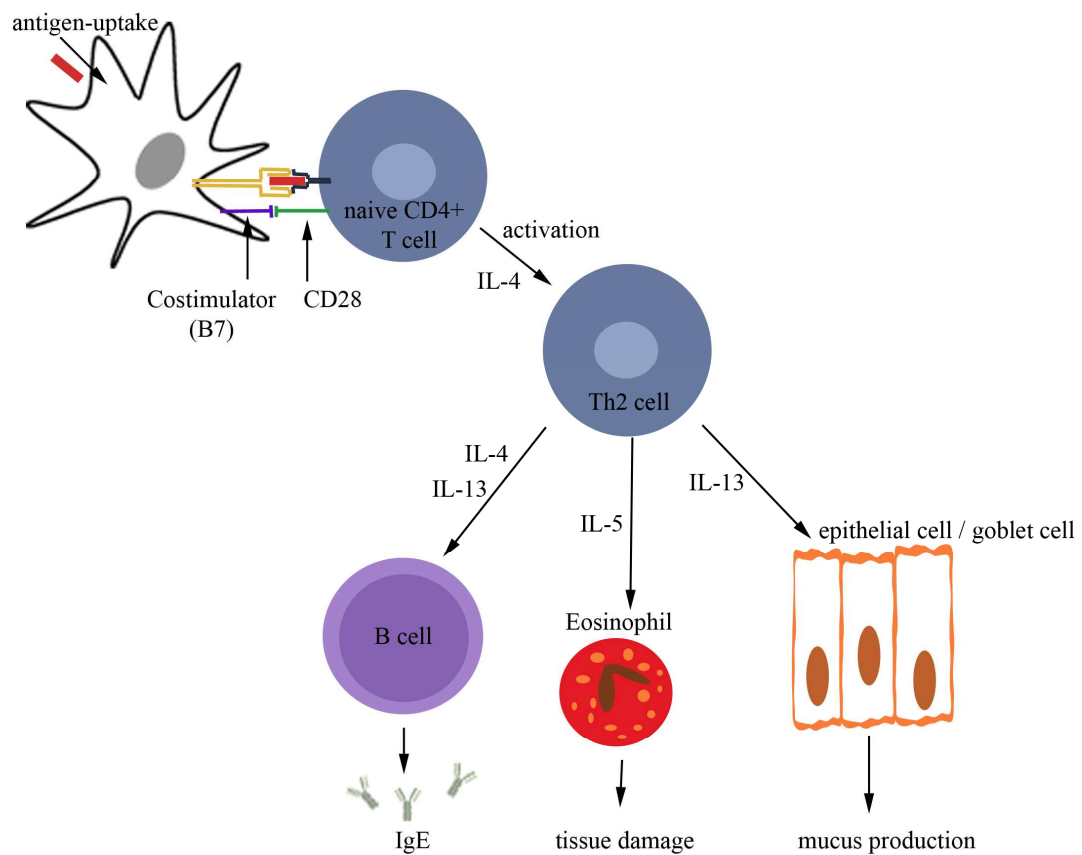
Fig. 1.3. Effector functions of Th2 cells. Following antigen-specific T cell activation, T cells produce IL-4, IL-5 and IL-13 cytokines. IL-4 and IL-13 in turn mediate IgE class switch of B cells. IL-13 stimulates epithelial cells / goblet cells leading to mucus production. IL-5 activates eosinophils leading to tissue damage.

1.2. The high-affinity IgE receptor – FcεRI

1.2.1. Expression and structure of the high affinity IgE receptor

The high affinity IgE receptor (FcεRI) is expressed in two isoforms. (i) The tetrameric ($\alpha\beta\gamma_2$) form (Fig. 1.4a) composed of one alpha, one beta and a gamma-chain dimer is expressed on mast cells and basophils [8, 9]. (ii) In humans, the trimeric ($\alpha\gamma_2$) form (Fig. 1.4b) lacking the beta-chain is expressed on Langerhans cells [10, 11], DCs [12, 13], monocytes [14], possibly also eosinophils [15] and platelets [16]. Noteworthy, mice do not express the trimeric form of FcεRI on APCs but express the tetrameric receptor on mast cells and basophils.

The FcεRIα-chain is a type I integral membrane protein composed of a C-terminal transmembrane anchor and one N-terminal extracellular part [17]. The α-chain is a 50 kDa, highly N-glycosylated subunit: FcεRIα reveals seven N-glycosylation sites in human [18] and six N-glycosylation sites in mouse [19]. The extracellular part of the α-chain is composed of two immunoglobulin-like domains (D1 and D2) [1] and contains the two IgE binding sites within the D2 domain. IgE-Fc binds to FcεRIα with a 1:1 stoichiometry and an affinity of $K_d < 10^{-9}$-10^{-10} M [20].

The β-chain is a 30 kDa subunit of FcεRI with four transmembrane domains. The NH_2 terminus and COOH terminus are both cytoplasmic. The β-chain contains an immunoreceptor tyrosine-based activation motif (ITAM) in the cytoplasmic tail near the C terminal end [21]. The β-chain amplifies signals mediated from the γ-chains [22]. The β-chain alone can not account for full signaling capacity [23]. Furthermore, the β-chain is able to amplify the surface expression of FcεRI. This explains the 10-100 fold higher expression of $\alpha\beta\gamma2$ receptors on mast cells and basophils compared to surface expression of the $\alpha\gamma2$ receptor [24].

The γ-chain is a 10 kDa subunit of the high-affinity IgE receptor. The γ-chains form a disulfide-linked homodimer. Each γ-chain consists of a short extracellular domain, a transmembrane domain and a cytoplasmic tail. Both γ-chains possess an ITAM in its cytoplasmic tail (25). The γ-chain of FcεRI is also a subunit from other Fc receptors like FcγRIII (human) and FcγRIIa (mouse) (26). Moreover, the γ-chain is required for surface expression of Fc receptors including FcεRI (25).

a

human	mouse
mast cells basophils	mast cells basophils

b

human	mouse
Langerhans cells dendritic cells monocytes eosinophils platelets	-
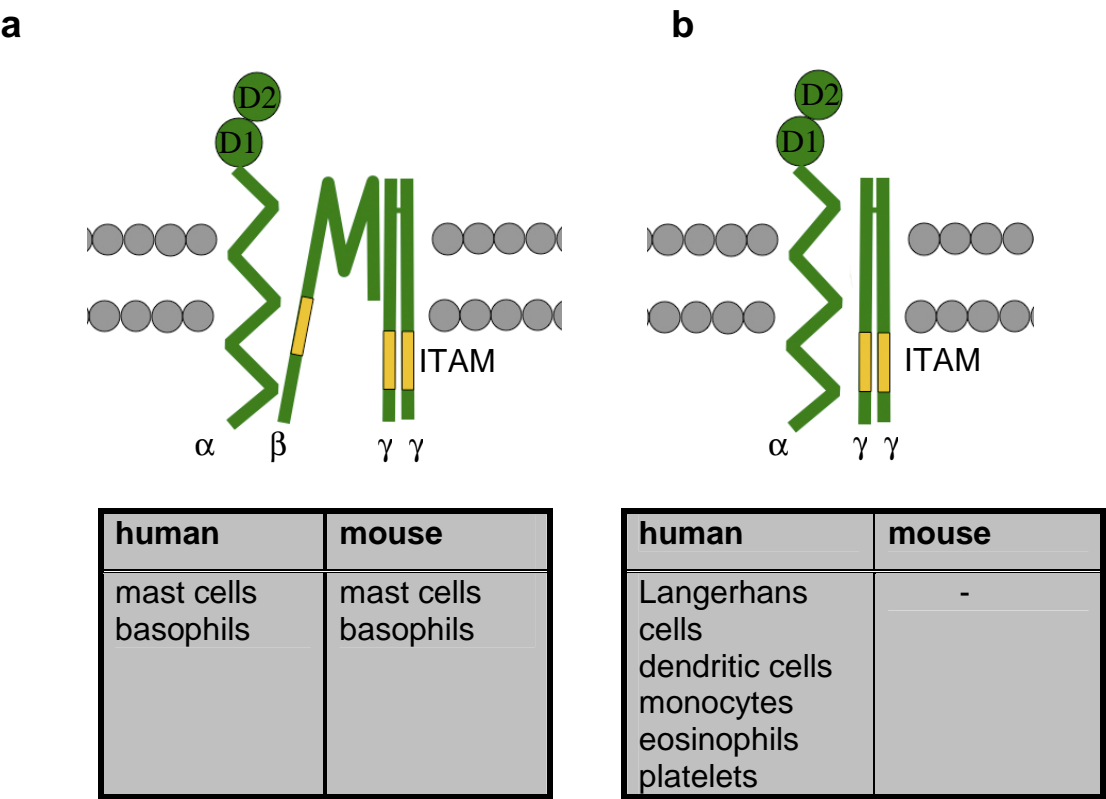
Fig. 1.4. Expression and structure of the high-affinity IgE receptor. FcεRI is expressed either as tetramer (a) or as trimer (b). The tetrameric form is composed of one alpha, one beta and a gamma-chain dimer whereas the trimeric form lacks the beta-chain. The $\alpha\beta\gamma_2$ form is expressed on mast cells and basophils. The $\alpha\gamma_2$ form is expressed in humans on Langerhans cells, dermal DCs, monocytes, eosinophils, peripheral blood DCs and platelets. The α-chain contains the two IgE binding sites within the D2 domain. The β-chain has four transmembrane domains and an ITAM in the cytoplasmic tail. The γ-chains form a disulfide-linked (S-S) homodimer. Each γ-chain contains an ITAM in its cytoplasmic tail.

1.2.2. Regulation of FcεRI expression

FcεRI cell surface expression is regulated by: (i) the existence of the γ-chain (ii) the existence of the β-chain, and (iii) IgE serum concentration and IgE binding to the α-chain.

The existence of the γ-chain is crucial for efficient cell surface transport of FcεRI. As we and others showed (Fig. 3.1), transfection of cells with the coding sequence for the α-chain only results in cytoplasmic FcεRI$^+$ expression, while co-transfection of the coding sequence for the γ-chain is sufficient for efficient FcεRI surface expression (27).

As aforementioned, the β-chain is able to amplify the surface expression of FcεRI resulting in 10-100 fold higher expression of αβγ2 receptors on mast cells and basophils compared to surface expression of the αγ$_2$ receptors (24).

In addition, there is a correlation between serum IgE and the density of surface expression of FcεRI (28). In healthy subjects, the serum concentration of IgE is much lower (about 100 ng/ml) than the concentration of IgG (2). In patients suffering from atopic diseases, the IgE serum concentration can dramatically increase. Increased serum IgE leads to upregulation of FcεRI surface expression by stabilization of FcεRI at the cell surface. Treatment of atopic patients with anti-IgE antibodies decreases free serum IgE and subsequent surface expression of FcεRI (29). Also, IgE does not influence the mRNA level for either α-, β- or γ- chain (30). Thus, the interaction of IgE with FcεRI is a main reason of posttranslational upregulation of receptor surface expression (31).

The effective concentration$_{50}$ (EC$_{50}$) for IgE-induced FcεRI upregulation is about 230 ng/ml (32). The mechanism of IgE-mediated FcεRI upregulation consists of three different factors: binding of IgE prevents the loss through receptor stabilization at the cell surface, increases the utilization of recycled and export of newly synthesized receptors (33).

22

1.2.3. Signaling via FcεRI

Following FcεRI aggregation on cell surface cell signaling is initiated (10). Aggregation leads to the activation of protein tyrosine kinases (PTKs) of the Src family including Lyn and Syk (34). The weakly associated PTK Lyn induces the phosphorylation of tyrosine residues within the β-chain ITAM (35). Interacting with the phosphorylated β-chain ITAM, additional recruited Lyn promotes the phosphorylation of tyrosine residues within the γ-chain ITAMs (22) and form binding sites for the PTK Syk. Syk is activated after ITAM binding (36). The PTK Syk is phosphorylated by Lyn but can also be autophosphorylated resulting in increased activity (37). Downstream events include the phosphorylation of LAT (linker for activation of T cells) subsequently essential for further downstream events resulting in the release of proinflammatory proteins (38).

In addition, a second – "complementary" – signaling pathway came up when Juan Rivera and his group described a Fyn-kinase dependent pathway (39). Within this cascade, Fyn becomes activated after FcεRI aggregation. This leads to the phosphorylation of GAB2 (growth-factor receptor-bound protein 2-associated binding protein 2) and subsequent to the binding of PI3K (phosphatidylinositol 3-kinase). Further downstream events result in the release of proinflammatory proteins without the requirement of LAT (39).

The existence of two different expression types of FcεRI raises the question of a difference in their signaling capabilities because of the lack of the β-chain within the $\alpha\gamma_2$ complex. Alber et al. showed that cells expressing an $\alpha\gamma_2$ complex are activated normally after FcεRI aggregation and have the ability to activate hematopoietic cells (40). The β-chain has the ability to amplify the Fcγ signal which leads to an amplified signaling mechanism including Syk activation and calcium mobilization (22). Bieber et al. concludes the lack of the β-chain on antigen-presenting cells (APCs) to functional differences like the high variability in surface expression (41).
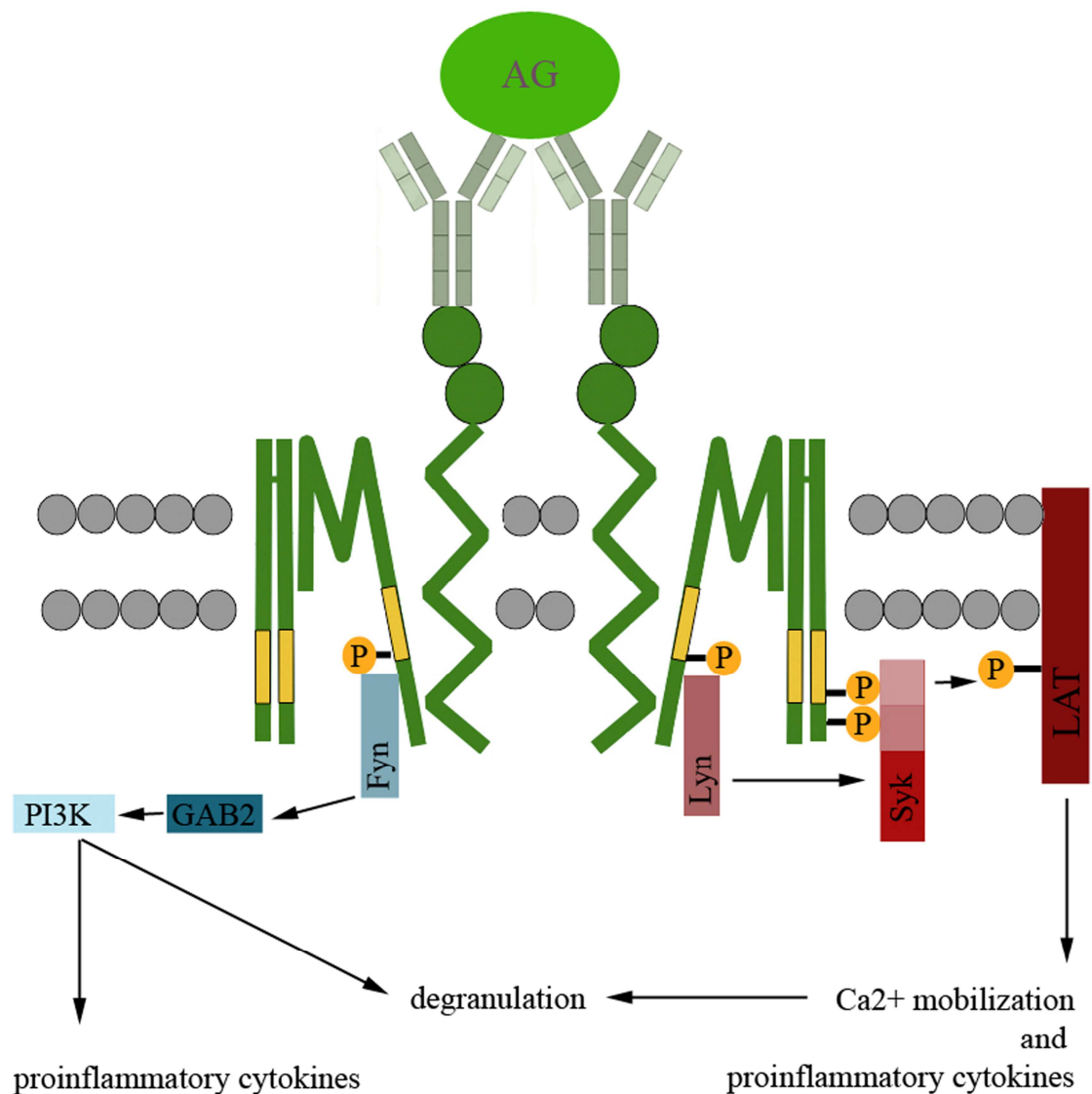
Fig. 1.5. Simplified scheme of the first events in FcεRI signaling. FcεRI aggregation leads to the activation of Lyn and Syk. Lyn induces the phosphorylation of the β-chain ITAM. Additional recruited Lyn promotes the phosphorylation of the γ-chain ITAMs and form binding sites for Syk which is activated after ITAM binding. Syk is phosphorylated by Lyn but can also be autophosphorylated. Downstream events include the phosphorylation of LAT resulting in the release of proinflammatory proteins.

Within the "complementary" signaling pathway Fyn becomes activated after FcεRI aggregation. This leads to the phosphorylation of GAB2 and subsequent to the binding of PI3K. Further downstream events result in the release of proinflammatory proteins without the requirement of LAT.

24

1.2.4. Biological function of FcεRI

FcεRI plays a central role in the pathophysiology of type 1 allergic reactions. Crosslinking of IgE bound to FcεRI on mast cells by allergen leads to mast cell activation and to the EAR which is often followed by a LAR. The characteristic chain of events in type 1 immediate allergic reactions includes (i) IgE production by B cells in response to allergen exposure, (ii) binding of IgE to Fcε receptors on the cell surface of mast cells and basophils, (iii) re-exposure to the same antigen which leads to interaction of allergen and FcεRI-bound IgE, and finally (iv) crosslinking of Fcε receptors which results in cell activation. Mast cell activation is followed by the release of preformed mediators like histamine and serotonin as well as the production and secretion of mediators like prostaglandins, leukotrienes, cytokines, interleukins and growth factors (7).

Furthermore, recent studies indicated an antigen-independent function of FcεRI. Asai et al. showed that IgE alone can partially activate FcεRI and enhance the survival of mast cells (42). Consequently, FcεRI bound monomeric IgE can increase allergic reactions not only by regulation of FcεRI expression, but also by regulation of mast cell homeostasis.

FcεRI on antigen-presenting cells enhances T cell activation. DCs can take up IgE-bound antigens, process them and present allergen-derived peptides. Maurer et al. showed that DCs from allergic patients more efficiently present allergen-derived peptide to T cells in the presence of allergen-specific IgE (43).

Furthermore, human epidermal Langerhans cells express FcεRI (11, 12). Jürgens et al. showed that crosslinking of FcεRI on Langerhans cells derived from patients with atopic dermatitis but not from healthy individuals results in calcium mobilization (44). In addition, upregulation of protein tyrosine kinases and subsequent activation of phospholipase C-γ1 (PLCγ1), essential for calcium mobilization, was detected only in Langerhans cells from atopic patients and not from healthy individuals (45). Moreover, crosslinking of FcεRI expressed on Langerhans cells of atopic patients leads to NF-κB activation which in turn results in the synthesis and secretion of proinflammatory cytokines like TNFα

and MCP-1 (46). To conclude, FcεRI expressed on antigen-presenting cells influences inflammatory and allergic reactions.

1.3. Dendritic cells and antigen-presentation

Skin cells with a "dendritic" nerve cell-like morphology were first described by Paul Langerhans in 1868. Today we know that Langerhans cells belong to the family of dendritic APCs. The term "dendritic cell" was coined in 1973 by Ralph M. Steinman and Zanvil A. Cohn to describe a previously unrecognized bone-marrow-derived cell species in peripheral lymphoid organs that has the unique ability to MHC-dependently activate resting T cells (47).

1.3.1. DC maturation and Th differentiation in response to DC stimuli

DCs have the ability to regulate immune responses: immunity against tolerance and Th1 against Th2. This ability is dependent on their state of maturation and the quality of the signals which they receive from the environment. Immature DCs are located in the peripheral tissues and are recruited into sites of inflammation where they have the ability to take up and process antigen. Following the receipt of certain signals (e.g. bacteria, viral products, inflammatory cytokines), DCs mature and migrate to lymphoid organs where they present allergen-derived peptides in the context of MHC molecules to T cells (48; Fig. 1.6). During DC maturation biologically important alterations occur: (i) upregulation and clustering of MHC (MHC-peptide complexes), B7 (CD80 and CD86) and CD40 molecules (49), (ii) synthesis of cytokines and chemokines (50) and (iii) switch in surface expression of chemokine receptors to control DC movement to lymphoid organs, e.g. upregulation of CCR7 to ensure DC homing to secondary lymphoid tissues (51).

The upregulation of MHC-peptide complexes determines the specificity of T cell response (signal 1) whereas the expression of B7 molecules allows expansion of T cells (signal 2). Furthermore DCs secrete cytokines (signal 3) in part in a polarized fashion towards the activated T cell which differ dependent on the nature of stimulus, stage of DC maturation and the already existing

27

environmental cytokines, determining the differentiation of naïve Th cells (ThN) towards Th1, Th2, Th17 and regulatory T cells (52, 53, Fig 1.7).

Key cytokines secreted by DCs include e.g. IL-2, IL-6, IL-10, IL-12, IL-18, IFN-α, IFN-ß, IFN-γ, TNF-α. Receiving lipopolysaccharide (LPS), poly(I:C), bacterial or viral signals, DCs secrete IL-12, the main Th1 polarizing cytokine, stimulating IFN-γ production in naïve T cells and promoting Th1 polarization. Engagement of CD40 on DCs with CD40 ligand (CD40L) primes mature DCs for maximal expression of IL-12. Binding of IL-12 to its appropriate receptor on antigen-stimulated CD4$^+$ T cells activates the transcription factors STAT1 and 4 (54). STAT1 stimulates the expression of T-bet which promotes IFN-γ production. STAT4 enhances IFN-γ production and seems to be an important factor in Th1 polarization since STAT4$^{-/-}$ mice show decreased secretion of IFN-γ and are defective in Th1 cell development (55). Moreover, IFN-γ augments its own expression by a STAT1-dependent positive feedback loop. Another Th1 polarizing cytokine secreted by DCs is IL-18. IL-18, unlike IL-12, only induces low levels of IFN-γ but in presence of IL-12 acts as a strong agonist (53). Type 1 interferons (IFN-α, β and ω) secreted by DCs also promote Th1 differentiation by activation of STAT4 in human but not murine T cells (56).

Receiving microbial or allergenic signals that cause repeated CD4$^+$ T cell stimulation, DCs stimulate the differentiation of naïve Th cells towards Th2 cells. One important event in Th2 differentiation can be the downregulation of IL-12 secretion. Furthermore, differentiation of T cells into Th2 cells depends on IL-4. Mainly, the Th cell itself produces IL-4, which is dependent on the activation of STAT6. The transcription factor STAT6 induces the expression of GATA3, the main transcription factor in Th2 differentiation by enhancing the expression of IL-4, IL-5 and IL-13 (57). Expressed GATA3 augments its own expression by a positive feedback loop (58) and inhibits IL-12 signaling by downregulation of IL-12 receptor β2-chain (IL-12Rβ2) expression (59).

The fact that differentiated CD4$^+$ Th2 cells are the main producers of IL-4 raises the question where does IL-4 originate before Th2 cell differentiation. ThN cells are capable of low-level secretion of IL-4, which will gradually enhance during

persistent low level antigen stimulation. Furthermore, other cells may be the source of IL-4 as Kelleher et al. showed the ability of Rauscher leukemia virus (RLV)-treated DCs to produce IL-4 (60). Crosslinking of FcεRI on mast cells and basophils is an essential event in the induction of allergic inflammation. Thus, these effector cells may be a source of IL-4. Plaut et al. demonstrated the capability of murine mast cells to secrete IL-4 and IL-5 upon FcεRI crosslinking (61) and Bradding et al. showed also human mast cells produce IL-4 (62). Basophils may be an additional source of the Th2-cytokine IL-4. Brunner et al. showed that basophils produce IL-4 after FcεRI stimulation (63), whereas studies by MacGlashan et al. indicate that basophils express IL-4 message even constitutively and upregulate IL-4 secretion after stimulation (64).

ThN cells can also differentiate into Th17 cells characterized by the secretion of IL-17. Th17 cells are pro-inflammatory (65) and play an essential role in defense against various bacteria and fungi. Th17 cells do not secrete IL-4 or IFN-γ and their differentiation is even antagonized by IL-4 and IFN-γ (66). The cytokines IL-6 and TGF-β are essential for the generation of Th17 cells (67) whereas IL-21 amplifies Th17 differentiation and IL-23 promotes the maintenance of Th17 cells (68).

DCs have also the capability of regulatory T cell induction. Regulatory T (Treg) cells can be distinguished between naturally occurring (nTreg) and induced regulatory T (iTreg) cells. nTreg cells are thymic derived CD4$^+$CD25$^+$Foxp3$^+$ Treg cells. iTreg cells are generated from peripheral ThN cells after activation by antigen-presenting DCs (53). Jonuleit et al. showed that immature DCs induce iTreg differentiation after repetitive stimulation (69) and McGuirk et al. demonstrated that pathogen-activated (e.g. Bordetella pertussis-treated) DCs can also induce iTreg development (70). In all studies, IL-10 plays an essential role in iTreg differentiation. Culture of human ThN cells with IL-10 results in the development of iTreg cells suppressing other Th cell proliferative responses (71). IL-10 indirectly influences tolerance since IL-10 inhibits full DC maturation, upregulation of costimulatory molecules and DC-dependent IL-12 secretion (72).

inflammatory cytokines
TNF-α
IL-1
or bacterial stimuli
or viral products

a

b

upregulation of

MHC I
MHC II
CD40

CD80
CD86
CCR7

antigen-uptake

T-cell priming
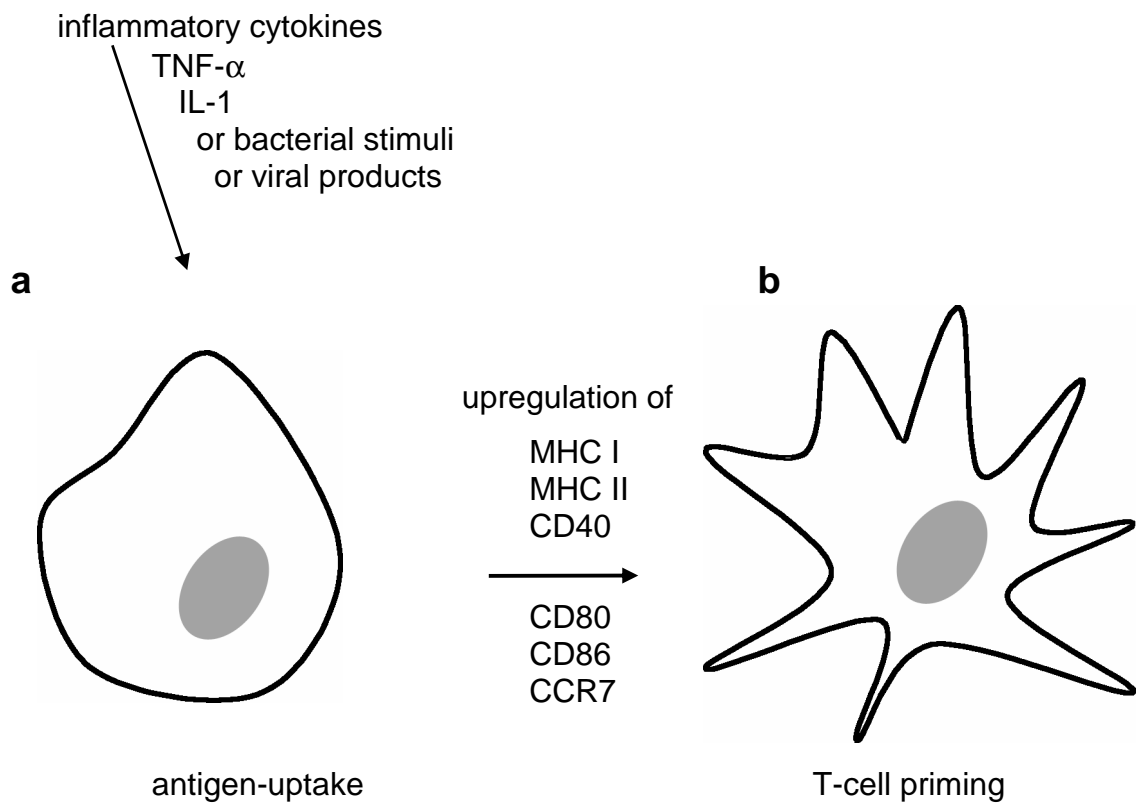
Fig. 1.6. DC-maturation. There are two states of DCs. (a) Immature DCs and (b) mature DCs. Stimuli like inflammatory cytokines or bacterial stimuli induce DC maturation thus including a phenotypic and functional alteration. Surface expression of MHC molecules, chemokine receptors and secretion of chemokines are upregulated.
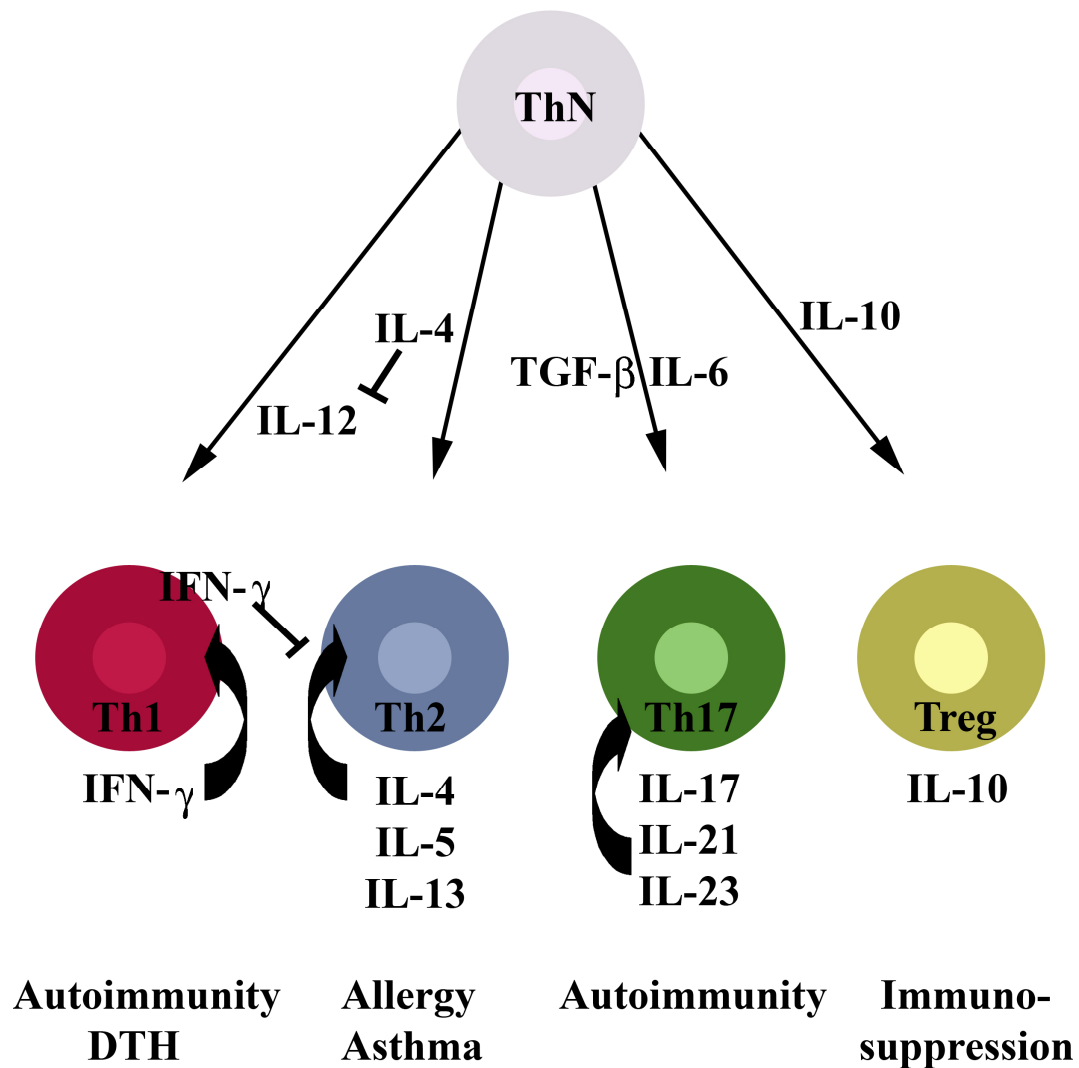
Fig. 1.7. Simplified scheme of Th subset development. Naïve T cells can differentiate into Th1, Th2, Th17 and regulatory T cells, depending on the signal they receive. IL-12 induces the differentiation towards Th1 and IL-4 towards Th2. IL-6 and TGF-β are essential for Th17 differentiation, whereas IL-10 acts in the development of regulatory T cells.

1.3.2. Antigen-uptake and presentation

To induce a T cell response, DCs have to present peptide in the context of MHC class I or II molecules expressed on their cell surface.

1.3.2.1.   MHC class I presentation

Intracellular antigens like intracellular bacteria or viruses are presented by MHC class I molecules to CD8$^+$ T cells (Fig. 1.8). The endogenous antigen is processed by the proteasome into small peptides. These peptides are transported via TAP (transporter associated with antigen presentation) into the endoplasmic reticulum (ER). In the ER, peptides are loaded onto newly synthesized MHC class I molecules. Peptide-loaded MHC molecules are transported through the Golgi apparatus to the cell surface (73).
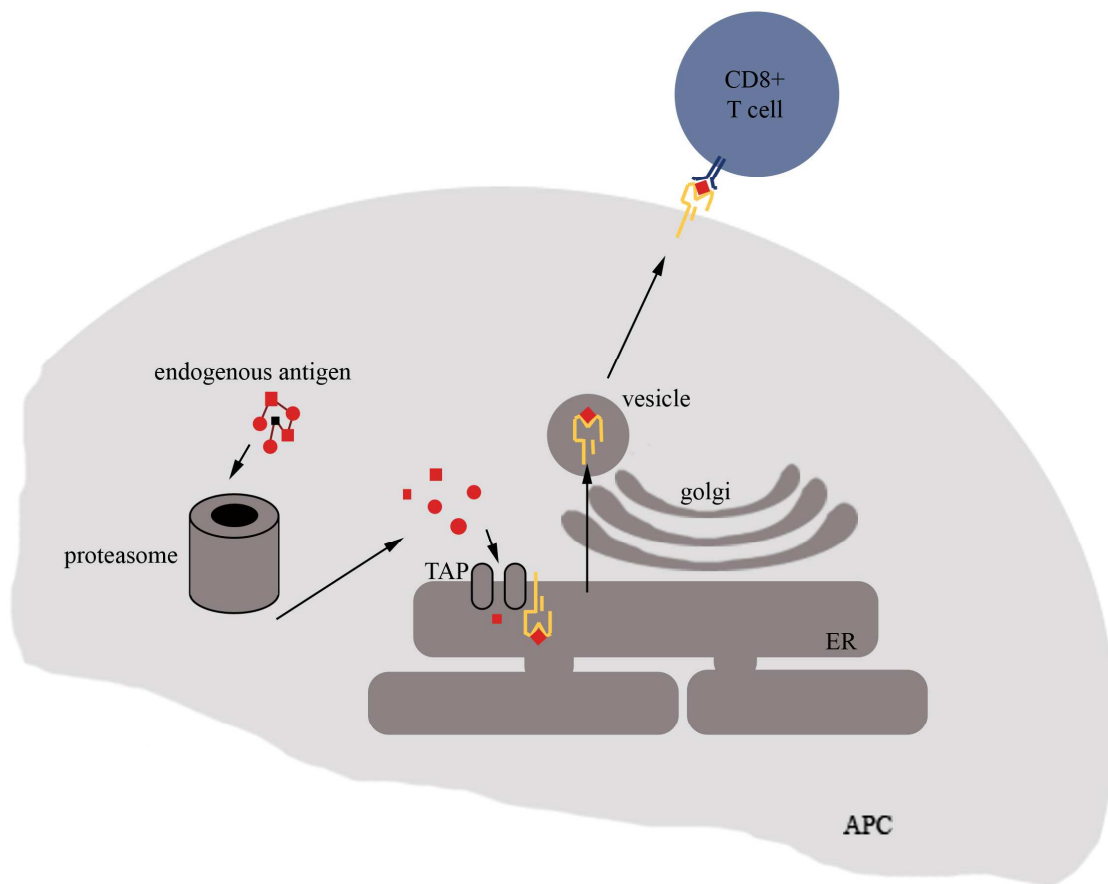
Fig. 1.8. MHC class I presentation. Endogenous antigen is degraded in the proteasome and transported via TAP into the ER. Peptides are loaded onto newly synthesized MHC class I molecules. Loaded MHC class I molecules are transported via the Golgi to the cell surface, where the peptide is presented to CD8$^+$ T cells. TAP transporter associated with antigen presentation; ER endoplasmic reticulum; APC antigen presenting cell; modified from (50).

1.3.2.2.   MHC class II presentation

Exogenous protein-derived peptides are presented in the context of MHC class II molecules to CD4$^+$ T helper cells (Fig. 1.9). DCs use phagocytosis or receptor-mediated antigen-uptake to internalize antigen and form the phagosome, which contains the sampled antigen (74). The phagosome fuses with the lysosome where the internalized antigen is processed. MHC class II molecules are synthesized into the endoplasmic reticulum (ER). To prevent MHC class II molecules of unintentional binding, the binding groove of the MHC class II molecule is occupied by the invariant chain Ii. Ii has further the function to determine the transport route of MHC class II molecules through the Golgi in the endosomal pathway (75). Vesicles containing the MHC class II molecule are delivered from the Golgi complex and associate with the phagosome / lysosome containing the degraded antigen. Ii is degraded leaving a short peptide – CLIP – in the binding groove (76). Activation of HLA-DM (in mouse H-2M) leads to the removal of CLIP and mediates the formation of a stable peptide-MHC class II complex ready for cell surface expression (77).

1.3.2.3.   Cross-presentation

DCs, in contrast to most other APCs, have the capacity to cross-present peptides (Fig. 1.10). Usually, the MHC class I pathway is restricted to the presentation of peptides derived from endogenous antigens. In DCs, the discrimination between MHC class I presentation of endogenous proteins and MHC class II presentation of exogenous antigens is not strict. DCs may also present exogenous antigens via the MHC class I pathway, referred as "cross-presentation" (73). The mechanism of cross-presentation is not fully understood. Recent studies showed that the phagosome containing exogenous antigens fuses with the ER that in turn contains newly synthesized MHC class I molecules and the TAP protein. Alternatively, exogenous antigens can be

transported into the DC cytosol and undergo conventional proteasomal degradation. Resulting peptides are transported via TAP into the ER entering the classical MHC class I pathway (78).
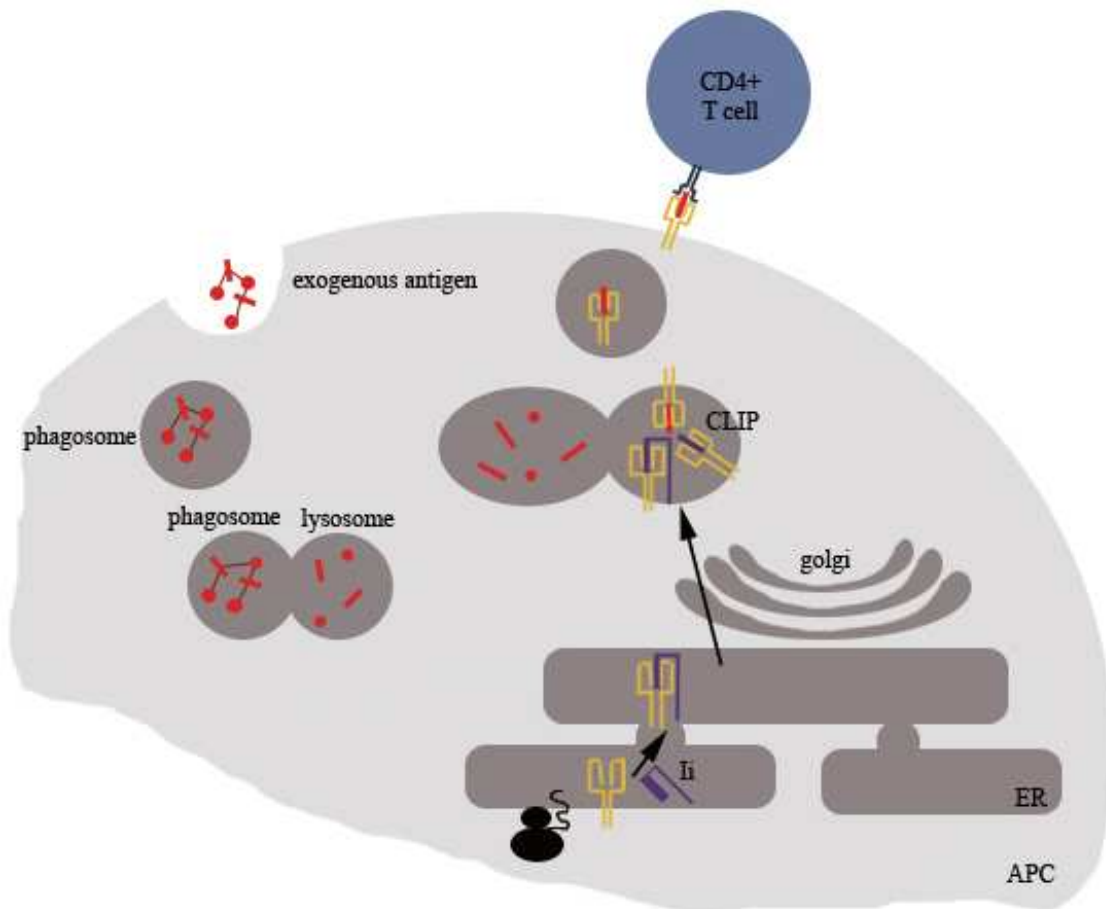
Fig. 1.9. MHC class II presentation. Extracellular antigens are phagocytized and processed in the phagolysosome. MHC class II molecules are synthesized into the ER and the peptide binding site is occupied by Ii. MHC class II molecules are transported through the Golgi to the lysosome. Ii is degraded leaving CLIP in the binding groove. Through activation of HLA-DM / H2-M CLIP is removed followed by the formation of a stable MHC class II-peptide complex which is transported to the cell surface to present peptides to CD4^{+} T cells. ER endoplasmic reticulum; APC antigen presenting cell; modified from (50).
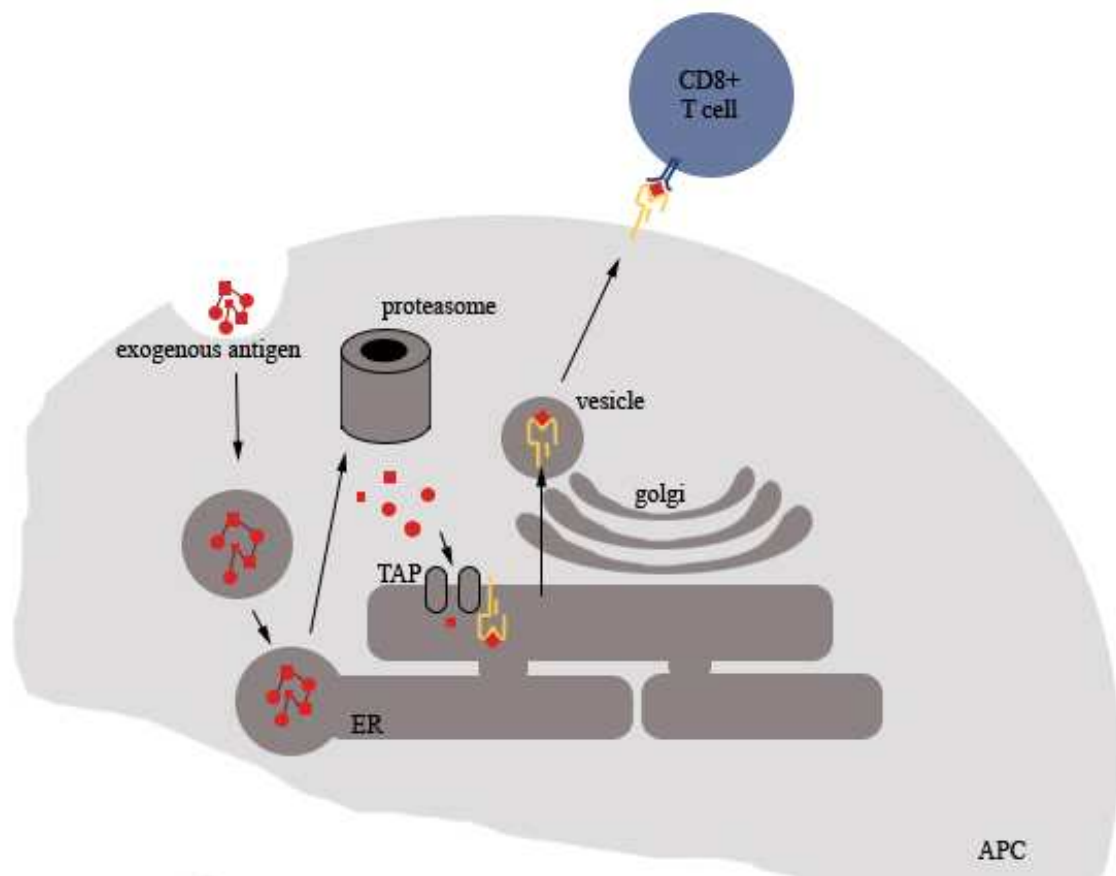
Fig. 1.10. Cross-presentation. Exogenous antigens are presented on MHC class I molecules to CD8^{+} T cells. The phagosome containing the antigen fuses with the ER. The antigen is transported into the cytosol where it is degraded by the proteasome. Peptides are transported via TAP into the ER. Peptides are loaded onto newly synthesized MHC class I molecules. Loaded MHC class I molecules are transported via the Golgi to the cell surface, where the peptide is presented to CD8^{+} T cells. TAP transporter associated with antigen presentation; ER endoplasmic reticulum; APC antigen presenting cell; modified from (73).

1.3.3. Murine dendritic cell subtypes

DCs can be divided in subtypes differing in function and expression of surface markers (Tab. 1.1). Basically, DCs can be divided into plasmacytoid and conventional DCs. Plasmacytoid DCs (pDCs) express the surface markers CD11c^{low} and B220. After viral stimulation via endosomal pDC-expressed TLR7 (recognizes ssRNA) and TLR9 (recognizes unmethylated CpG DNA) (75), interferon regulatory factor 7 (IRF7) is activated (80) and type I IFNs (IFN-α/β), mainly IFN-α are transcribed and secreted by pDCs (81, Fig. 1.11). Contrary to other cell types, pDCs are not reliant on IRF3 in the activation of IFN genes since pDCs from IRF3$^{-/-}$ mice produce the same amounts of IFN as pDCs from WT mice. (82). Type I IFNs bind to the IFN-α receptor (IFNAR) composed of two subunits, IFNAR1 and IFNAR2. IFNAR1 and IFNAR2 are associated with the Janus family tyrosine kinases Tyk2 and Jak1, respectively. Upon IFN binding Tyk2 and Jak1 become activated leading to phosphorylation of STAT1 and STAT2 (83), formation of STAT1/STAT2 dimers and recruitment of IRF9. STAT1/STAT2 dimers and IRF9 proteins form trimeric complexes which translocate into the nucleus and induce the activation of gene transcription as a result of trimer binding to IFN-stimulated response elements (ISREs) (84, Fig. 1.12). Type I IFN induced gene transcription includes e.g. the synthesis of enzymes like serine/threonine protein kinase (PKR16) and RNase L18 resulting in viral transcription/translation blocking and viral RNA degradation, respectively. pDCs appear not play a crucial role in antigen-presentation, but their secretion of large amounts of IFN-α is essential for blocking viral replication and may contribute to prime other DC subtypes (73). Conventional DCs can be further divided into five subtypes. Due to the expression of CD4 and CD8, three subtypes can be distinguished. There are CD11c^{+}CD8^{+}CD4^{-} lymphoid DCs, CD11c^{+}CD8^{-}CD4^{+} myeloid DCs and CD11c^{+}CD8^{-}CD4^{-} DCs (85). Conventional DCs have the ability to present protein-derived peptides in the context of MHC molecules to T cells and induce the immune response. Furthermore CD8^{+} DCs have also the ability of cross-presentation and cross-priming (73). The remaining two DC subtypes are Langerhans cells and

interstitial dermal DCs (DDC). They are characterized by their expression of DEC-205 (86). Langerhans cells and DDCs can further be distinguished by the different level expression of DEC-205 (high on Langerhans cells and intermediate on dermal DCs). Langerin was thought to distinguish between Langerhans cells and DDC (87) but recent studies showed a population of Langerin$^+$ DDCs. Bursch et al. demonstrated that the expression of the cell adhesion molecule EpCAM allows distinguishing Langerhans cells from EpCAM$^-$ DDCs (88, 89). Langerhans cells and DDCs have the capacity of self-renewal under stady-state conditions within the skin (90). Only after skin injury caused by e.g. UV irradiation, depleted DCs are replaced by circulating precursors (91). Langerhans cells capture antigen in the skin and carry them to the draining lymph nodes where they prime T cells and induce immune responses (92). DDCs have been described to mainly induce CD4$^+$ T cell responses (93, 94).

DC subtype	surface marker				
	CD11c	CD4	CD8	B220	DEC-205
CD4$^+$ DC	+	+	-	-	-
CD8$^+$ DC	+	-	+	-	+
CD4$^-$ CD8$^-$ DC	+	-	-	-	-
Langerhans cells	+	-	-	-	high
dermal DCs	+	-	-	-	+
plasmacytoid DC	+	+/-	+/-	+	-

Table 1.1. Surface expression markers of DC subtypes. DCs can be divided into six subtypes. The main discrimination is made between plasmacytoid DCs (pDCs) and conventional DCs. Conventional DCs can further be divided through the surface expression of CD4 and CD8. Additional, there are Langerhans cells and dermal DCs; modified from (73)
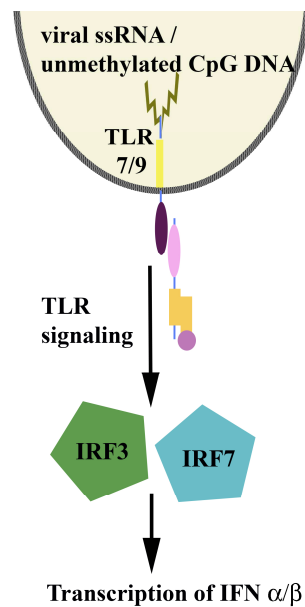
Fig. 1.11. Production of IFN-α/β. After viral stimulation via endosomal pDCs-expressed TLR7 and TLR9, IRF7 is activated and type IFNs are transcribed; modified from (4)
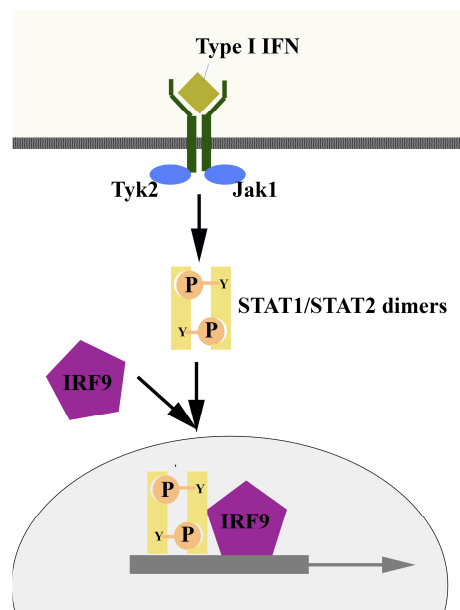
Fig. 1.12. Response to type I IFNs. Type I IFNs bind to IFNAR. The two subunits, IFNAR1 and IFNAR2, are associated with Tyk2 and Jak1, respectively. Upon IFN binding Tyk2 and Jak1 become activated leading to phosphorylation of STAT1 and STAT2, formation of STAT1/STAT2 dimers and recruitment of IRF9. STAT1/STAT2 dimers and IRF9 proteins form trimeric complexes which translocate into the nucleus and induce the activation of gene transcription as a result of trimer binding to ISREs; modified from (4).

38

1.3.4. Dendritic cells in the lung

DCs are found in all lymphoid organs (47), in the blood (95), in the bone marrow (96) as well as in other organs like the lung (97). Within the lung, DCs are localized in the airway epithelium, lung parenchyma and pleura (97). DCs and macrophages, both are APCs expressing CD11c on their cell surface. DCs are more potent stimulators of immune responses than macrophages. Thus, discrimination of these two populations is indeed important. CD11b can not be used as marker for discrimination between pulmonary macrophages and DCs. Pulmonary macrophages in general and various DCs, depending on their anatomical location, express CD11b. Vermaelen et al. studied the accurate discrimination of lung DCs and macrophages by their expression of CD11c and their level of autofluorescence (98) and showed a clear discrimination of two populations among CD11c-bright lung cells. Characteristics of autofluorescence allow discrimination between CD11c^{+} lung DCs and CD11c^{+} macrophages: low autofluorescent DCs can easily be distinguished from high autofluorescent macrophages (99).

DCs are present both in normal and in inflamed lung tissue. However, inflammatory stimuli increase the number of DCs in the lung (100).

Due to the location of DCs within the lung and their capacity of efficient antigen-presentation, DCs seem to be important also in allergic lung inflammation. Lambrecht et al. showed that depletion of DCs during the induction of airway inflammation results in an almost totally suppressed eosinophil-dependent inflammation (101).

In addition, pulmonary DCs in humans express FcεRI. Comparing the number of FcεRI[+] DCs in normal and asthmatic airways, Tunon-De-Lara and colleagues demonstrated an increase of FcεRIα-expressing DCs in asthma. Thus, FcεRI expression on DCs may contribute to the occurrence and the regulation of magnitude of allergic lung inflammation (102).

1.4. Allergy and atopic diseases

"The conception that antibodies, which should protect against disease, are also responsible for disease, sounds at first absurd. " (Clemens von Pirquet, 1906)

Clemens von Pirquet first introduced the term "allergy" in 1906 to describe a disease complex that is mediated by altered reactivity of the immune system (103). In 1963, Gell and Coomb classified hypersensitivity reactions into four groups whereas IgE-mediated allergy was referred as type 1 (immediate) hypersensitivity reaction (104). Allergic diseases include rhinoconjunctivitis, allergic asthma, atopic dermatitis and food anaphylaxis. Pathophysiologically, type 1 hypersensitivity reactions can be divided into two phases: (i) the EAR occurs within minutes after allergen exposure and (ii) the LAR, which persists for hours to days.

1.4.1. Causes of allergy

1.4.1.1.   Allergens

"What makes an allergen to allergen?" (Kjell Aas, 1978). Molecular investigation showed some common characteristics of allergens: Allergens are soluble and stable proteins, many of them having enzymatic function. Furthermore, the allergenic property of an antigen depends on the particle size (105), normally ranging from 5 to 80 kDa. Allergens are classified according to their origin (e.g. food allergens, allergens of animal hair, pollen allergens) and to their mode of entry (e.g. inhalation, food).

1.4.1.2.   Genetic predisposition

Family and twin studies allow an investigation in the predisposition for allergies. Family studies showed that children from healthy individuals have a relative risk ranging from 9 to 18% to develop allergies. The risk to develop an allergic disease for children with one parent being atopic is about 50% and with both parents being atopic even 70% (106). Comparing monozygotic and dizygotic twins, Hopp et al. showed a heritability of total serum IgE, methacholine sensitivity and total skin test scores (107). Studies on chromosomal regions relevant for the development of allergies identified e.g. chromosome 11q13 encoding the β-chain of FcεRI (108, 109) and 5q31-33 encoding for Th2 cytokines like IL-4 and IL-5 (110). Holt et al. showed an association of allergy with delayed postnatal maturation of T-cell competence: the capacity of T cells from children with family risk for atopy to produce IFN-γ is significantly decreased (111).

1.4.1.3.   Hygiene hypothesis

In 1989, David P. Strachan first hypothesized an inverse relation between allergic disease and household size due to transmission of more bacterial and viral infections in these families (112). This hypothesis is used to link the increased prevalence of allergic disease in developed countries with reduced exposure to bacteria, viruses and microbes in modern civilizations. The possible mechanism behind is a suppression of Th2-mediated allergic responses through bacterial or virus-elicited Th1 immune response during early life. Supporting the hygiene hypothesis, Matricardi et al. demonstrated that exposure to foodborne and orofecal microbes results in less frequent occurrence of respiratory allergy (113). Conversely, contradicting the hygiene hypothesis, Benn et al. showed that early infections do not protect from allergic disease (114). Recent studies favored a different model: regulatory T cells

balance Th1 and Th2 responses by secretion of regulatory cytokines (IL-10 and TGF-β) (115) and are decisive in the development of allergic disease. How their generation and function are linked to the theorem of the hygiene theory remains to be elucidated.

1.4.2. Reactions of type 1 allergic hypersensitivity

Type 1 allergic hypersensitivity consists of an early (EAR) and a late-phase allergic reaction (LAR). The EAR occurs within seconds to minutes after re-exposure to an antigen whereas the LAR develops 2 – 24 h later.

1.4.2.1.   The early-phase allergic reaction

Upon first exposure to antigen, APCs take up antigen, migrate to lymph nodes, process the antigen and present antigen-derived peptides to naïve CD4$^+$ T cells. T cells differentiate into Th2 cells secreting IL-4 and IL-13 and thus promote heavy chain isotype switching in allergen-specific B cells and IgE secretion. Circulating allergen-specific IgE binds to FcεRI receptors on the cell surface of mast cells and basophils. Re-exposure to the same antigen leads to interaction of allergen and FcεRI-bound IgE and thus crosslinking of FcεRI-bound IgE resulting in mast cell/basophil activation. This cell activation includes (i) release of preformed mediators (e.g. histamine), (ii) new synthesis and secretion of lipid mediators (e.g. leukotrienes) and (iii) new synthesis and secretion of cytokines (e.g. TNF) (116). Mast cells are the most crucial cell type in the EAR. The necessity of FcεRI expressed on mast cells was demonstrated in a study by Dombrowicz et al. using FcεRIα$^{-/-}$ mice. After intravenous IgE-injection, FcεRIα$^{-/-}$ mice, in contrast to WT mice, fail to develop cutaneous and systemic anaphylaxis (117).

1.4.2.2.   The late-phase allergic reaction

The LAR developing hours after allergen re-exposure may follow the EAR. Cytokines and chemokines secreted during the EAR initiate the LAR. The LAR is characterized by recruitment and activation of leukocytes like DCs, T lymphocytes and eosinophils to sites of allergen exposure (1). Th2 cells do not only play an essential role in the induction of EARs, LARs are strictly Th2 cell-dependent allergic responses. Th2 cells secrete cytokines like IL-4, IL-5 and IL-13 (118). IL-4 promotes the production of IgE by B cells (1), IL-13 stimulates epithelial cells leading to increased mucus production (119) and IL-5 activates eosinophils (120). Eosinophils are normally not present in peripheral tissue. After IL-5 dependent activation and chemokine (e.g. eotaxin, RANTES) attraction eosinophils are recruited to sites of inflammation. Robinson et al. showed in a study examining patients with atopic asthma an increase of Th2 cell activation, Th2 cytokine mRNA expression and eosinophils recruitment after allergen challenge concluding that Th2 produced cytokines directly contribute to the magnitude of LARs (121). Furthermore, studies using IL-4 neutralization or IL-4$^{-/-}$ mice demonstrate that Th2 cytokines are required for the development of LARs since the lack of IL-4 reduces eosinophilic inflammation of the lung (122). The LAR differs from classical delayed-type hypersensitivity reactions (DTH) in which Th1 but not Th2 cells are most important. Constant and repeated allergen exposure results in chronic allergic inflammation and irreversible tissue damage.

LARs may occur independently of EARs. This was shown in studies using mast cell-deficient mice (123). Moreover, in IgE-deficient mice, eosinophilic bronchial inflammation develops normally (124). Thus, these studies demonstrate that IgE, mast cells and FcεRI-expressed on mast cells are not important for the development of LARs.

In contrast to mice, human LARs are IgE-dependent. Anti-IgE treatment studies in human asthmatic revealed that application of a humanized murine monoclonal antibody directed to the FcεRI-binding domain of IgE decreases serum IgE and drastically reduces the LAR (125).
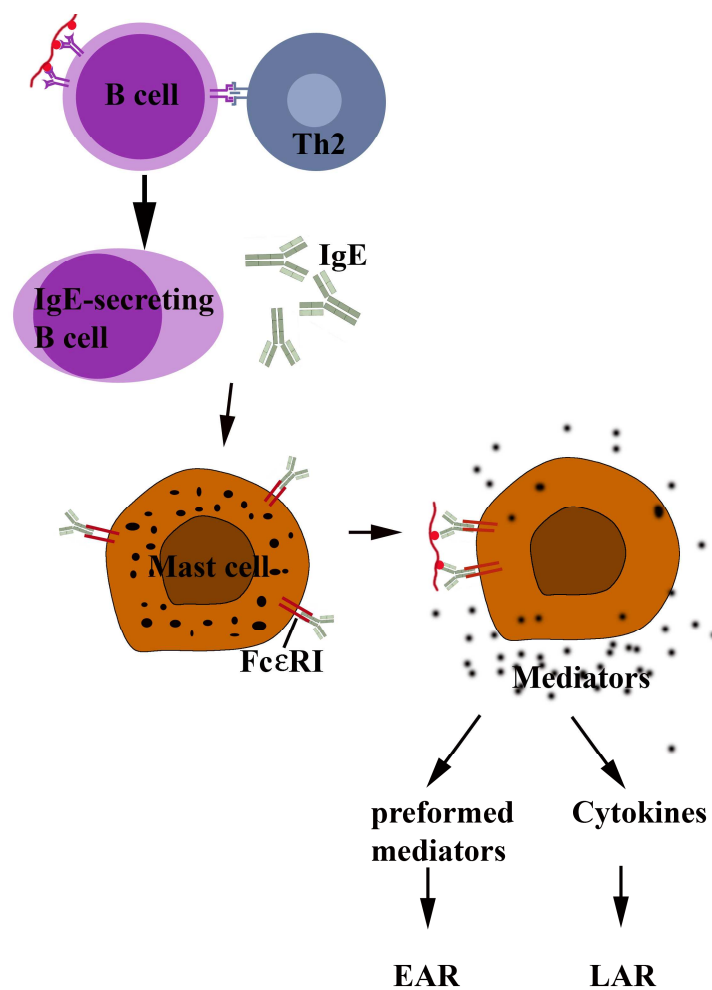
Fig. 1.13. Type 1 allergic hypersensitivity. Type 1 hypersensitivity consists of the EAR and the LAR. They are initiated by exposure to an antigen, followed by differentiation of ThN cells into Th2 cells and production of antigen-specific IgE by B cells. IgE binds to FcεRI on mast cells. Crosslinking of FcεRI by allergen leads to mast cell activation and the release of preformed mediators and the synthesis of cytokines; modified from (4).

1.5. α-DC transgenic mice: the tool of my study

FcεRI is expressed in two isoforms: (i) the tetrameric form composed of one alpha, one beta and two gamma-chains is expressed in humans and mice on mast cells and basophils; (ii) the trimeric form lacking the beta-chain is only expressed in humans and not in mice.

To study the in vivo role of FcεRI on DCs, our laboratory has generated α-DC TG mice. These mice display an overall "human-like" FcεRI expression pattern which allowed us to study this receptor's contribution to immunity and allergic reactions in a fashion reflecting the human situation.

The transgenic construct generated is driven by a CD11c promoter that induces transcription of the human FcεRIα-chain and the fluorescent dye eGFP in a simultaneous fashion selectively on DCs (Fig. 1.9).

Fig. 1.14. Construct for constitutive DC-targeted expression of FcεRI. CD11c promoter (pCD11c)-driven bicistronic construct for DC-targeted expression of huFcεRIα and eGFP; IRES, internal ribosome entry site.

1.6. Overall aim and concept of this study

Allergic inflammation is a severe disease whose incidence has increased over the last few decades. Allergic asthma is characterized by chronic inflammation of the lung and mucus overproduction. Type 1 allergic reactions consist of an early (EAR) and a late-phase allergic reaction (LAR). During the EAR, crosslinking of IgE/allergen complexes bound to FcεRI on mast cells leads to mast cell activation. This includes the release of preformed, pharmacologically active mediators like histamine and serotonin as well as the production and secretion of mediators like prostaglandins, leukotrienes, cytokines, interleukins and growth factors (7). EARs occur within minutes after allergen exposure but, by definition, are short-lived. In many instances the EAR is followed by a delayed-type inflammatory response, the LAR. Unlike EARs, LARs are characterized by chemokine and cytokine-induced recruitment of leukocytes like DCs, T lymphocytes and eosinophils to sites of allergen exposure (1) resulting in tissue inflammation, mucus production and allergic asthma. Frequent occurrence of severe LARs can cause irreversible fibrotic lung pathology. As a consequence, LARs, even more the EARs, are the main reason of morbidity and mortality in human type 1 allergy (126).

Mechanistically, the EAR and the LAR in humans are clearly independent as e.g. shown by the inability to prevent LAR-associated lung inflammation using drugs that inhibit mast cell secretion or the subsequent effects of their mediators. Despite evident mechanistic dissociation of the mast cell-mediated EAR and the LAR, they both are driven by IgE in humans. This was clearly shown in IgE neutralization studies in asthmatic patients. Thus, cells other than mast cells respond to IgE and are pathophysiologically relevant for the elicitation of human LARs.

Besides its presence on mast cells, FcεRI is also expressed on human antigen-presenting cells such as DCs in various tissues like the lung. FcεRI expressed by DCs amplifies allergen-specific T cell responses in atopy (12). However, the

46

in vivo relevance of FcεRI on DCs in the induction of allergic inflammation in peripheral tissues like the lung remains unknown. This is probably due to the lack of a suitable mouse model to study the role of FcεRI in allergic reactions. Noteworthy, mice express FcεRI on mast cells and basophils but lack the expression on APCs and are thus no suitable animal model to investigate in the in vivo role of FcεRI on APCs. In order to obtain a powerful mouse model to study allergic reactions in the respiratory tract in a fashion relevant for human allergic inflammation, our laboratory has generated transgenic mice that display a "humanized" cellular FcεRI expression pattern. In this α-DC TG mouse line expression of the human FcεRIα is driven by the DC-specific CD11c promoter. This transgenic mouse model is the tool of my study to define the importance of FcεRI for DC function, T cell activation and, subsequently, its contribution to atopic inflammation in the respiratory tract.

2. Materials and Methods

2.1. Culture media

2.1.1. Culture medium for CHO transfectants

10 %	FCS
2 mM	L-glutamine
100 U/ml	penicillin
100 µg/ml	streptomycin

add IMDM ad 500 ml

filter sterile (0.22 µm)

2.1.2. Culture medium for JW8/5/13 cells

2 mM	L-glutamine

add CD Hybridoma Medium ad 1000 ml

2.1.3. Culture medium for proliferation assays

10 %	FCS
2 mM	L-glutamine
100 U/ml	penicillin
100 µg/ml	streptomycin
10 mM	HEPES
1 mM	sodium pyruvate
0.5 mM	β-mercaptoethanol
1 x	non-essential amino acids

add RPMI 1640 ad 500 ml

filter sterile (0.22 µm)

2.1.4. Washing medium

10 %	FCS
2 mM	L-glutamine
100 U/ml	penicillin
100 µg/ml	streptomycin

add RPMI 1640 ad 500 ml

filter sterile (0.22 µm)

2.2. Buffers

2.2.1. Erythrocyte lysis buffer

0.15 M	NH_4Cl	8.29 g
1 mM	$KHCO_3$	1 g
0.1 mM	EDTA	37.2 mg

add ddH_2O ad 800 ml

adjust pH to 7.2 – 7.4 with HCl

add ddH_2O ad 1000 ml

filter, store at RT

2.2.2. MACS buffer

0.5 %	BSA
2 mM	EDTA

add 1x PBS ad 400 ml

adjust pH to 7.2

add 1x PBS ad 500 ml

filter and store at 4°C

2.2.3. Biotinylation buffer

0.1 M	NaHCO$_3$	8.4 g
1 M	NaCl	58.4 g

add ddH$_2$O ad 1000 ml

2.3. Cell lines

Chinese hamster Ovary (CHO) transfectants, coexpressing the human FcεRIα-
and FcεRIγ-chain (CHOαγ) have been previously described (11). CHOαγ were
used to test IgE binding.

JW8/5/13 cells were purchased from ECACC. The hybridoma cell line JW8/5/13
(transfected DNA: mouse VH gene + human C (epsilon) gene) secretes
chimeric IgE anti-NP.

2.4. Propagation of adherent cells

- remove medium
- flush 75 cm^2 culture flask with 10 ml PBS
- add 5 ml of Trypsin/EDTA solution
- incubate at RT until the cells disassociate from the culture flask (careful
  knocking)
- take 500 µl of Trypsin/EDTA- cell suspension
- wash the cells with washing medium
- resuspend cell pellet in 5 ml culture medium
- add 15 ml of culture medium into a new 75 cm^2 culture flask
- add 5 ml of cell suspension

- add 1.28 mg of Geneticin (microbiological potency of 516 µg/ml) /ml medium (selection on stable $\alpha\gamma$-transfectants)
- incubate for 3 – 4 days at 37 °C, 5 % CO_2 and 95 % relative humidity

2.5. Cultivation of JW8/5/13 cells

We used the hybridoma cell line JW8/5/13, to produce chimeric IgEαNP. Cell culture supernatant or purified IgEαNP was used for experimentation.

- culture cells in CD Hybridoma medium supplemented with 2 mM L-glutamine
- change medium every 3 – 4 days
- incubate cells at 37 °C, 5 % CO_2 and 95 % relative humidity

2.6. Biotinylation of proteins

- adjust protein to a concentration of 1 mg/ml
- dialyze against biotinylation buffer ON at 4 °C
- solve biotin-X-NHS in DMF (10 mg/ml)
- add 10 µl of biotin-X-NHS in DMF to 1 ml antibody drop by drop
- rotate 3 h at RT
- dialyze against PBS ON at 4 °C

2.7. Mice

Male and female C57BL/6, BALB/c, OT-II and DO11.10 mice were obtained from the Jackson Laboratory. IgE$^{-/-}$ mice were a gift from H.C. Oettgen. Generation of the α-DC TG mice was created in our laboratory. Under the control of the constitutively active CD11c promoter, mice express the IgE binding human FcεRIα-chain and eGFP (Fig. 1.14). Southern Blot analysis of DNA isolated from mouse tails shows presence of huFcεRIα-DNA sequence in α-DC TG mice but not in wildtype (WT) littermate controls (Fig 2.1). The transgenic strain was bred on both BALB/c and C57BL/6 backgrounds. α-DC TG mice were crossed into the IgE$^{-/-}$ BALB/c background. Mice were genotyped by PCR amplification of mouse tail DNA. All mice were housed under specific pathogen-free conditions.

tg PCR +   -
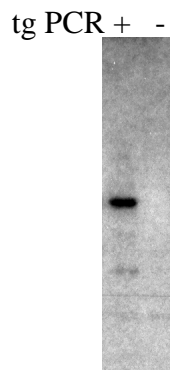
Fig. 2.1. Southern blot analysis of DNA extracted from α-DC TG (left lane) and WT mice (right lane). Existence of transgenic DNA was verified using α32P dATP-labelled hybridization probe.

2.8. Immunization and lung challenge

Mice were immunized with 100 µg Ovalbumin (Ova) dissolved in PBS intraperitoneally four times in one week intervals. Control mice were injected with PBS alone.

Allergic asthma was induced after immunization by aerosol challenge with 4 % (w/v) Ova one week after the last i.p. immunization on two successive days. Three days later, mice were sacrificed.
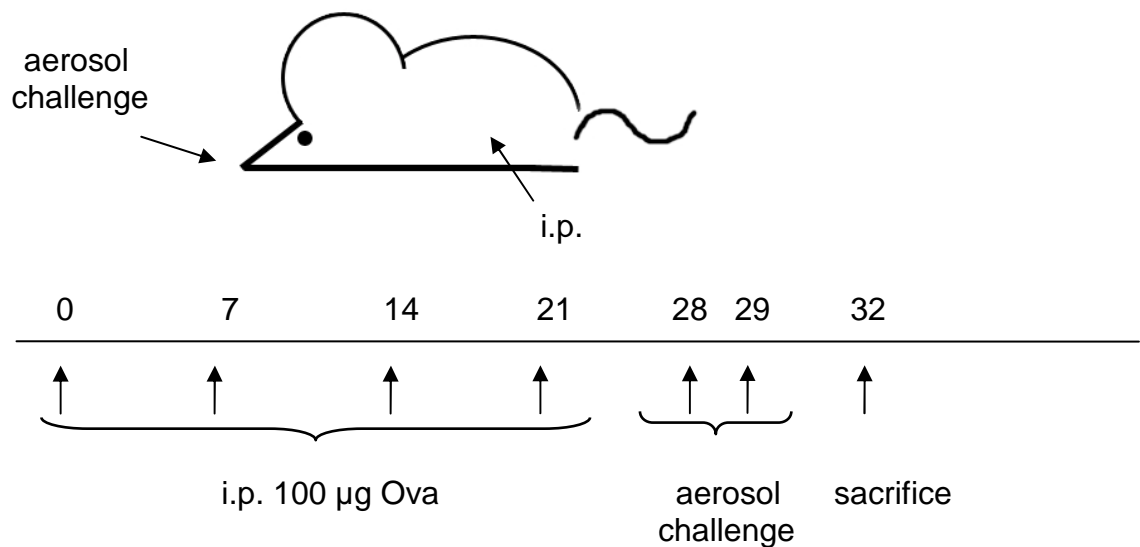
Fig. 2.2. Immunization scheme of mice.

2.9. Collection of blood samples

2.9.1. Collection of blood samples by tail bleeding

- warm the mouse by using infrared heat lamp
- place the mouse on the top of the cage

- hold the tail loosely above the collection tube

- carve the vein using a scalpel

- collect blood as long as drops appear

- using sterile kitchen roll swab the wound and apply pressure to stop bleeding

- allow clotting of blood for 3 h at RT

- centrifuge for 10 min at 3,500 rpm

- remove serum

- use it immediately for analyzes or store at -20 ℃

2.9.2. Collection of blood samples by cardiac puncture

When the subsequent experimental procedure permitted cardiac puncture (terminal method, not useful if the peritoneum needs to be lavaged), we used this method to collect large blood samples.

- anesthetize mouse
- lay the mouse on the back
- take a syringe and penetrate the sternum into the heart
- if blood does not emerge, try a different angle
- gently pull back the plunger and collect blood sample
- allow clotting of blood for 3 h at RT
- centrifuge for 10 min at 3,500 rpm
- remove serum
- use it immediately for analyzes or store at -20 ℃

2.10. Determination of ovalbumin-specific mouse IgE

The quantification of Ovalbumin specific mouse IgE was carried out by using Mouse Ovalbumin specific IgE ELISA ASSAY KIT (Serotec) according to the manufacturer's protocol. We used BioTek ELx50 microplate washer to wash the ELISA plates. An ELISA reader (BenderMedSystems) was used to measure the absorbance at 450 nm (reference wavelength: 620 or 630 nm). Preparation of standard curve and reading of IgE concentration in the samples was performed by ELISA reader using point to point curve fit method (lin/lin).

- keep reagents to RT
- dilute wash buffer concentrate 10-fold with purified water
- add 500 µl of purified water to standard A-F and let stand for 15 min
- decant the contents of each well used
- dispense 150 µl buffer into microplate for pre-dispensing samples
- dispense 15 µl of sample or standard solution into this mircoplate
- keep the plate 10 min at RT
- dispense 110 µl of the diluted sample or standard into the pre-coated wells
- agitate the plate and incubate the plate covered with aluminum foil for 60 min at RT
- wash the plate three times with wash buffer, 300 µl for each well
- add 100 µl of antibody-enzyme conjugate
- agitate the plate and incubate the plate covered with aluminum foil for 30 min at RT
- wash the plate three times with wash buffer, 300 µl for each well
- add 100 µl of substrate
- agitate the plate and incubate the plate covered with aluminum foil for 30 min at RT
- add 100 µl of stop solution

- measure the absorbance at 450 nm (reference wavelength: 620 or 630 nm)
- preparation of standard curve and reading of IgE concentration in the samples was performed

2.11. Adoptive Transfer of CFSE-labelled T cells

To study in vivo T cell responses in mice, we performed adoptive transfer of CFSE-labelled T cells. T cells were purified as described under "Isolation of CD4$^+$ T cells" and labelled with CFSE as described under point 2.13.

- wash cells twice with PBS and resuspend the cell pellet in PBS (5 x 10^6 CFSE-labelled T cells / 200 µl / mouse)
- put the mouse in an animal restraint which allow tail exposure
- warm mouse tail in hand-hot water for 3-5 min
- allow T cell solution to warm to RT
- prepare syringe with a 30 gauge needle
- draw up the T cell solution
- insert the needle into the tail vein
- dispense 200 µl (5 x 10^6 CFSE-labelled T cells) into the vein
- return the mouse into the cage

2.12. Preparation of animals

Mice were killed by cervical dislocation. Before peritoneal wall incision, the abdomen was disinfected with 70 % ethanol. All organs were removed under sterile conditions.

2.12.1. Removal of spleen

2.12.1.1.   Dissection of the spleen only

- place the mouse on its right side
- cut the skin and the muscle layer above the spleen and liver
- hold the spleen with a forceps
- remove the spleen from attached organs
- place the spleen in a PBS-containing tube

Fig. 2.3. Removal of the spleen.

2.12.1.2. Dissection of the spleen if further organs are needed

- fix the mouse
- cut the skin and the muscle layer along the median axis
- the spleen is located on the left side of the mouse, next to the left lobe of the liver
- take the spleen with a forceps
- remove the spleen from attached organs
- place the spleen in a PBS-containing tube
- proceed to the dissection of further needed organs
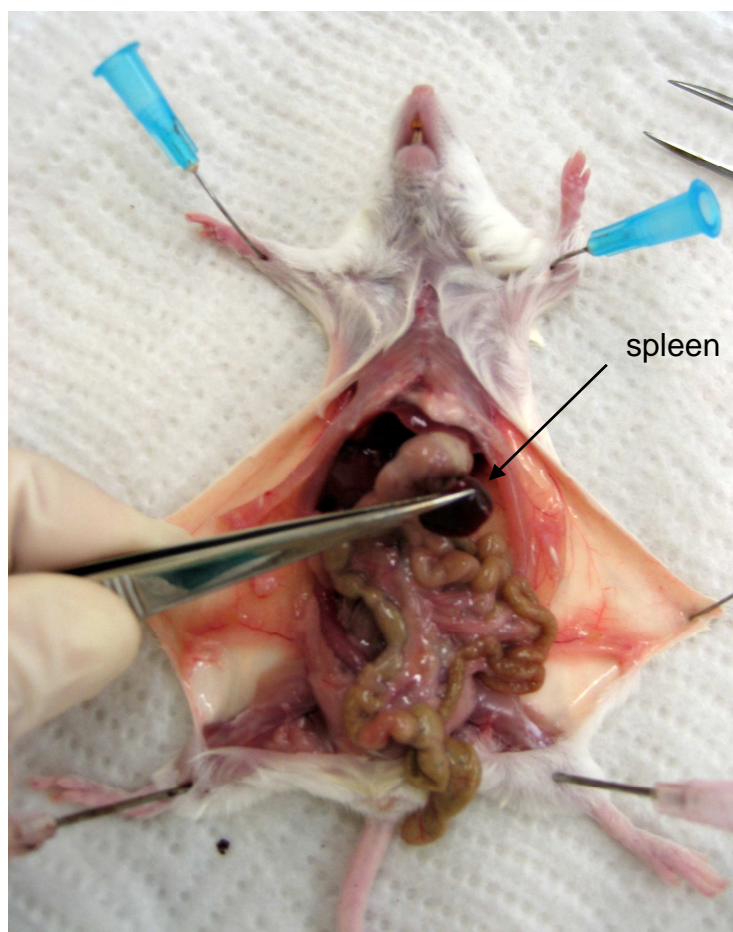
Fig. 2.4. Removal of the spleen if you need further organs.

2.12.2. Removal of mesenteric and inguinal lymph nodes

- fix the mouse
- cut the skin and the muscle layer along the median axis
- identify inguinal lymph nodes
- take the lymph nodes with a forceps
- pull the lymph node out of the attached tissue
- place the lymph nodes in a PBS-containing tube
- take the blind gut and place it to the right side next to the foot
- take the intestinal loops and place them to the right side
- identify mesenteric lymph nodes
- take the lymph nodes with a forceps
- pull the lymph node out of the attached tissue
- place the lymph nodes in a PBS-containing tube
- as control: lymph nodes go down in contrast to fat tissue

a   **b**
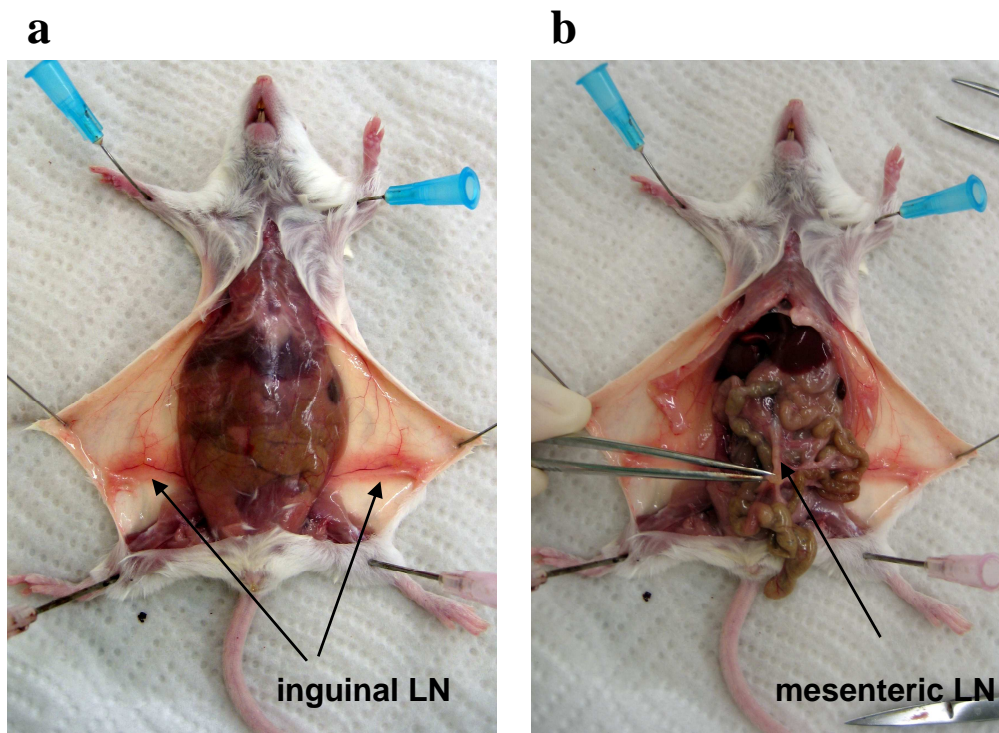
Fig. 2.5. Removal of lymph nodes. (a) Removal of inguinal lymph nodes. (b) Removal of mesenteric lymph nodes.

2.12.3. Removal of lung

- open the rib cage
- remove the whole thoracic organs by intersecting the esophagus, vena cava and thoracic aorta
- hold the lung with a forceps
- cut the attachment under the lung towards the neck
- remove the whole thoracic organs
- remove the lung from the remaining organs
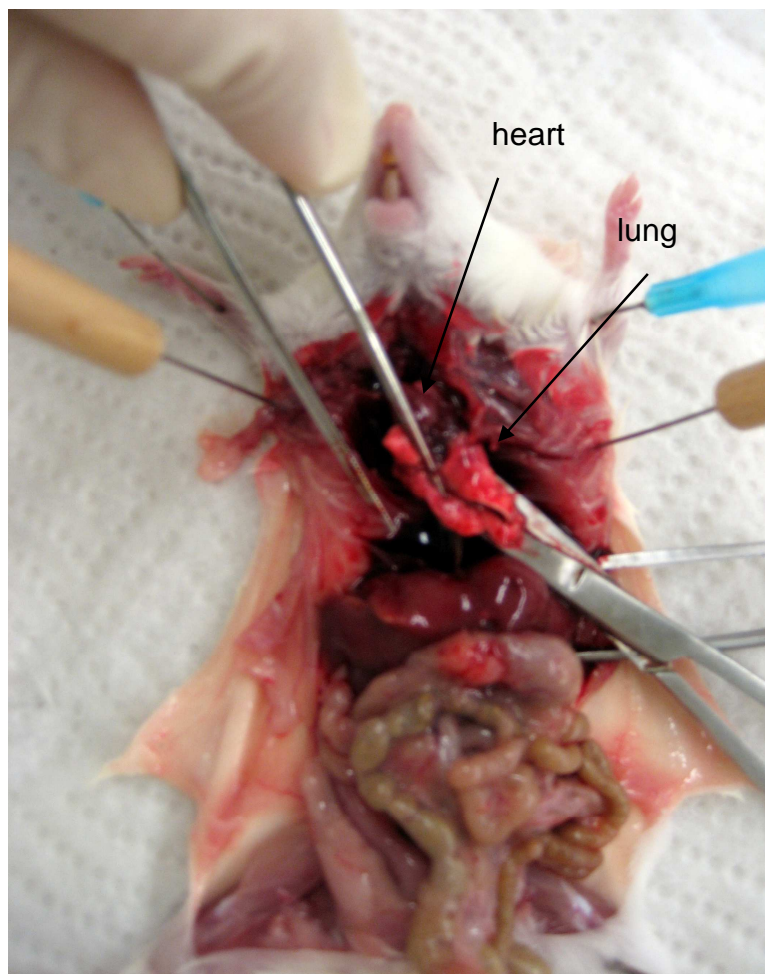
Fig. 2.6. Removal of the lung.

2.12.4. Removal of the intestine

- fix the mouse
- cut the skin and the muscle layer along the median axis
- take the intestinal loops and cut the intestine directly below the stomach and above the rectum
- the blind gut is located between the small intestine and the ascending colon
- free the intestines from any fatty tissue
- defecate the intestine
- flush the intestine with PBS carefully using a syringe

2.12.5. Removal of the liver

- fix the mouse
- cut the skin and the muscle layer along the median axis
- the liver is located below the sternum
- take the liver with a forceps
- remove the liver from attached organs
- place the liver in a PBS-containing tube

2.12.6. Removal of the kidneys

- fix the mouse
- cut the skin and the muscle layer along the median axis
- the kidneys is located on the dorsal wall of the abdominal cavity
- take the kidneys with a forceps carefully (don't damage!)

- remove the kidney
- place the kidneys in a PBS-containing tube

2.12.7. Removal of the brain

- cut off the head
- remove excess tissue using a forceps until you be able to see the cerebellum
- cut the skullcap sagittal using a scissor
- remove the skullcap by breaking off small pieces with a forceps
- avoid injuring to the brain
- turn the head upside down
- carefully remove structures anchoring the brain
- take off the brain
- place the brain in a PBS-containing tube

2.13. Cell preparation

2.13.1. Splenic single cell suspension

- place isolated spleens in a well of a 6-well plate with 5 ml collagenase D (1 mg/ml, Roche Applied Science)
- flush the spleen with collagenase D using a 1 ml syringe
- cut the tissue in small pieces
- incubate for 40 min at 37 ℃
- apply the whole material on a 40 µm pore-size cell strainer placed on a 50 ml tube
- squeeze the whole material through the cell strainer by gentle agitation with the top part of the pestle of a small syringe
- flush the strainer frequently during this process with chilled washing medium
- wash cells with chilled PBS
- resuspend the cell pellet in 5 ml erythrocyte lysis buffer
- incubate for 5 min at RT
- stop the lysis by addition of approximately 30 ml washing medium
- wash cells with chilled PBS
- resuspend the cell pellet in PBS or appropriate medium depending on further procedure

2.13.2. Lymph node and lung single cell suspension

- place isolated lymph nodes or lung on a 40 µm pore-size cell strainer placed on a 50 ml tube

- squeeze the lymph nodes / tissue through the cell strainer by gentle agitation with the top part of the pestle of a small syringe
- flush the strainer frequently during this process with chilled washing medium
- wash cells with chilled PBS
- resuspend the cell pellet in PBS or appropriate medium depending on further procedure

2.14. Immunomagnetic cell purification

2.14.1. General materials

MS, LS, and CS separation columns, magnetic separator (all from Miltenyi Biotec)

2.14.2. Isolation of CD11c$^+$ cells

2.14.2.1. Isolation of splenic CD11c$^+$ cells

- wash spleen cells twice with chilled PBS
- resuspend the cell pellet in MACS buffer (400 µl / 10^8 cells)
- add 100 µl of CD11c MicroBeads per 10^8 total cells
- mix well and incubate for 15 min at 4 – 8°C
- wash cells with 30 ml MACS buffer
- resuspend the cell pellet in 500 µl MACS buffer per 10^8 cells
- choose column size depending on the cell number

- place the column in the magnetic separator
- rinse the column with MACS buffer (volume depending on the column size)
- apply cells onto the column
- flush the column thrice with the appropriate amount of MACS buffer (depending on the column size)
- remove column from the separator
- place the column on a 14 ml polypropylene tube (Falcon)
- apply 4 ml washing medium onto the column
- flush out fraction with the magnetically labelled cells by applying the plunger supplied with the column
- wash the cells
- resuspend 2×10^5 cells in 100 µl PBS
- preincubate the cells with rat and hamster serum for at least 15 min on ice
- add PE-labelled hamster anti-mouse CD11c and PE-Cy5.5-labelled rat anti-mouse CD19 (5 µg/ml each)
- mix well and incubate for 30 min on ice
- wash cells twice
- sort cells for CD11c$^+$ and CD19$^-$

2.14.2.2. Isolation of CD11c$^+$ lung cells

- wash the cells
- resuspend 2×10^5 cells in 100 µl PBS
- preincubate the cells with rat and hamster serum for at least 15 min on ice
- add APC-Alexa Fluor 750-labelled hamster anti-mouse CD11c (5 µg/ml) and APC-labelled rat anti-mouse CD45 (1 µg/ml)
- mix well and incubate for 30 min on ice

- wash cells twice
- sort cells for CD11c$^+$ and CD45$^+$

2.14.3. Isolation of CD4$^+$ T cells

- wash spleen cells twice with chilled PBS
- resuspend cell pellet in chilled PBS (30 x 10^6 /ml)
- label cells by addition of biotinylated mAbs: anti-CD11c, anti-CD19, anti-B220, anti-GR-1, anti-TER, anti-CD11b, anti-CD8 and anti-NK-1.1 (2 µg/ml each)
- mix well and incubate for 30 min on ice
- wash cells twice with chilled PBS
- resuspend the cell pellet in 80 µl MACS buffer per 10^7 cells
- add 20 µl of MACS anti-Biotin MicroBeads per 10^7 cells
- mix well and incubate for 15 min at 4 – 8°C
- wash cells with 30 ml MACS buffer
- choose column size depending on the cell number
- prepare the column following the instructions of the manufacturer
- apply cells onto the column and collect non-retained cells
- flush the column thrice with the appropriate amount of MACS buffer (depending on the column size)
- wash the cells

2.15. Flow cytometry analysis

Three-color FACS-analysis was performed on a FACScan, six-color analysis on a FACSAria (Both from BD Biosciences, San Jose, CA). Antibodies were used at the concentrations indicated by the manufacturers. If directly labelled antibodies

were used, non-specific binding of antibodies was prevented by blocking with 10% rat serum and/or with 10% hamster serum depending on the host species used for antibody production.

2.15.1. General protocol of direct labelling

- wash cells twice in chilled PBS
- resuspend 2×10^5 cells in 100 µl PBS
- preincubate the cells with animal serum for 15 min on ice
- add fluorochrome-conjugated mAbs at the concentration indicated by the manufacturer
- mix well and incubate for 30 min on ice
- wash cells twice
- resuspend cells in 100 µl PBS
- analyze cell on a flow cytometer

2.15.2. General protocol of indirect labelling

- wash cells twice in chilled PBS
- resuspend 2×10^5 cells in 100 µl PBS
- add biotin-conjugated mAbs at the concentration indicated by the manufacturer
- mix well and incubate for 30 min on ice
- wash cells twice
- add appropriate second step antibody at the indicated concentration
- incubate for 25 min on ice
- wash cells twice with PBS
- resuspend cells in 100 µl PBS

- analyze cells on a flow cytometer

2.15.3. Fluorescence-activated cell sorting

Cell sorting was carried out on a FACSAria flow cytometer (BD Biosciences).

- stain cells according to the general protocol of direct / indirect labelling
- wash cells with chilled PBS
- resuspend the cell pellet in washing medium (10×10^6 /ml)
- filter cells through a 40 µm pore-size cell strainer
- sort the cells of interest into polystyrene tubes that have been rinsed with washing medium

2.16. CFSE labelling

- solve CFSE in DMSO at 10 mM
- purify cells of interest, wash twice in cold PBS
- dilute CFSE in PBS to 1 µM for in vitro T cell stimulation and to 5 µM for adoptive transfer of T cells
- resuspend the cell pellet in CFSE solution (1 ml/10^7 cells)
- mix well and incubate for 10 min at RT
- stop labelling by addition of 1 volume FCS
- wash cells twice with PBS supplemented with 10 % FCS
- control CFSE labelling by FACS analysis
- for adoptive transfer wash cells twice with PBS and resuspend the cell pellet in PBS

- for in vitro T cell stimulation wash cells twice with washing medium and resuspend cell pellet in appropriate culture medium

2.17. Stimulation of T cell proliferation

- incubate $3x10^4$ CD11c$^+$ DCs with $6x10^5$ Ova-specific DO11.10 T cells in a total of 200 µl culture medium for proliferation assays in a 96-well round-bottom plate; culture medium for proliferation assays was used for background control. Conditions are tested in triplicates.
- pulse cells with defined concentrations of Ova protein or 4-hydroxy-3-nitrophenylacetyl hapten- (NP-) conjugated Ova protein
- if required, add chimeric IgE anti-NP
- incubate the plates for 72 h at 37 °C and 5 % CO_2 and 95 % relative humidity
- take off 100 µl supernatant for cytokine determination
- add 1 µCi of [*methyl*-^{3}H]thymidine (GE Healthcare) per well
- incubate the plates for 18h at 37 °C and 5 % CO_2 and 95 % relative humidity
- determine ^{3}H-thymidine-uptake using a Wallac 1205 Betaplate Liquid Scintillation counter

2.18. Determination of ^{3}H-thymidine-uptake

- harvest 96-well round-bottom plate using a Harvester 96 Mach II on a pre-wet glass fibre filter according to the manufacturer's protocol
- dry the filter for 45 sec at 600 W in a microwave
- melt-on scintillator sheet on the top of the filter in a sample bag for 1 min using a T-Tray Heatsealer

- measure ^{3}H-thymidine-uptake using a Wallac 1205 Betaplate Liquid
  Scintillation counter according to the manufacturer's protocol

2.19. Cytokine measurement in cell culture supernatants

The quantification of mouse IL-2, IL-4, IL-5, IFN-γ and TNF was carried out by
using the Mouse Th1/Th2 Cytokine CBA (BD Biosciences) according to the
manufactureres protocol. Samples were acquired on a FACScan using BD
CellQuest Software and BD CBA Multiplex Template. Analysis of CBA data was
performed using BD Cytometric Bead Array Analysis.

2.19.1. Preparation of samples

- reconstitute 1 vial of lyophilized Mouse Th1/TH2 Cytokine Standard
  with 0.2 ml of Assay Diluent; allow the standard to equilibrate for at
  least 15 min
- prepare the top standard by addition of 100 µl of 10x bulk standard to
  900 µl assay diluent
- perform a 1:2 serial dilution coming up to a 1:256 dilution
- mix 10 µl of each vortexed capture bead for each assay tube (=
  mixed capture beads)
- add 50 µl of the mixed capture beads to the assay and control tubes
- add 50 µl of the Mouse Th1/Th2 Cytokine Standard dilution to the
  control tubes
- add 50 µl of each sample to the assay tube
- add 50 µl of the Mouse Th1/Th2 PE Detection Reagent to each tube
- mix well
- incubate for 2 h at RT and protect from light

- add 1 ml of Wash Buffer
- centrifuge for 5 min at 1600 rpm
- aspirate the supernatant
- add 300 µl Wash Buffer to each tube and resuspend the pellet
- analyze sample on the flow cytometer

2.19.2. Cytometer setup

BD CBA instrument Setup template was used for cytometer setup

- add 50 µl of Setup Beads to three setup tubes labelled A, B and C
- add 50 µl of FITC Positive Control to tube B
- add 50 µl of PE Positive Control to tube C
- incubate for 45 min and protect from light
- add 450 µl Wash Buffer to tube A and 400 µl of Wash Buffer to tubes B and C
- follow the instructions of BD CBA set up template

2.20. Immunohistochemistry

2.20.1. General Immunohistochemistry

- dissect tissues and mount in OCT
- freeze in liquid nitrogen and store at -20°C
- cut 7 µm sections on a cryomicrotome
- fix sections in acetone for 10 min on ice
- incubate in 2 % BSA / PBS for 10 min

- block with 0.3 % H_2O_2 for 20 min
- block non-specific antibody binding with 2 % mouse serum in 2 % BSA / PBS
- overlay sections with biotinylated primary antibody (anti-huFcεRIα mAb 15-1-biotin or cIgE-biotin) diluted in 2 % BSA / PBS for 1 h at RT
- wash 5 times with PBS
- overlay sections with the detection enzyme (SA-HRP) diluted in 2 % BSA / PBS for 40 min at RT
- wash 5 times with PBS
- cover the sections with AEC substrate chromogen (approximately 2 drops)
- incubate for 5 min at RT
- wash 5 times with PBS
- counter stain with filtered haematoxylin for 10 sec
- wash 5 times with water
- mount in aqueous mounting medium

2.20.2. Immunofluorescence

- dissect tissues and incubate organs 4.5 h in 5 % formalin
- mount in OCT
- freeze in liquid nitrogen and store at -20 °C
- cut 7 µm sections on a cyromicrotom
- wash sections with PBS
- mount in VectaShield Mounting medium
- examine sections using a LSM 520 confocal microscope (Zeiss)
- record fluorescence light emission of 505-550 nm (green) and 560-615 (red)

2.20.3. Scoring of H&E-stained lung sections

Lungs were removed, fixed in buffered formaldehyde and embedded in paraffin. The morphological signs of LAR severity were ascertained by Dr. Antal Rot, Novartis Institutes for BioMedical Research, Vienna under the microscope in 5 µm H&E stained sections.

2.21. Protein quantification

We used BCA Protein Assay Kit (Pierce) to quantify protein concentrations.

- prepare a dilution series of BSA protein (2,000 µg/ml – 25 µg/ml) using the same buffer in which the protein of interest is dissolved
- prepare working reagent: mix 50 parts of BCA reagent A with 1 part of BCA reagent B
- add 100 µl of each standard and unknown sample into a disposable plastic cuvette
- add 2 ml working reagent to each cuvette
- mix well
- incubate for 30 min at 60 °C
- cool all cuvettes to RT
- measure absorbance at 562 nm in a spectrophotometer
- subtract the blank absorbance from sample and standard absorbances
- draw a standard curve by plotting absorbance at 562 nm for each BSA standard versus its concentration in µg/ml
- interpolate the concentration of unknown samples using a linear regression line

2.22. List of reagents

2.22.1. Antibodies

2.22.1.1. Antibodies for immunomagnetic depletion

Specificity	Clone	Conjugate	Manufacturer	Cat#
CD8a	53-6.7	Biotin	eBiosciences	13-0081
CD11b	M1/70	Biotin	BD Biosciences	553309
CD11c	HL3	Biotin	BD Biosciences	553800
CD19	1D3	Biotin	BD Biosciences	553784
B220	RA3-6B2	Biotin	BD Biosciences	553086
Gr-1	RB6-8C5	Biotin	BD Biosciences	553125
NK1.1	PK136	Biotin	eBiosciences	13-5941
TER-119	TER-119	Biotin	BD Biosciences	553672

2.22.1.2. Antibodies for cell characterization

Specificity	Clone	Conjugate	Manufacturer	Cat#
CD3 Molecular Complex	17A2	Purified	BD Biosciences	555273
CD3 Molecular Complex	17A2	PE	BD Biosciences	555275

Specificity	Clone	Conjugate	Manufacturer	Cat#
CD3e	145-2C11	APC	BD Biosciences	553066
CD3e	17A2	APC-Alexa Fluor 750	eBioscience	27-0032
CD4	H129.19	PE-Cy5	BD Biosciences	553654
CD4	L3T4	PerCP	BD Biosciences	553052
CD4	H129.19	PE-Cy5	BD Biosciences	553654
CD8a	53-6.7	PerCP	BD Biosciences	553036
CD8a	53-6.7	APC	BD Biosciences	553035
CD8a	53-6.7	PE-Cy7	eBioscience	25-0081
CD11c	HL3	PE	BD Biosiences	553802
CD11c	HL3	APC	eBioscience	550261
CD11c	N418	APC-Alexa Fluor 750	eBioscience	27-0114
CD11b	3A33	PE-Cy7	Abcam	ab25506
CD19	6D5	PE-Cy5.5	Abcam	ab25548
CD19	6D5	PE-Cy7	Abcam	ab25509
CD40	3/23	PE	BD Biosciences	553791
CD45	30-F11	APC	BD Biosciences	559864
CD80	16-10A1	PE	BD Biosciences	553769
CD86	GL1	PE	BD Biosciences	553692
B220	RA3-6B2	PE	BD Biosciences	553090
B220	RA3-6B2	PerCP	BD Biosciences	553093
DO11.10 TCR	KJI-26	PE	BD Biosciences	551772
F4/80	BM8	PE	eBioscience	12-4801

Specificity	Clone	Conjugate	Manufacturer	Cat#
GR-1	RB6-8C5	PerCP-Cy5.5	BD Biosciences	552093
human FceRIα	Cra1	Purified	eBioscience	16-5899
human FceRIα	Cra1	Biotin	eBioscience	13-5899
human FceRIα	Cra1	PE	eBioscience	12-5899
human FceRIα	Cra1	APC	eBioscience	17-5899
human IgE	B3102E8	Biotin	SouthernBiotech	9160-08
mouse IgE	R35-72	Biotin	BD Biosciences	553414
mouse IgE	23G3	Biotin	SouthernBiotech	1130-08
mPDCA	JF05-1C2.4.1	PE	Milteny Biotec	130-091-962
MHC Class II	M5/114.15.2	PE	BD Biosciences	557000
MHC Class II	M5/114.15.2	PE-Cy5	eBioscience	15-5321

2.22.1.3. Antibodies against chemokine receptors

Specificity	Clone	Conjugate	Manufacturer	Cat#
CCR3	83101	PE	R&D	FAB729P

2.22.1.4. Other antibodies

Specificity	Description	Clone	Conjugate	Manufacturer	Cat#
NP	chimeric human IgE	JW8/1	Purified	Serotec	MCA333B
Ovalbumin	mouse IgE	2C6	Purified	Serotec	MCA2259
Ovalbumin	mouse IgE		Purified	Serotec	PMP68
Ovalbumin	mouse IgE	C38-2	Purified	BD Biosciences	557079

2.22.1.5. Isotype controls

Host species	Isotype	Conjugate	Manufacturer	Cat#
Mouse	IgG1	Purified	Simga-Aldrich	M9269
Mouse	IgG2a	Purified	Simga-Aldrich	M9144
Mouse	IgG2b	Purified	Simga-Aldrich	M8894
Rat	IgG1	PE	BD Biosciences	553925
Rat	IgG1	APC	BD Biosciences	550884
Rat	IgG1	PE-Cy7	BD Biosciences	557645
Rat	IgG2a	PE	BD Biosciences	553930
Rat	IgG2a	PerCP	BD Biosciences	553933
Rat	IgG2a	APC	BD Biosciences	554690
Rat	IgG2a	PE-Cy7	BD Biosciences	552784
Rat	IgG2b	PE	BD Biosciences	553989
Rat	IgG2b	APC	BioLegend	400612

Host species	Isotype	Conjugate	Manufacturer	Cat#
Rat	IgM	PE-Cy7	SouthernBiotech	0120-17
Hamster	IgG1	PE	BD Biosciences	553954
Hamster	IgG1	APC	BD Biosciences	553956
Hamster	IgG1	APC-Alexa Fluor 750	eBiosciences	27-4888

2.22.1.6. Second-step reagents

Reagent	Abbreviation	Conjugate	Manufacturer	Cat#
Streptavidin	SA-PE	PE	BD Biosciences	349023
Streptavidin	SA-APC	APC	BD Biosciences	349024

2.22.2. Peptides and proteins

Protein/Peptide	Abbreviation	Conjugate	Manufacturer	Cat#
Bovine Serum Albumin Grade 5	BSA		Sigma-Aldrich	A2153
Bovine Serum Albumin	NP-BSA	4-Hydroxy-3-nitrophenylacetyl	Biosearch Technologies	N-5050-10
Ovalbumin Grade V	Ova		Sigma-Aldrich	A5503
Ovalbumin Grade V	NP-Ova	4-Hydroxy-3-nitrophenylacetyl	Biosearch Technologies	N-5051-10
SIINFEKL (Ova 257 – 264)	pOva		Anaspec	60193-5

2.22.3. General reagents

Reagent	Abbreviation	Manufacturer	Cat#
4-(2-hydroxyethyl)-1-piperazineethanesulfonic acid	HEPES	GIBCO BRL	15630-049
4-Hydroxy-3-nitrophenylacetyl hapten-PE	NP-PE	Biosearch Technologies	N-5070-1
5(6)-Carboxyfluorescein diacetate N-Succinimidyl ester		Sigma-Aldrich	21888-25MG-F
β-Mercaptoethanol			
Acetone		Merck	8.22251.2500
Aluminum hydroxide	alum	Serva	12261.01
Anti-Biotin MicroBeads		Miltenyi Biotec	130-090-485
Biotin – X – NHS		Calbiochem	203188
CD11c MicroBeads		Miltenyi Biotec	130-052-001
CD Hybridoma Medium		Invitrogen	VX11279023
Collagenase D		Roche	11088866001
Dimethylsulfoxide	DMSO	MERCK	1.09678
Ethanol, 96%	EtOH	Pharmacy, AKH	58601
Foetal calf serum (heat inactivated)	FCS	Invitrogen	10500-064
Formaldehyde 7.5%		SAV Liquid Products	N-29401
Geneticin G-418 Sulphate		GIBCO BRL	11811-023

Reagent	Abbreviation	Manufacturer	Cat#
Goat serum		Sigma-Aldrich	G9023
Hamster serum		Jackson Immuno Research	007-000-120
Human IgE, myeloma		Calbiochem	401152
Ionomycin	Iono	Sigma-Aldrich	I0634
Iscove´s modified Dulbecco´s medium	IMDM	GIBCO BRL	21980-032
L-glutamine		GIBCO BRL	25030-024
Mouse serum		Chemicon	S25-10ml
Non-essential amino acids, 100x	NEA	Biochrom AG	K0293
NaCl		MERCK	106.404
NaOH		MERCK	106.498
O.C.T.		Sakura	4583
ODN 2395	CpG	Alexis Biochemicals	ALX-746-020-T100
Penicilin/streptomycin	PenStrep	GIBCO BRL	15140-114
Phorbol 12-myristate 13-acetate	PMA	Sigma-Aldrich	P8139
Phosphate-buffered saline	PBS	GIBCO BRL	14190-094
Rat IgG		Simga-Aldrich	I4131
Rat serum		PAA	B02037
RPMI 1640		GIBCO BRL	52400-025
Sodium pyruvate, 100x		GIBCO BRL	11360-039
Trypsin-EDTA, 0.05%		GIBCO BRL	25300-054

Reagent	Abbreviation	Manufacturer	Cat#
VectaShield Mounting medium		Vector Labs	H-1000
Water, double distilled	ddH2O	Fresenius Kabi	11500293

2.22.4. Used commercial kits

- BCA Protein Assay Kit, Pierce
    - BCA Reagent A
    - BCA Reagent B
    - Albumin Standard Ampules

- Mouse Ovalbumin specific IgE ELISA ASSAY KIT
    - Standard A (lyophilized)
    - Standard B (lyophilized)
    - Standard C (lyophilized)
    - Standard D (lyophilized)
    - Standard E (lyophilized)
    - Standard F (lyophilized)
    - Buffer
    - Detection conjugate
    - Antibody-coated assay plate
    - Wash buffer concentrate
    - Substrate
    - Stop solution
    - Microplate for predispensing samples

- Mouse Th1/Th2 Cytokine CBA
    - Mouse IL-2 Capture Bead
    - Mouse IL-4 Capture Bead
    - Mouse IL-5 Capture Bead
    - Mouse IFN-γ Capture Bead
    - Mouse TNF Capture Bead
    - Mouse Th1/Th2 PE Detection Reagent
    - Mouse Th1/Th2 Cytokine Standards
    - Cytometer Setup Beads
    - PE Positive Control Detector
    - FITC Positive Control Detector
    - Wash Buffer
    - Assay Diluent

3. Results

3.1. Transgenic mice with FcεRI expression on dendritic cells

Murine DCs, in contrast to human DCs do not express FcεRI constitutively. As described under point 1.5 (α-DC transgenic mice: the tool of my study), our laboratory created α-DC TG mice harboring a germ line-integrated construct expressing the human IgE-binding FcεRIα-chain and eGFP under control of the DC-restricted, constitutively active CD11c promoter (Fig 1.14).

To study FcεRI surface expression and eGFP expression in vitro, HEK cells were transfected either with a mock construct or the construct containing the human α-chain gene and eGFP. We could determine only eGFP expression but no receptor surface expression after vector transfection. However, co-transfection of this construct with a vector harboring the murine FcεRIγ-chain gene – in vivo provided by DCs themselves – revealed green fluorescent transfectants expressing a huαmuγFcεRI receptor on their surface as revealed by murine IgE binding and anti-FcεRIα immunoreactivity (Fig. 3.1).

The fact that in our model huFcεRIα surface expression requires co-expression of the myeloid-restricted murine FcεRIγ (19, Fig. 3.1) contributes to DC-restriction of FcεRIα expression in a transgenic promoter-independent fashion.
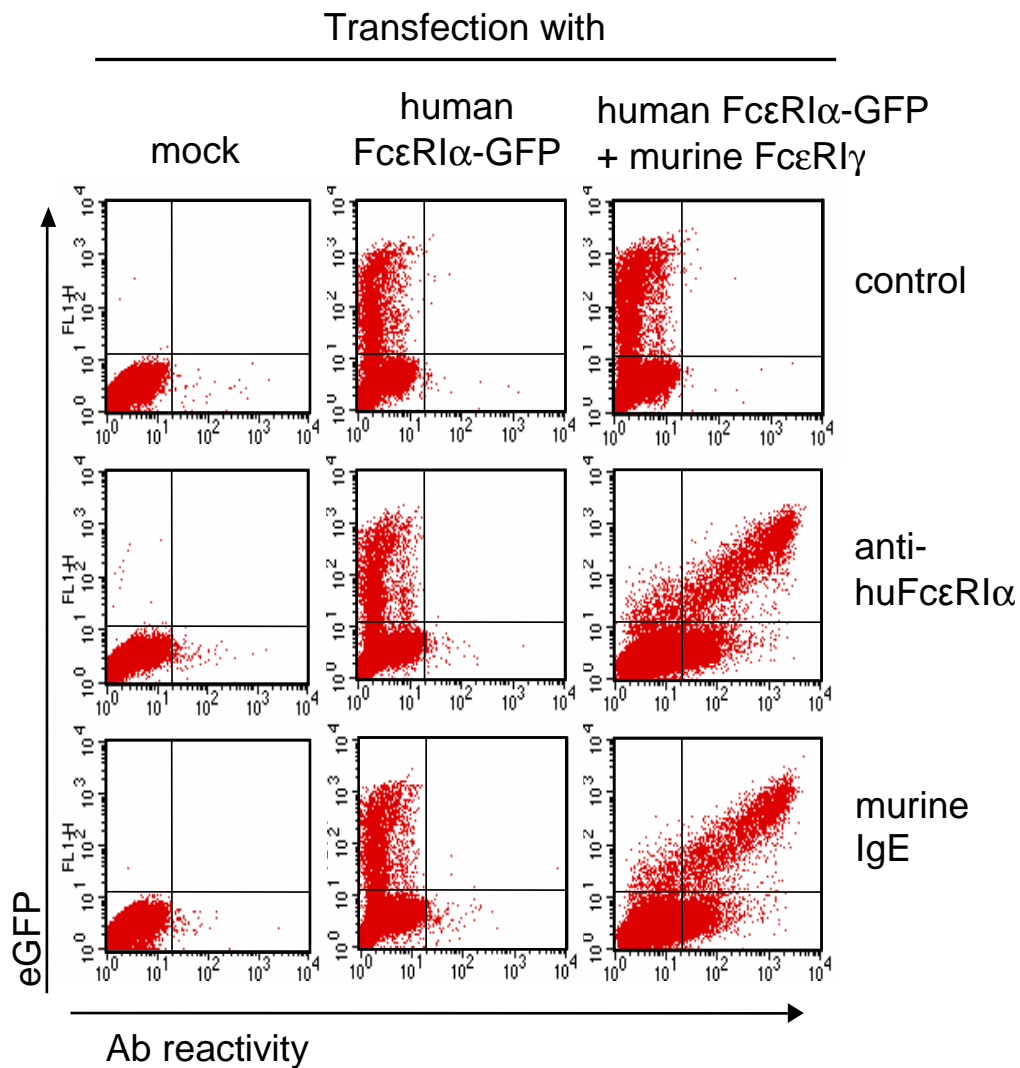
Fig. 3. 1. Murine γ-chain revealed surface expression of huFcεRIα. Facs analysis of mock (left), huFcεRIα (middle) and huFcεRIαmuFcεRIγ transfected HEK 293 T cells. T cells were stained with either control antibody (first panel), 15-1 antibody (anti-FcεRIα; second panel) or bound with murine IgE (last panel).

To analyze DC-restricted transgen expression in various tissues of α-DC TG mice, we measured eGFP expression by FACS analysis. In α-DC TG mice, discrete populations of eGFP-expressing cells were detected in lymphoid (spleen, lymph nodes) and non-lymphoid organs (e.g., lung, intestine, liver; Fig. 3.2). 1.1% (spleen), 0.9% (lymph nodes), 0.1% (lung), 0.02% (intestine), 0.01% (liver), 0.1% (kidney) and 0.0% (brain) of total cells expressed eGFP (Fig. 3.2). eGFP$^+$ cells in the various organs were DCs as shown by their high MHC class

II expression, display of co-stimulatory molecules, and superior T cell stimulatory capacity (Fig. 3.2, 3.3, 3.5). Binding of monomeric IgE to FcεRI-expressed DCs does not alter the expression level of co-stimulatory molecules and antigen presentation capacity (Fig. 3.3, 3.4).
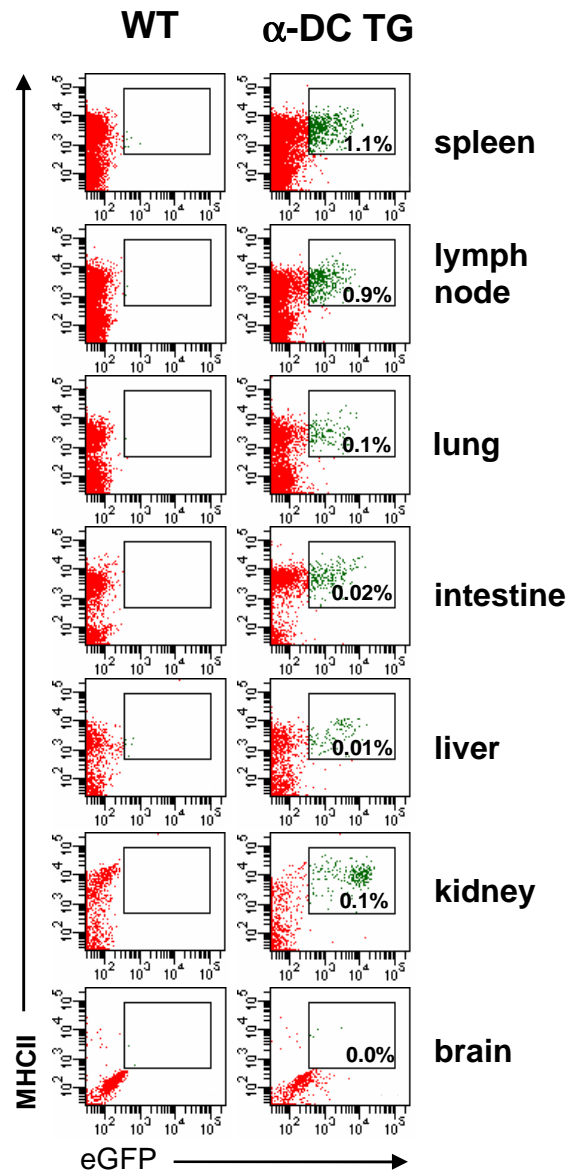

Fig. 3. 2. DCs from lymphoid organs as well as from non-lymphoid organs express human FcεRIα. Multi-organ double immunofluorescence analysis of eGFP (horizontal) and MHC class II expression (vertical) in WT (left panels) and α-DC TG mice (right panels). Cells shown were gated for CD45 expression. Panels (from top panel): spleen, lymph node, lung, intestine, liver, kidney and brain.
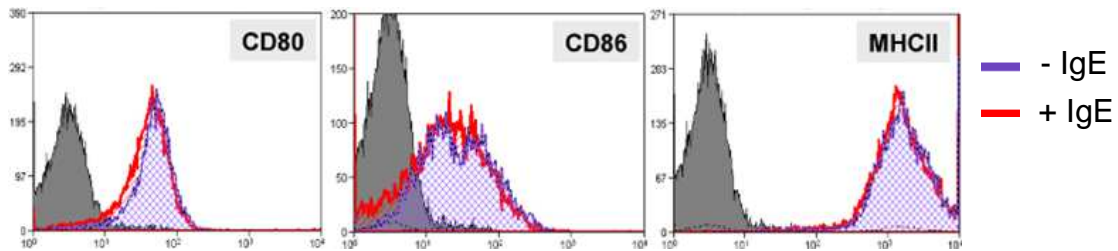
Fig. 3.3. Expression of co-stimulatory molecules on DCs from α-DC TG mice is not altered in the presence of IgE. Demonstration of CD86 (left panel), CD80 (middle panel) and MHC class II expression (right panel) in eGFP$^+$ FcεRIα$^+$ splenocytes. Cells were incubated in the presence (red) or the absence (purple) of IgE. Black histograms denote the reactivity of isotype-matched control mAbs. Experiment was performed in collaboration with E. Fiebiger.
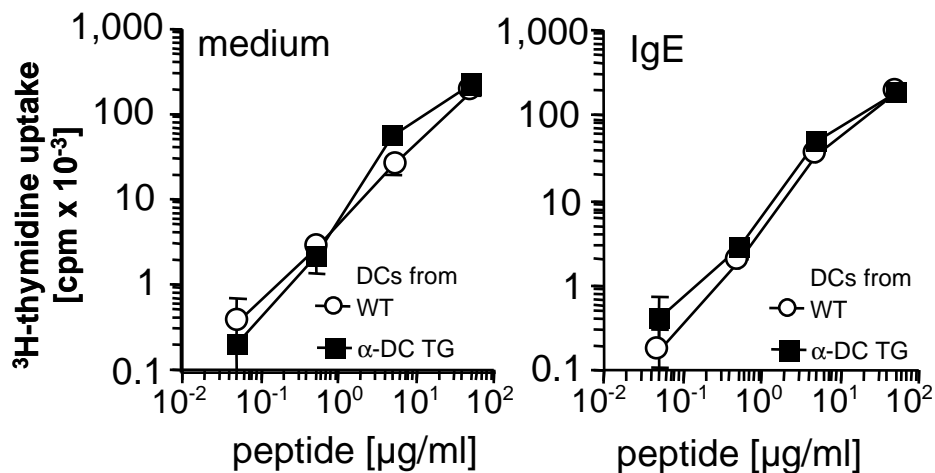

Fig. 3. 4. Binding of monomeric IgE does not alter antigen presentation capacity. DCs isolated from α-DC TG (closed squares) and WT mice (open circles) were cultured with naïve Ova-specific DO11.10 T cells in the presence of graded concentrations of Ova peptide (Ova323-339; ISQAVHAAHAEINEAGR) in absence (left) or presence (right) of antigen-unspecific IgE. ^{3}H-thymidine uptake was measured (mean cpm of triplicate cultures $\pm$ s.e.m.; vertical).
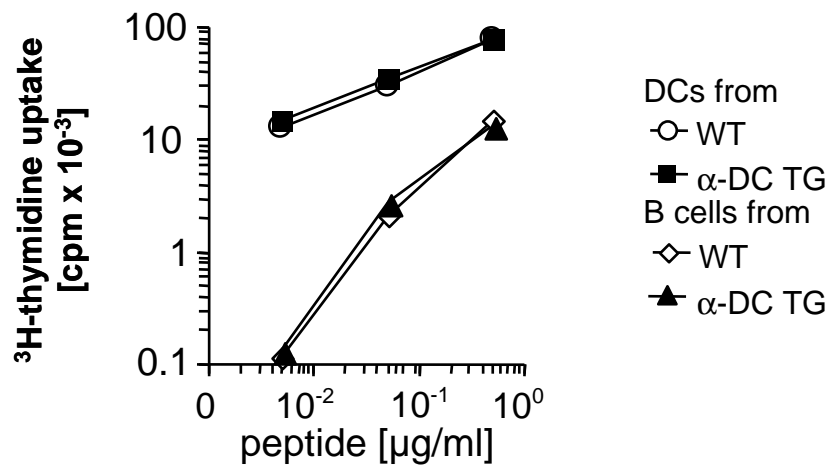
Fig. 3. 5. DCs from α-DC TG mice present exogenously added peptide to T cells at the same efficacy as DCs from WT mice. Sorted splenic CD11c^{+} DCs from α-DC TG (closed squares) and WT mice (open circles) and, for control purposes, CD19^{+} B cells from α-DC TG (closed triangles) and WT mice (open diamonds) were assayed for presentation of a synthetic Ova peptide (Ova323-339; ISQAVHAAHAEINEAGR). ^{3}H-thymidine uptake of Ova-specific T cells (cpm; vertical) in response to graded concentrations of Ova peptide (horizontal) was measured. Mean cpm ($\pm$ s.e.m.) of triplicate cultures are shown.

Gating for splenic CD11c^{+} DCs further revealed that the vast majority of all DCs expressed eGFP (Fig. 3.6, Fig 3.7). FcεRIα-chain surface expression was largely restricted to eGFP^{+} DCs as shown by anti-huFcεRIα immunoreactivity (Fig. 3.6, Fig. 3.7). The vast majority of CD11c^{+} DCs from both C57BL/6 and BALB/c mice expressed eGFP and human FcεRIα at comparable frequencies (Fig. 3.6, Fig. 3.7).

Importantly, DCs from α-DC TG mice bound human as well as murine IgE in cell suspensions and on tissue sections (Fig. 3.8; Fig. 3.9) showing transgenic receptor expression in a functional configuration. Using immunohistochemistry we determined the distribution of transgene-expressing DCs in the spleen. We stained for human FcεRIα-expressing cells and showed that perifollicular IgE-

binding, FcεRIα$^+$ cells are detectable in α-DC TG mice but not in WT littermate controls (Fig. 3.8).

In contrast, isolated and in situ DCs from WT mice did not bind IgE (Fig. 3.8; Fig. 3.9). Cellular characterization showed huFcεRIα expression on DCs but not on other cell types from α-DC TG mice like T cells, B cells, mast cells and basophils (Fig. 3.10, Fig 3.11).

Fig. 3. 6. Demonstration of huFcεRIα and eGFP expression in splenic CD11c$^+$ cells from C57BL/6 mice by flow cytometry. Upper left panel: Gating of DCs from dot plots showing CD11c expression (horizontal) versus 90° light scat tering (SSC, vertical). Upper right panel: anti-huFcεRIα immunoreactivity of CD11c$^+$ cells from WT (gray histogram) and α-DC TG mice (red histogram). Lower panels: dot plots showing eGFP (vertical) versus huFcεRIα expression (horizontal) in CD11c$^+$ cells from WT (left) and α-DC TG mice (right). Experiment was performed in collaboration with E. Fiebiger.
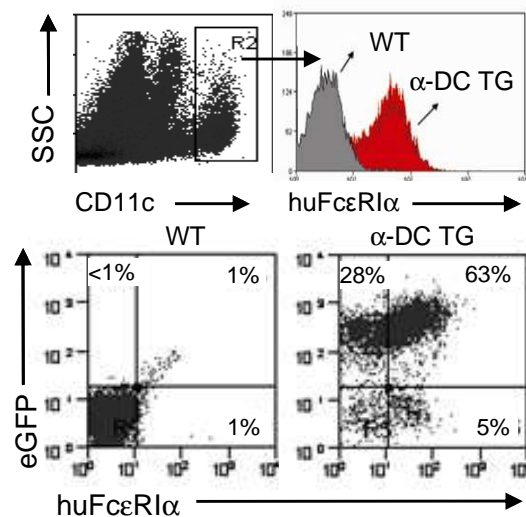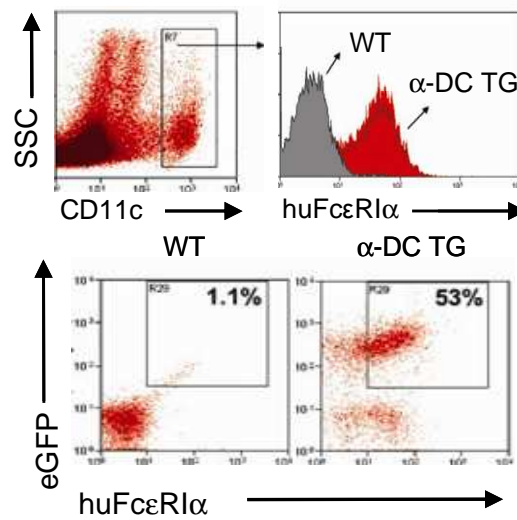
Fig. 3. 7. Demonstration of huFcεRIα and eGFP expression in splenic CD11c⁺ cells from BALB/c mice by flow cytometry. Upper left panel: Gating of DCs from dot plots showing CD11c expression (horizontal) versus 90° light scat tering (SSC, vertical). Upper right panel: anti-huFcεRIα immunoreactivity of CD11c⁺ cells from WT (gray histogram) and α-DC TG mice (red histogram). Lower panels: dot plots showing eGFP (vertical) versus huFcεRIα expression (horizontal) in CD11c⁺ cells from WT (left) and α-DC TG mice (right). Experiment was performed in collaboration with E. Fiebiger.

WT   **α-DC TG**

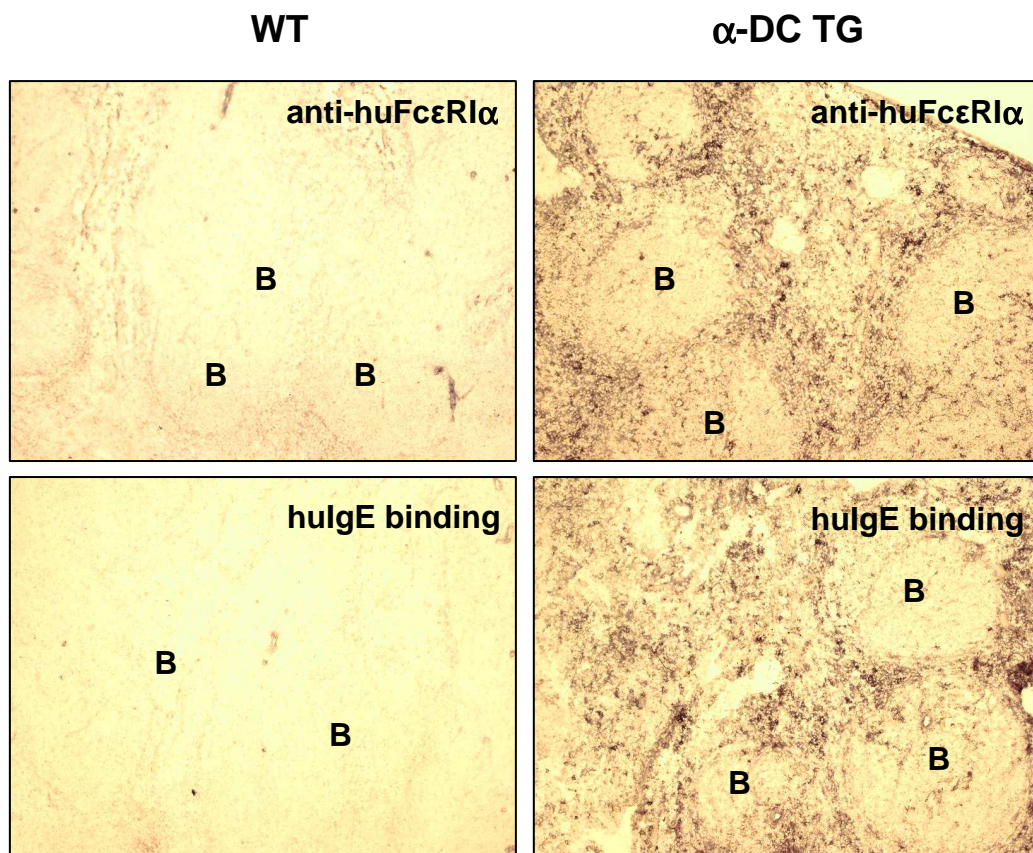**Fig. 3. 8. FcεRI[+] DCs are located in the T cell zones of lymphoid organs.** Detection of huFcεRIα expression (upper panels) and human IgE binding (lower panels) on spleen sections from WT (left) and α-DC TG mice (right). HRP-based visualization of Ab-bound cells reveals huFcεRIα expression and IgE binding to perifollicular cells with dendritic morphology (insets, right panels); B, B cell follicle.
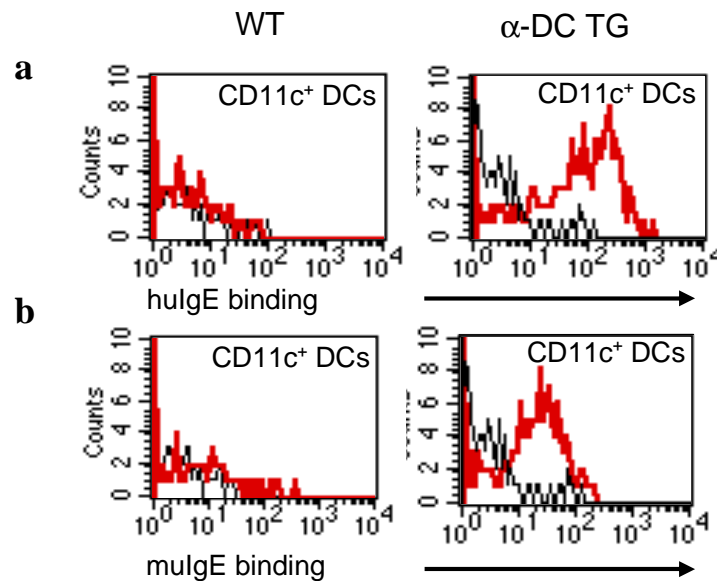
Fig. 3. 9. Transgenic CD11c^{+} DCs have the capability to bind human and murine IgE.
Detection of human (upper panels) and murine IgE (lower panels) binding to isolated DCs from
α-DC TG and WT mice (right and left panels, respectively) by anti-human and anti-murine IgE
mAbs and flow cytometry (red histograms). Black histograms denote the reactivity of isotype-
matched control mAbs.

Fig. 3. 10. CD11c^{+} DCs but not B cells or T cells from α-DC TG mice express FcεRIα.
Analysis of huFcεRIα expression in splenic DCs (left), B cells (middle) and T cells (right) of α-
DC TG mice. Lines in histograms denote the upper limit of the reactivity of isotype-matched
control mAbs.
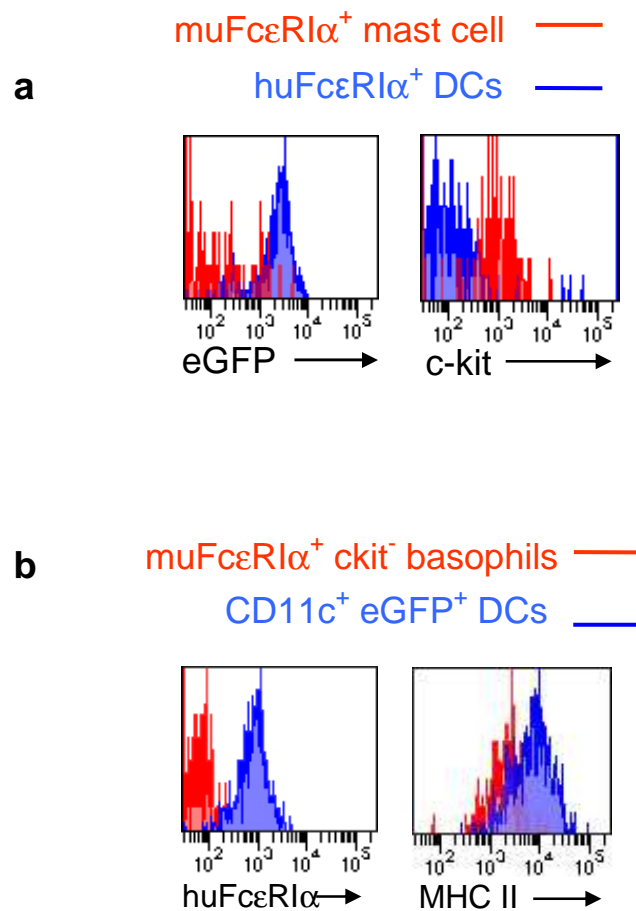
Fig. 3. 11. Mast cells and basophils do not express human FcεRIα. (a) Analysis of eGFP (left) and c-kit expression (right) in muFcεRIα$^+$ mast cells (red) and huFcεRIα$^+$ DCs (blue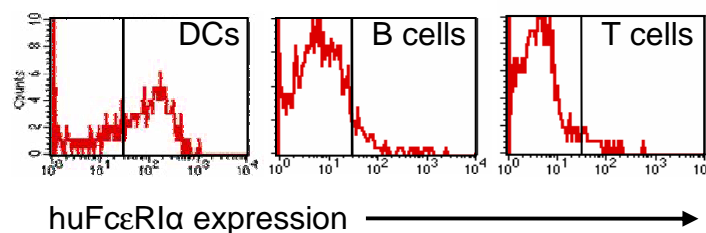) by flow cytometry. (b) Analysis of huFcεRIα (left) and MHC class II expression (right) in muFcεRIα$^+$c-kit$^-$ basophils (red) and CD11c$^+$eGFP$^+$ DCs (blue) by flow cytometry.

FcεRI on human DCs is expressed as αγ2 trimer (12). To glean information on the structural composition of FcεRI expressed on murine transgenic DCs, FcεRI receptors were immunoprecipitated. In DCs, FcεRI was assembled as a trimeric complex containing a huFcεRIα-chain (approx. 50 kDa) and a muFcεRIγ dimer (approx. 20 kDa, Fig. 3.12) and lacked FcεRIβ (data not shown). Control precipitates (without initial IgE binding) displayed no reactivity with either anti-human α-chain or anti-murine γ-chain antibody. Thus, chimeric FcεRI on DCs of TG mice has the same molecular subunit composition as FcεRI on human DCs (12).
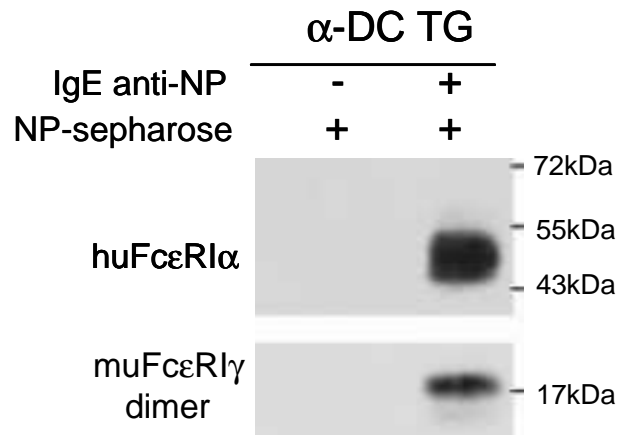
Fig. 3. 12. Immunoprecipitation of FcεRI complexes composed of huFcεRIα and muFcεRIγ from DCs. NP-sepharose precipitates from IgE anti-NP-loaded (right lanes) and unloaded α-DC TG DCs (left lanes) were analyzed by anti-huFcεRIα (upper panel) and anti-muFcεRIγ immunoblotting (lower panel). The co-precipitated 18 kDa moiety in the lower panel corresponds to dimers of muFcεRIγ. Experiment was performed in collaboration with E. Fiebiger

In a next set of experiments, we studied the huFcεRIα expression pattern on different DC subtypes including myeloid (CD4$^+$ CD11c$^+$), lymphoid (CD8$^+$ CD11c$^+$) and plasmacytoid DCs (B220$^+$, CD19$^-$, CD11c^{low}, mPDCA-1$^+$). In analogy to their CD11c expression level, myeloid DCs from α-DC TG mice expressed the highest level of huFcεRIα (Fig. 3.13a) while lymphoid and plasmacytoid DCs were rather devoid of huFcεRIα expression (Fig. 3.13b), a pattern that matches FcεRI expression on DC subsets in humans (123). Myeloid, lymphoid and plasmacytoid DCs from wild-type controls showed no huFcεRIα immunoreactivity or IgE-binding ability (Fig. 3.13).
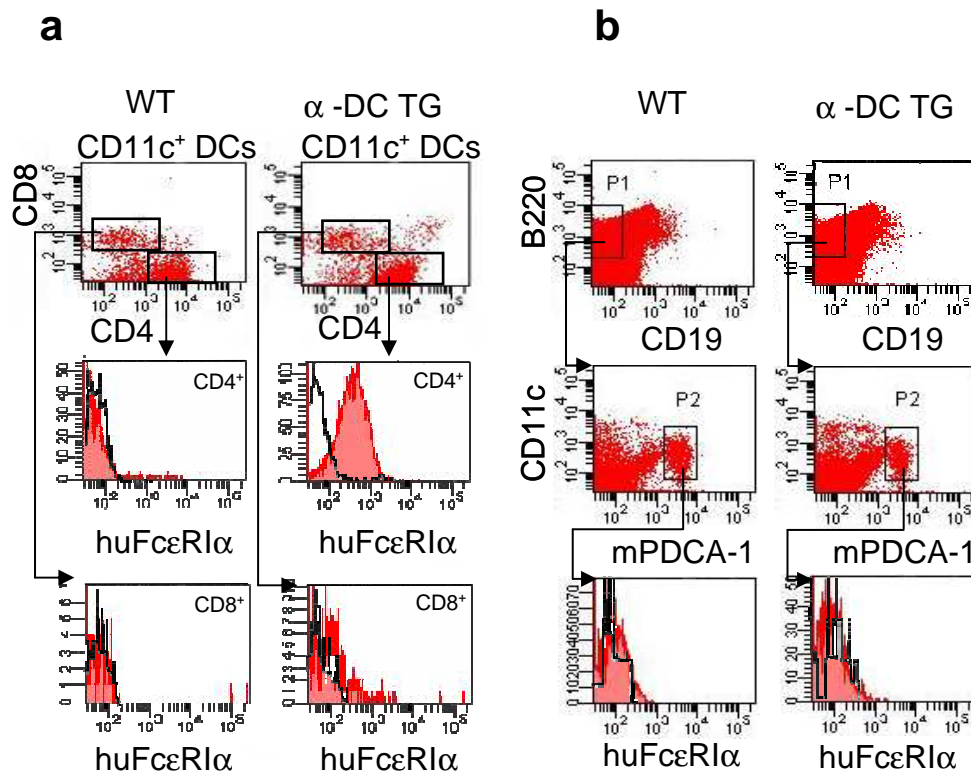
Fig. 3. 13. FcεRI expression on different α-DC subtypes. **(a) CD4⁺ CD11c⁺ myeloid DCs from α-DC TG mice express FcεRI.** Demonstration of huFcεRIα expression of subtypes of splenic CD11c⁺ cells from α-DC TG and WT mice (right and left panels, respectively) by flow cytometry. Top panels: dot plots showing CD4 (horizontal) versus CD8 expression (vertical). Middle panels: anti-huFcεRIα immunoreactivity of CD4⁺CD11c⁺ cells (red histograms). Bottom panels: anti-huFcεRIα immunoreactivity of CD8⁺CD11c⁺ cells (red histograms). Black histograms denote the reactivity of isotype-matched control mAbs. **(b) Plasmacytoid DCs from α-DC TG mice do not express the high affinity IgE receptor.** Analysis of huFcεRIα expression in splenic pDCs from α-DC TG and WT mice (right and left panels, respectively) by flow cytometry. Top panels: dot plots showing CD19 (horizontal) versus B220 expression (vertical). Middle panels: gated B220⁺CD19⁻ cells (P1) were analyzed for mPDCA-1 (horizontal) versus CD11c expression (vertical). Lower panels: anti-huFcεRIα immunoreactivity of B220⁺CD19⁻CD11c^low and mPDCA-1⁺ cells (red). Black histograms denote the reactivity of isotype-matched control mAbs.

Next, we asked wether DC-expressed FcεRI is functional. To address this, we tested whether DCs from α-DC TG mice are capable of FcεRI-dependent antigen uptake.

Comparing fluid phase and FcεRI-dependent antigen uptake, we showed that DCs from α-DC TG mice, but not DCs from WT mice, internalized full protein antigens in an IgE-dependent fashion (Fig. 3.14). Fluid phase antigen uptake, in contrast, was identical in DCs from α-DC TG and WT mice (Fig. 3.14).
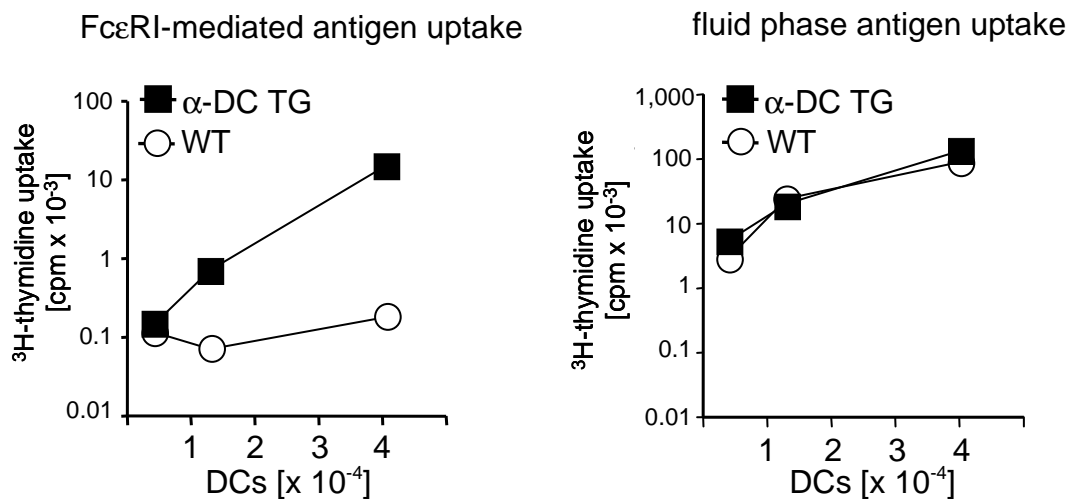
Fig. 3. 14. FcεRI and IgE-mediated antigen uptake in DCs. DCs from α-DC TG (closed squares) and WT mice (open circles) were loaded with NP-Ova under conditions permitting FcεRI-mediated (left panel) or fluid phase antigen uptake (right panel). ^{3}H-thymidine uptake of Ova-specific T cells (cpm; vertical) was used to measure uptake and presentation of NP-OVA by graded numbers of DCs (horizontal). For FcεRI-mediated antigen uptake CD11c^{+} DCs were loaded with IgE anti-NP ON before incubation with 1 mg NP-Ova /10[6] cells for 1 h on ice. DCs were washed three times and allowed to internalize and process IgE-bound antigen for 2 h at 37℃. For fluid-phase antigen uptake, CD11c^{+} DCs were pulsed with NP-OVA for 2 h at 37℃. Experiment was performed in collaboration with E. Fiebiger.

To conclude, α-DC TG mice display a "human-like" expression pattern of functional FcεRI on their DCs and are therefore a unique model to study the functional role of DC-expressed FcεRI in vivo.

3.2. DCs use FcεRI and antigen-specific IgE to augment antigen-specific T cell responses in vivo

The FcεRI-mediated IgE binding to DCs was studied in vivo in naïve mice and mice immunized with Ova under conditions promoting antigen-specific IgE responses. DCs from WT mice displayed no surface-bound IgE irrespective of whether the mice were immunized or were not immunized with Ova (Fig. 3.15) showing that endogenous IgE receptors are not up-regulated on WT DCs during a Th2-dominated immune response. B cells from WT mice had bound some IgE under non-immunized and, more so, under immunized conditions (Fig. 3.15) indicating that B cells are the major IgE binding APCs in normal WT mice. In contrast, DCs from α-DC TG mice showed in vivo IgE binding under baseline conditions and further 5-10-fold increased levels of surface-bound IgE following immunization (Fig. 3.15). In vivo IgE binding to DCs was at least one order of magnitude higher than IgE binding to B cells in α-DC TG mice. Thus, DCs are the essential IgE binding APCs in α-DC TG mice what corresponds to the situation in allergic humans (128).

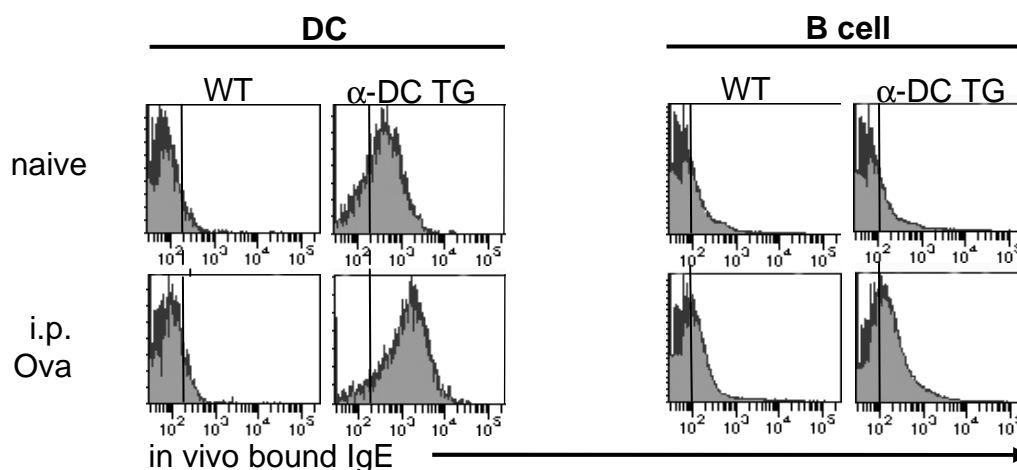**Fig. 3. 15. FcεRI-expressing DCs bind the highest amounts of IgE in vivo.** Detection of IgE bound to DCs (left panels) and B cells (right panesl) from i.p. Ova-immunized (lower panels) and non-immunized (upper panels) WT and α-DC TG mice (left and right panels, respectively) by anti-murine IgE mAbs and flow cytometry. Vertical lines in histograms denote the upper cut-off of the reactivity of isotype-matched control mAbs.

To study a potential impact of the IgE-FcεRI interaction on DCs for antigen-specific T cell activation in vivo, α-DC TG and WT mice were immunized repeatedly. The spleen cells recovered were restimulated with Ova in vitro and the T cell proliferation was measured by ^{3}H-thymidine uptake. As shown in Fig. 3.16, antigen-specific splenocytes proliferation was enhanced in Ova-immunized α-DC TG mice as compared to WT controls.
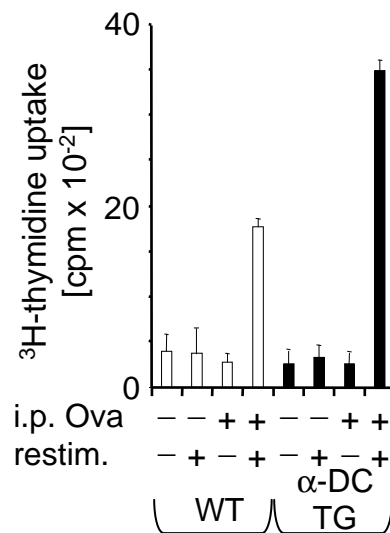
Fig. 3. 16. Augmented antigen-specific splenocyte proliferation in α-DC TG mice. Splenocytes from naïve and Ova-immunized α-DC TG (black bars) and WT mice (white bars) were cultured in the presence or absence of Ova (20 µg/ml) and ^{3}H-thymidine uptake was measured (mean cpm of triplicate cultures + s.e.m.; vertical).

Next we asked if the IgE-bound DCs are the stimulatory principle of this enhanced T cell response.

α-DC TG mice and WT littermate controls were immunized with Ova. Spleens were harvested and CD11c$^+$ cells were FACS-purified. These DCs were used as stimulators of Ova-primed T cells. We show that IgE-bearing DCs from α-DC TG were far more potent stimulators of Ova-specific recall T cell activation than were IgE$^-$ DCs from WT controls (Fig. 3.17a). Moreover, a 50-fold lower antigen concentration was required to initiate T cell proliferation with IgE$^+$ DCs from α-

DC TG than with IgE⁻ DCs from WT mice. This indicates a functionally relevant lower antigen threshold necessary for T cell activation in α-DC TG mice.

Next, IgE-bearing DCs from α-DC TG were used as stimulators of T cells which had been purified from Ova-immunized α-DC TG and WT mice. As shown in Fig. 3.17b, the Ova-specific proliferation of T cells from α-DC TG mice was higher than the proliferation of T cells from WT mice. Thus, the Ova-specific memory T cell response established in vivo is greater in α-DC TG than in WT mice.

a   **b**
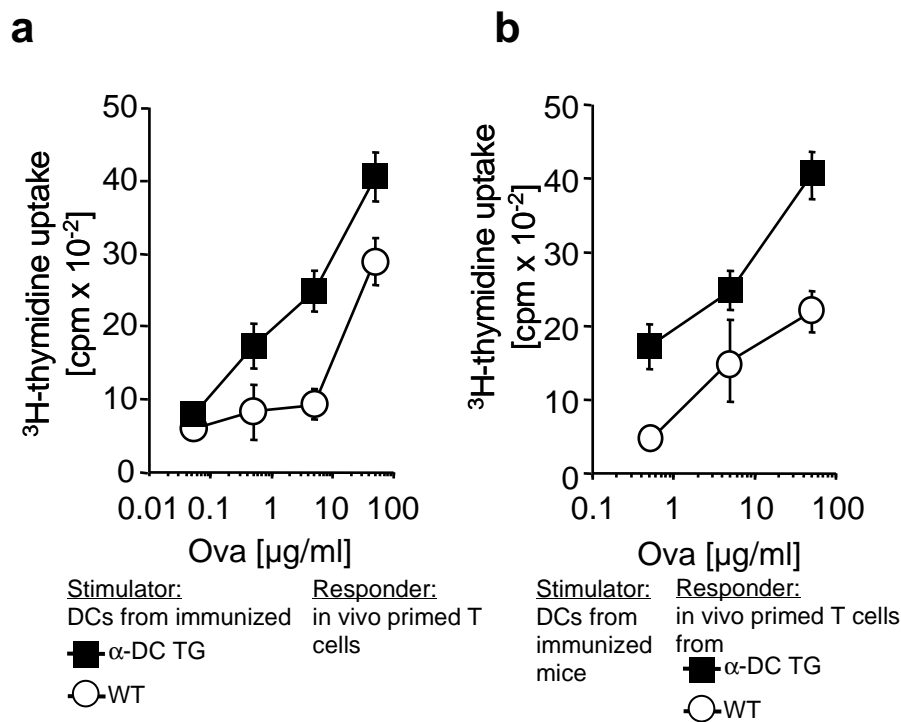
Fig. 3. 17. (a) FcεRI⁺ DCs loaded with antigen-specific IgE following immunization in vivo are superior stimulators of antigen-specific memory T cell responses. Splenic DCs isolated from Ova immunized α-DC TG (black squares) and WT mice (white circles) were cultured with isolated T cells from Ova immunized mice in the presence of graded concentrations of Ova (horizontal). ³H-thymidine uptake was measured (mean cpm of triplicate cultures ± s.e.m.; vertical). **(b) Augmented in vivo antigen-specific T cell response in α-DC TG mice.** T cells isolated from Ova immunized α-DC TG (black squares) and WT mice (white circles) were cultured with isolated DCs in the presence of graded concentrations of Ova (horizontal). ³H-thymidine uptake was measured (mean cpm of triplicate cultures ± s.e.m.; vertical).

Next, we analyzed whether the interaction of IgE with FcεRI is responsible for the enhanced T cell response observed. To address this issue, we used IgE-deficient (IgE$^{-/-}$) mice and crossed them into the α-DC TG background. IgE$^{-/-}$α-DC TG, α-DC TG and WT mice were immunized and spleen cells recovered were restimulated with defined concentrations of Ova protein. IgE$^{-/-}$α-DC TG mice had an Ova-specific T cell response that is greatly reduced in comparison to that of IgE-proficient α-DC TG mice, yet comparable to that of WT mice (Fig. 3.18). Thus, we conclude that the binding of antigen-specific IgE to FcεRI on DCs in vivo resulted in the enhanced antigen-specific memory T cell response due to antigen targeting to DCs in an IgE and FcεRI-dependent fashion.
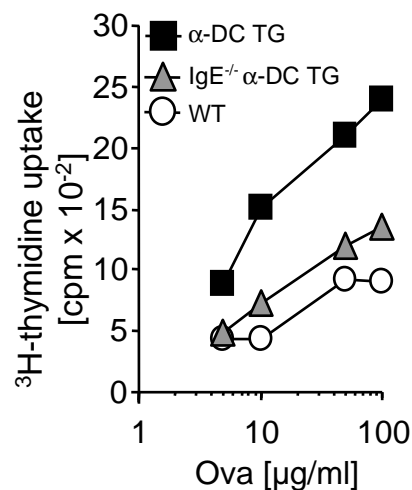

Fig. 3. 18. The augmented antigen-specific proliferative response in α-DC TG mice depends on the presence of IgE in vivo. Splenocytes from Ova-immunized α-DC TG (black sqaures), IgE$^{-/-}$ α-DC TG mice (gray triangles), and WT mice (white circles) were cultured in the presence of graded concentrations of Ova and ^{3}H-thymidine uptake was measured (mean cpm; vertical).

3.3. FcεRI⁺ DCs efficiently prime naïve T cells for Th2 development and amplify antigen-specific Th2 responses in vivo

IgE-FcεRI-dependent amplification of T cell responses in vivo can be explained by enforced T cell expansion at the memory cell level due to repetitive antigen exposure and accumulating antigen-specific IgE. Besides, the possibility exists that IgE-FcεRI interactions allow DCs to increase their ability to activate and recruit greater cell numbers of antigen-specific naïve T cells.

To test this, purified DCs were used as stimulators of naïve and primed Ova-specific TCR transgenic T cells (DO11.10) in the presence or the absence of haptenized (NP-) Ova and hapten- (NP-) specific IgE. DCs isolated from non-immunized WT and α-DC TG mice induced the same amount of T cell proliferation (Fig. 3.19a). However, addition of antigen-specific IgE caused a much stronger CD4$^+$ T cell proliferation (Fig. 3.19b) and TNFα and IL-2 cytokine production (Fig. 3.20) when FcεRI$^+$ DCs are present in the cultures than in the absence of FcεRI. The T cell proliferation-promoting effect of IgE was clearly evident over almost the entire dose range of antigen tested, yet became gradually less explicit with increasing antigen concentrations probably due to the saturable nature of FcεRI-dependent antigen uptake.

Mechanistically, we found that IgE-FcεRI-facilitated T cell proliferation occurs due to (i) an increased rate of naïve T cells entering the cell cycle (Fig. 3.21) and, for cells that have already entered cell cycle, (ii) an accelerated propagation through consecutive rounds of cell division (Fig. 3.22). Interestingly, the proliferation-inducing effect of IgE-FcεRI-dependent antigen presentation was more critical for the proliferation of naïve T cells than for primed T cells (Fig. 3.23). This suggests that enhanced stimulation of the naïve T cell pool is essential for the augmented total antigen-specific T cell response in α-DC TG mice.

102
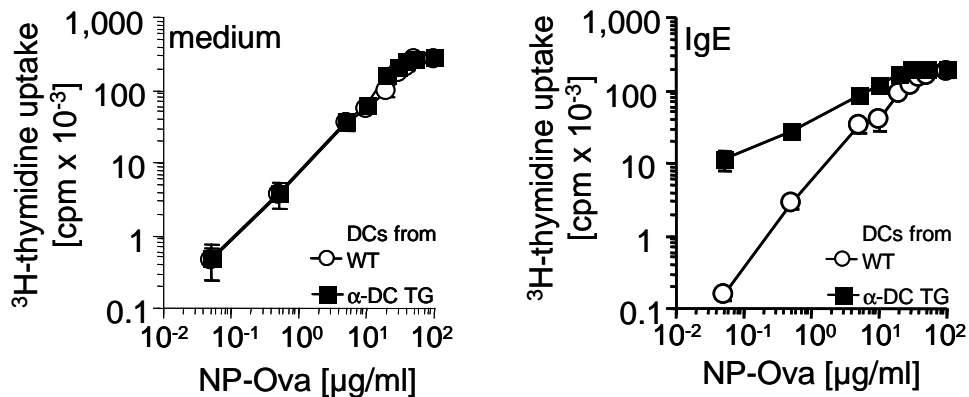
Fig. 3. 19. IgE/antigen (Ova) complexes are more effectively presented by FcεRI-expressing DCs to Ova-specific T cells. DCs isolated from α-DC TG (black squares) and WT mice (open circles) were cultured with naïve Ova-specific DO11.10 T cells in the presence of graded concentrations of haptenized (NP-)Ova (horizontal). Where indicated NP-specific IgE (right panel) was added. ^{3}H-thymidine uptake was measured (mean cpm of triplicate cultures + s.e.m.; vertical). Unlike in its presence, in the absence of NP-specific IgE (left panel), DCs from α-DC TG and WT mice induced the same level of T cell proliferation. Equal IgE-dependent naïve T cell activation by FcεRI$^+$ DCs was seen in the BALB/c (responders: DO11.10 T cells) and the C57BL/6 background (responders: OTII T cells; data not shown).
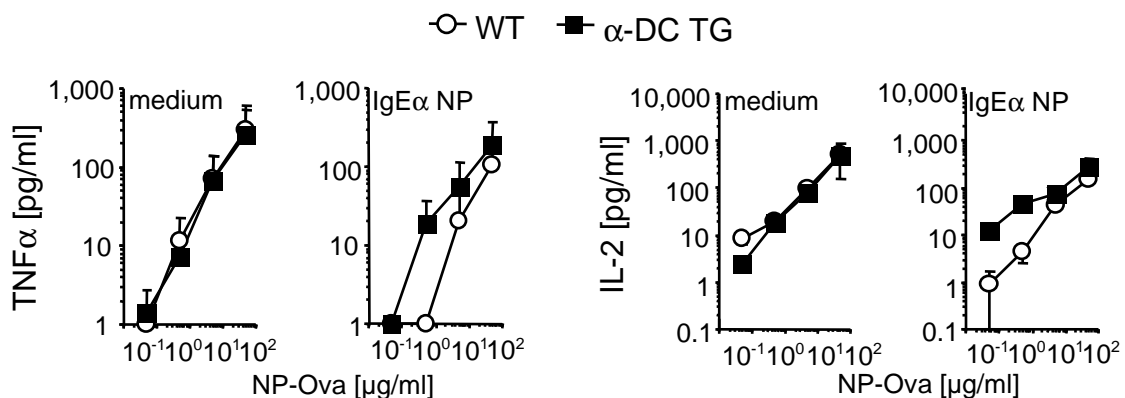
Fig. 3. 20. IgE/FcεRI-dependent amplification of the T cell response results in increased TNFα and IL-2 secrection. DCs isolated from α-DC TG (black squares) and WT mice (open circles) were cultured with naïve Ova-specific DO11.10 T cells in the presence of graded concentrations of haptenized (NP-)Ova (horizontal). Where indicated NP-specific IgE (right) was added. TNFα (left panels) and IL-2 (right panels) secretion was measured on day 3. Data presented as the mean [pg/ml] ± s.e.m. of triplicate cultures.
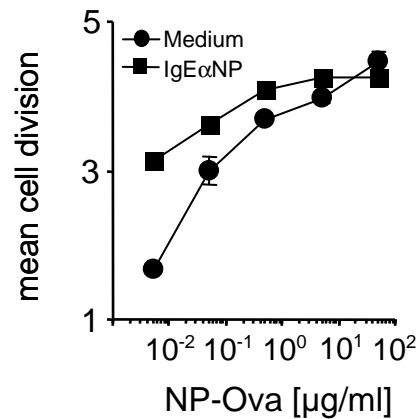
Fig. 3. 21. IgE-enhanced cell division numbers in naïve T cells stimulated by FcεRI⁺ DCs.
DCs from α-DC TG mice were cocultured with CFSE-labelled Ova-specific T cells in the
presence (squares) or the absence of IgE anti-NP (circles) and graded concentrations of NP-
Ova (horizontal). Mean division numbers of cycling Ova-specific T cells ($\pm$ s.e.m., vertical) are
shown as a function of the concentration of NP-Ova. Mean cell division numbers were
calculated using the cell numbers contained in the individual peaks of the CFSE fluorescence
histograms.
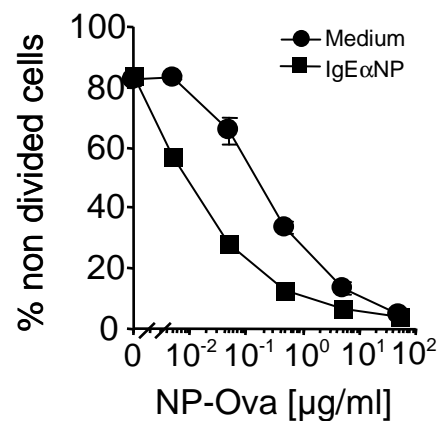
Fig. 3. 22. IgE-enhanced cell cycle entry of naïve T cells stimulated by FcεRI⁺ DCs. DCs
from α-DC TG mice were cocultured with CFSE-labelled Ova-specific T cells in the presence
(squares) or the absence of IgE anti-NP (circles) and graded concentrations of NP-Ova
(horizontal). The mean percentage ($\pm$ s.e.m.) of non-divided cells (i.e., cell which have undiluted
CFSE fluorescence, vertical) is shown as the function of the concentration of NP-Ova.
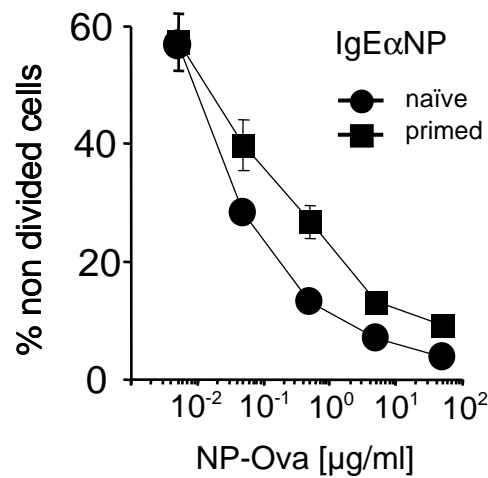
Fig. 3. 23. IgE and FcεRI-dependent induction of proliferation is functionally more relevant for naïve T cells than for primed T cells. DCs from α-DC TG mice were cocultured with CFSE-labelled Ova-specific naïve T cells (circles) or in vivo primed T cells (squares) in the presence of IgE anti-NP and graded concentrations of NP-Ova (horizontal). The mean percentage (± s.e.m.) of non-divided cells (vertical) is shown as the function of the concentration of NP-Ova.

To analyze if FcεRI-IgE-antigen crosslinking is sufficient to induce enhanced T cell proliferation, we cultured purified DCs with Ova-specific TCR transgenic T cells (DO11.10) and added defined concentrations of NP-BSA in presence of NP-specific IgE and Ova. DCs from WT and α-DC TG mice induced the same T cell response (Fig. 3.24). Thus, BSA-induced FcεRI crosslinking alone is not followed by enhanced T cell proliferation. Hence, we conclude that FcεRI-enhanced antigen uptake but not FcεRI-dependent DC activation is the major principle of exacerbated T cell activation in α-DC TG mice.
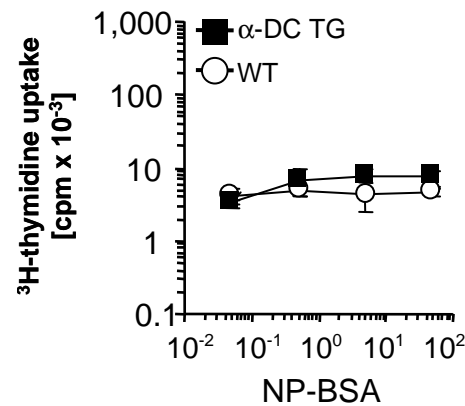
Fig. 3. 24. BSA-induced crosslinking of FcεRI is not sufficient to induce enhanced T cell proliferation. DCs isolated from α-DC TG (closed squares) and WT mice (open circles) were cultured with naïve Ova-specific Do11.10 T cells in the presence of graded concentration of NP-BSA (horizontal) in the presence of NP-specific IgE and Ova. ^{3}H-thymdine uptake was measured (mean cpm of triplicate cultures ± s.e.m.; vertical)

Naïve CD4^{+} T cells can differentiate into Th1 or Th2 cells, characterized by their pattern of cytokine secreted. Whereas Th1 cells predominantly secrete IFN-γ, Th2 cells produce IL-4. We asked whether DCs from α-DC TG mice induced altered Th differentiation as compared to WT DCs. Thus, we analyzed whether the binding of antigen-IgE complexes to FcεRI on DCs influences the differentiation of antigen-specific naïve Th cells activated by these cells. For this, we used antigen loading conditions to separately analyze FcεRI-dependent and fluid phase antigen uptake (Fig. 3.14).

After antigen uptake in fluid phase, DCs primed naïve Ova-specific T cells to differentiate into Th1 cells, whereby IFN-γ dominated the cytokine secretion (Fig. 3.25). In contrast, when Ova was targeted to FcεRI on DCs, these cells induced IL-4-dominated Th2 differentiation (Fig. 3.25).
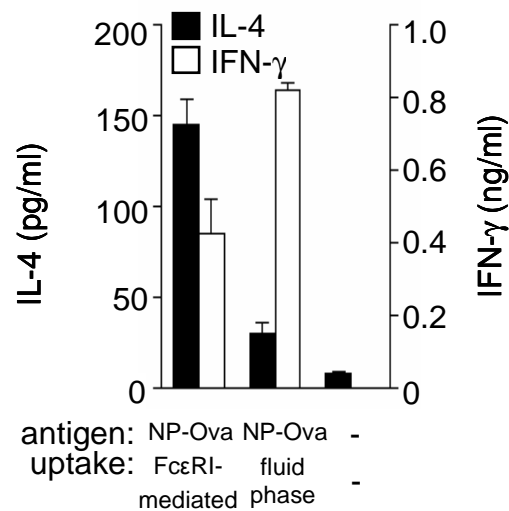
Fig. 3. 25. Augmented IL-4 and reduced IFN-γ secretion by Ova-specific T cells primed by DCs after IgE- and FcεRI-dependent antigen uptake. FcεRI⁺ DCs loaded with NP-specific IgE or unmodified DCs were pulsed with NP-Ova or medium only and co-cultured with naïve OVA-specific T cells. Mean concentrations (+ s.e.m.) of IL-4 (pg/ml, left vertical axis) and IFN-γ (ng/ml; right vertical axis) in culture supernatants as obtained in three independent experiments are shown. Experiments were performed in collaboration with E. Fiebiger

To see whether this IgE-FcεRI-mediated Th2-skewing has a correlate in vivo, α-DC TG and WT mice were immunized with Ova intraperitoneally and epicutaneously, isolated spleen cells were restimulated in vitro and analyzed for Th1 and Th2 cytokine secretion. Following immunization via either anatomic route of antigen delivery, we observed strongly amplified Th2 responses in α-DC TG mice, as evidenced by increased antigen-dependent secretion of IL-4 and IL-5 as well as by increased Th2:Th1 cytokine ratios (Fig. 3.26a-e). Th2-dominated cytokine production was not only seen with Ova, but also after the immunization with the structurally unrelated birch pollen allergen Betv1, a major allergen in humans (Fig. 3.26f)
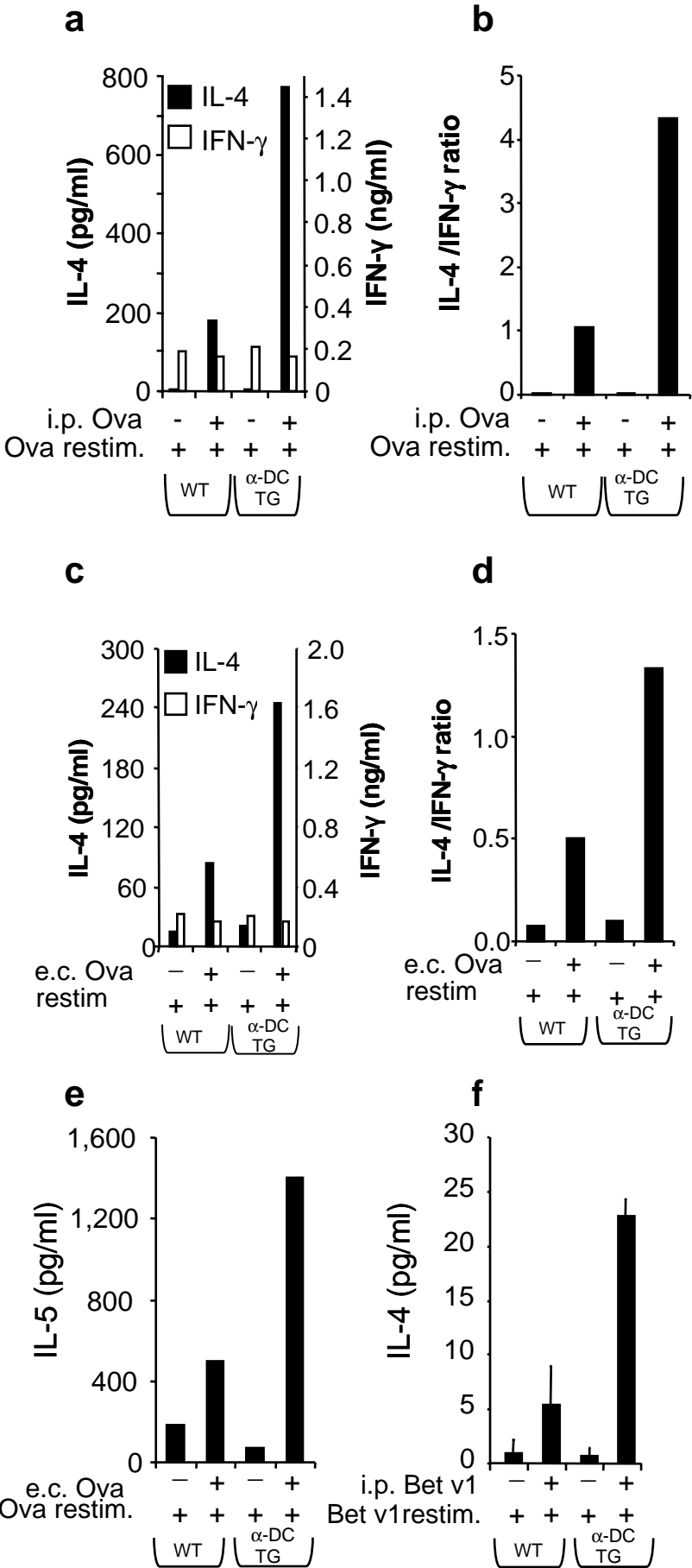
Fig. 3. 26. Augmented Ova-specific in vivo Th2 responses in α-DC TG mice. (a)
Splenocytes from naïve and Ova-immunized α-DC TG (closed bars) and WT mice (open bars)
were cultured in the presence of Ova. Pooled splenocytes from three mice per group were
used. Concentrations of IL-4 (pg/ml, left vertical axis) and IFN-γ (ng/ml; right vertical axis) were
determined by ELISA. **(b)** IL-4 /IFN-γ ratios from experiment shown in (a) **(c)** Th2-skewed
antigen-specific T cell responses in epicutaneously Ova-sensitized α-DC TG mice. Spleen cells
from epicutaneously Ova-sensitized or non-sensitized α-DC TG and WT mice were exposed to
Ova in vitro. IL-4 (black bars, left vertical axis) and IFN-γ concentrations (open bars, right
vertical axis) in supernatants of splenocytes pooled from three mice per group are shown. **(d)**
IL-4 /IFN-γ ratios from experiment shown in (c). **(e)** IL-5 secretion measured in experiment
shown in (c). **(f)** Th2-skewed antigen-specific T cell responses in i.p. birch pollen-sensitized α-
DC TG mice. Spleen cells from i.p. Betv1-sensitized or non-sensitized α-DC TG and WT mice
were exposed to Betv1 in vitro. Mean concentrations (+ s.e.m.) of IL-4 (vertical) in supernatants
of splenocytes obtained from 5 mice per group are shown. Experiment was done by N. Duschek
in collaboration with U. Wiedermann-Schmidt.

The in vivo relevance of this enhanced antigen-specific Th2 cytokine secretion
in α-DC TG mice is further corroborated by the observation of increased serum
levels of antigen-specific IgE in these mice (Fig. 3.27). Thus, the biological role
of FcεRI on DCs in vivo is not only to promote T cell expansion both from the
naïve and memory pool but also to induce and amplify type 2 T cell responses.

Fig. 3. 27. Antigen-specific serum IgE is augmented in α-DC TG mice. Elisa-based detection of Ova-specific serum IgE in α-DC TG mice (black bars) and WT mice (open bars). Mice were immunized i.p. with Ova or were non-immunized (PBS). Mean concentrations of Ova-specific IgE (+ s.e.m.) obtained with three mice per group are shown.
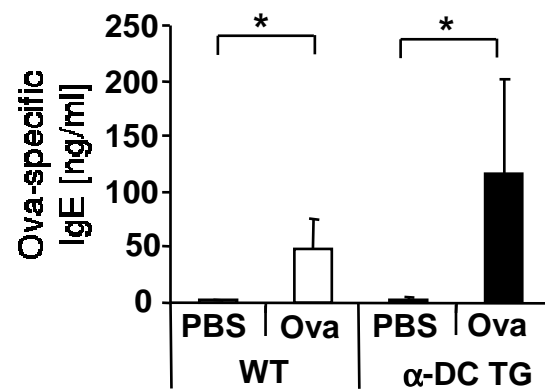
3.4. Exacerbation of allergic late-phase inflammation in α-DC TG mice

To explore whether the expression of FcεRI on DCs modifies allergic tissue inflammation, we induced pulmonary LARs in α-DC TG and WT mice. To induce allergic asthma, mice were immunized and sacrificed 72 h after challenge with aerosolized antigen.

H&E-stained lung sections evaluated in a blinded fashion (cf. 2.20.3) point showed significantly increased inflammatory cell infiltration in lungs of α-DC TG mice (Fig 3.28). Lungs of α-DC TG mice, as compared to those of WT mice, had denser perivascular and peribronchial inflammatory cuffs frequently covering the entire circumferences of those structures (Fig 3.29). Moreover, inflammatory cell infiltrates in α-DC TG mice were spread over larger areas of lung tissue than in WT controls where infiltrates occurred in a patchy distribution. The cellular infiltration tended to extend into the peri- and interalveolar space more prominently in α-DC TG than in WT mice (Fig. 3.28 and 3.29).

Next, we analyzed and quantified the cell subtype composition of lung infiltrates. Using FACS analysis, we measured the number of CD45$^+$ leukocytes in lung cell suspensions prepared from immunized and non-immunized α-DC TG and WT mice exposed to aerosolized Ova 72 h before sacrifice. In this analysis, the number of CD45$^+$ hematopoietic cells was significantly increased in allergen-exposed lungs of α-DC TG mice compared to WT controls (Fig. 3.30), supporting the histological observations.

Quantification of cell subtypes within the infiltrate showed that eosinophils were present in significantly increased proportions within the CD45$^+$ lung infiltrates of α-DC TG mice as compared to those of WT controls (Fig. 3.31). A relative

increase in CD11c^{+} lung-infiltrating cells was also noted in α-DC TG mice (Fig. 3.31) which becomes more evident taken into account the increase in total CD45^{+} lung cells in these animals. The proportions of other myelomonocytic cell subsets and T cells were not significantly different in the lungs of α-DC TG and WT mice. Hence, we conclude that the expression of FcεRI on DCs enhances both the magnitude and the eosinophil and, possibly, DC component of inflammatory cell infiltration in allergic pulmonary late-phase reactions.
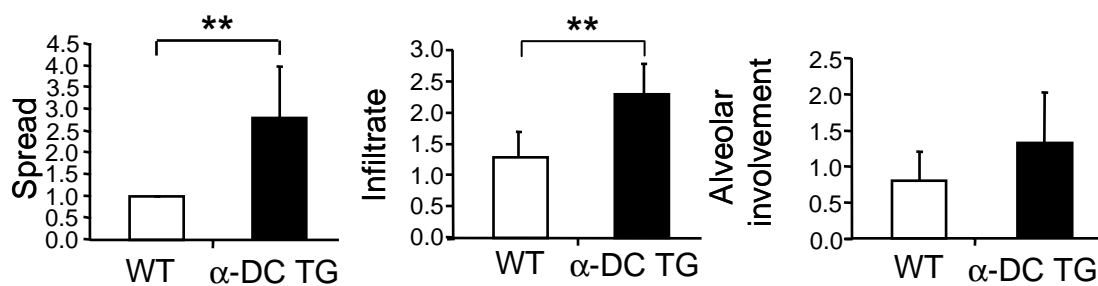
Fig. 3. 28. Increased pulmonary infiltration in α-DC TG mice. The spread of the infiltrate (left panel), the extent of infiltration (middle panel) and its extension into the peri- and intraalveolar space (right panel) were quantified, in a blinded fashion, by microscopic scoring of H&E-stained lung sections from i.p. Betv1-immunized and allergen aerosol-challenged α-DC TG (black bars) and WT mice (open bars). Results are presented as mean scores (+ s.e.m.) as obtained with lungs of 7 mice per group. **, p<0.01. Experiment was performed in collaboration with A. Rot.
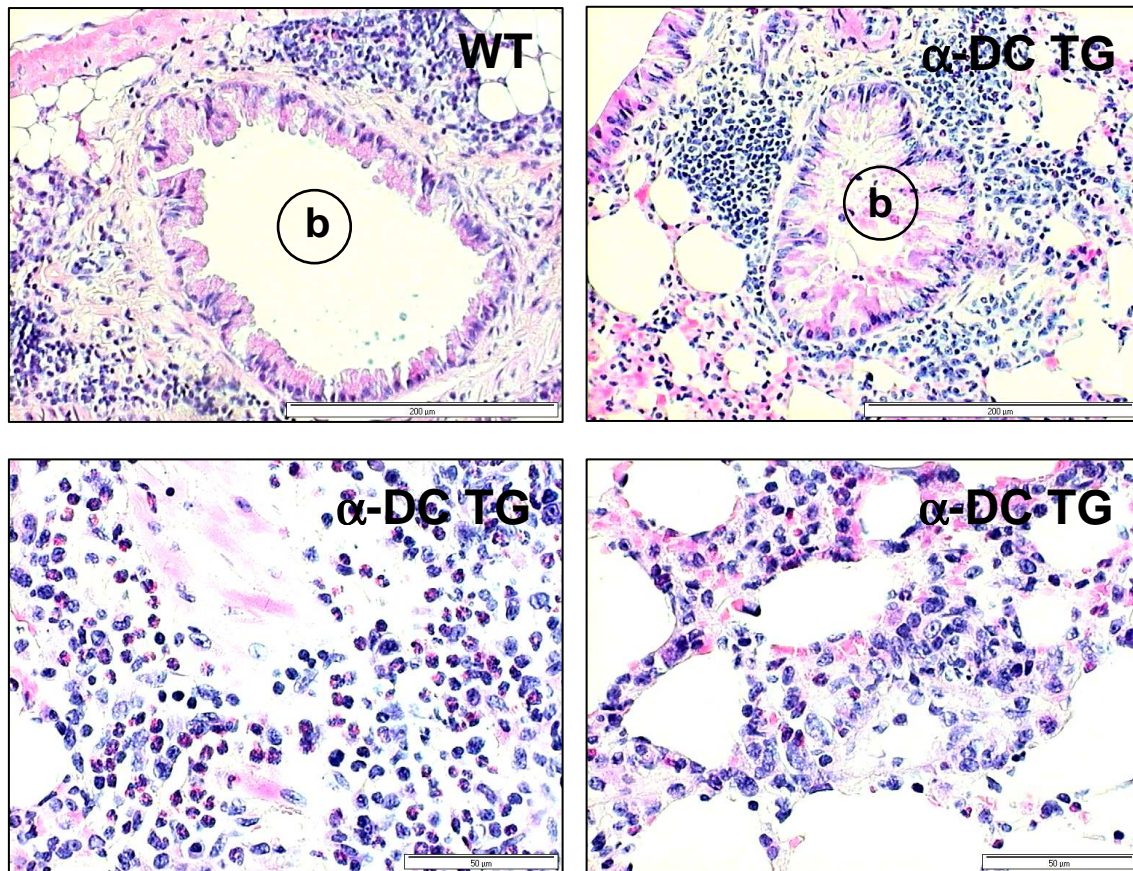
Fig. 3. 29. Representative examples of inflammatory lung pathology in α-DC TG and WT mice. H&E-stained lung sections from WT mice show patchy inflammatory infiltrates that are demarcated from bronchi/bronchioli (upper left panel). In α-DC TG lungs, inflammatory infiltrates form peribrochial cuffs frequently covering the entire circumference of these structures (upper right panel). Infiltrates are not demarcated from but intimately associated with bronchi/bronchioli. This subepithelial, peribronchial area is the very location of FcεRI$^+$ DC accumulation in inflamed α-DC TG lungs (see text). The inflammatory infiltrates in α-DC TG lungs are formed by mononuclear cells and contain a prominent proportion of eosinophils both in parenchymal (lower left panel) and alveolar regions (lower right panel); b, bronchus/bronchiolus. Experiment was performed in collaboration with A. Rot.
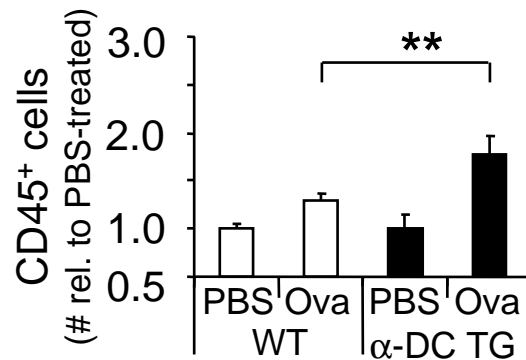
Fig. 3. 30. Quantification of allergen-induced lung infiltration with CD45+ hematopoietic cells. Naïve and i.p. Ova-immunized α-DC TG (black bars) and WT mice (open bars) were exposed to aerosolized Ova. The number of CD45+ cells contained in lung single cell suspensions was measured by flow cytometry and normalized to the content of CD45+ cells in lungs of non-immunized mice. The mean (+s.e.m.) of data obtained with three mice per group is shown.
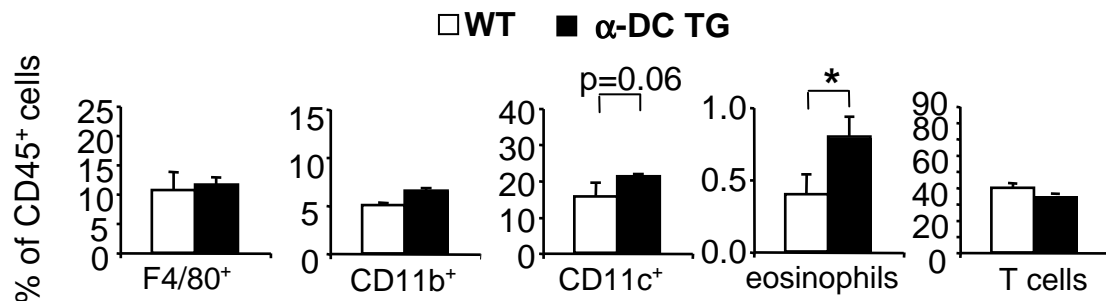
Fig. 3. 31. Increased pulmonary infiltration with CD11c+ hematopoietic cells and eosinophils in α-DC TG mice. Subtyping analysis of the hematopoietic inflammatory lung infiltrates in Ova-sensitized and Ova-challenged α-DC TG (black bars) and WT mice (open bars). The mean percentual contribution (+ s.e.m.) of F4/80+ macrophages, CD11b+ and CD11c+ myeloid cells, eosinophils, and T cells to the CD45+ lung infiltrate as determined in three mice per group is shown. *, p<0.05; **, p<0.01.

3.5. Airway-associated FcεRI⁺ DCs accumulate in allergic lung inflammation

The observation of larger numbers of CD11c$^+$ cells in lungs of α-DC TG mice than of WT mice led us to analyze the nature, localization and pulmonary recruitment of transgene-expressing lung DCs in greater detail.

Thus, we examined eGFP-expressing cells in lungs harvested from immunized and aerosol-challenged mice. Only few eGFP$^+$CD11c$^+$ DCs were present in single cell suspensions prepared from lungs of naïve, of Ova-challenged or of Ova-immunized but only mock-challenged α-DC TG mice (Fig. 3.32, 3.33).

In contrast, the lungs of Ova-sensitized and Ova-challenged mice contained a large population of eGFP$^+$CD11c$^+$ DCs (Fig. 3.33 and 3.35). Analyzing this large eGFP$^+$ population, we showed that these cells express FcεRI. Isolated eGFP$^+$CD11c$^+$ lung cells expressed FcεRI and strongly stimulated Ova-specific T cell proliferation (Fig. 3.33, 3.34). eGFP$^-$CD11c$^+$ lung cells, in contrast, did not express FcεRI and were poor stimulators of T cell proliferation (Fig. 3.33, 3.34). Thus, eGFP expression in α-DC TG mice is a marker of lung DCs since eGFP expression visualizes the functionally competent FcεRI$^+$CD11c$^+$ lung DC population in these animals. Furthermore, eGFP$^+$ cells showed only low-autofluorescence thus excluding transgene expression in macrophages which are characterized by high level autofluorescence in both WT and α-DC TG mice (98, 99, Fig. 3.37).

In mock-challenged α-DC TG mice, the eGFP$^+$ DCs localized in close proximity to bronchioli but did not infiltrate the lung parenchyma (Fig. 3.34). In Ova-sensitized and Ova-challenged mice, eGFP$^+$ DCs infiltrated in large numbers bronchioli and small bronchi as well as the alveolar lung parenchyma (Fig. 3.35). Closer inspection of the airway-associated DCs revealed that their cell body localized just beneath the bronchial epithelium and that these cells, from their apical aspect, project a discontinuous network of dendrite-like cell protrusions into the basal lamina of the small airways (Fig. 3.34). In contrast to

sensitized and challenged mice, mice that were only sensitized or were only exposed to aerosolized antigen did not show any alteration of lung DC number or localization (Fig. 3.31, 3.32, 3.34). Thus, the recruitment of FcεRI$^+$ DCs to the lung is linked to the elicitation of an antigen-specific immune response in situ.
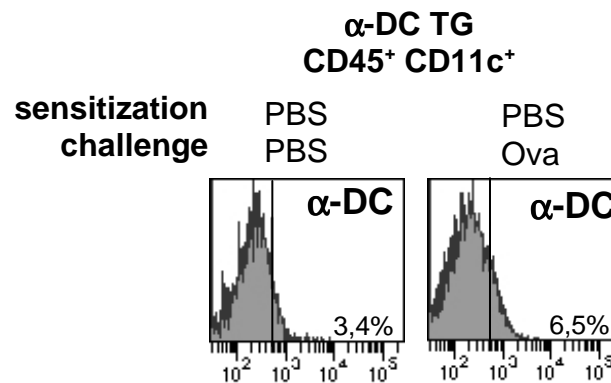
Fig. 3. 32. No alteration of lung DC number in naïve or only aerosol-challenged mice. eGFP expression of CD45$^+$CD11c$^+$ lung cells from naïve α-DC TG mice (left histogram) and naïve α-DC TG mice after inhalation of aerosolized Ova (right histogram) Vertical lines indicate the upper cut-off of autofluorescence of CD45$^+$CD11c$^+$ lung cells from WT mice.
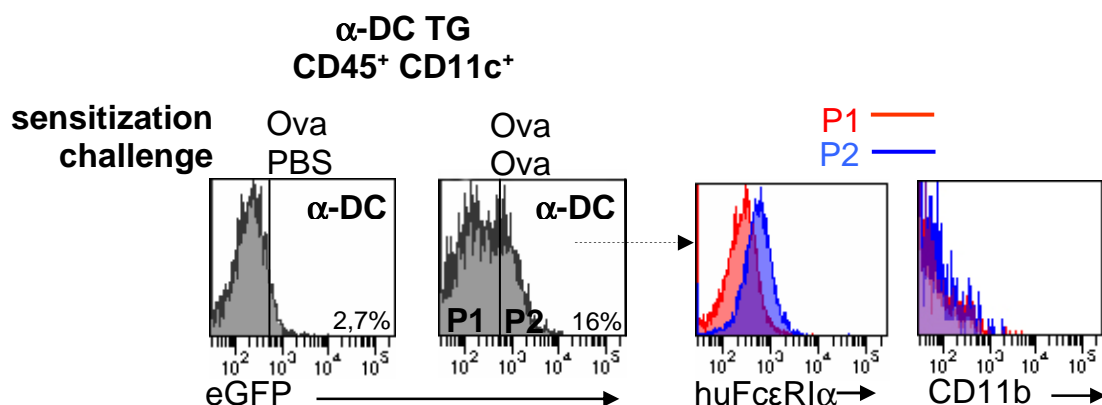
Fig. 3. 33. The number of eGFP$^+$CD11c$^+$ cells is greatly increased in allergic lung inflammation. eGFP expression of CD45$^+$CD11c$^+$ lung cells from i.p. Ova-immunized α-DC TG mice after inhalation of aerosolized Ova (right histogram, left panel) or PBS only (left histogram, left panel). Vertical lines indicate the upper cut-off of autofluorescence of CD45$^+$CD11c$^+$ lung cells from WT mice. Gated eGFP$^+$ (P2, blue), but not eGFP$^-$ (P1; red) CD11c$^+$ lung cells express human FcεRIα (left histogram, right panel). Both, eGFP$^+$ and eGFP$^-$CD11c$^+$ lung cells lack CD11b (right histogram, right panel).

116
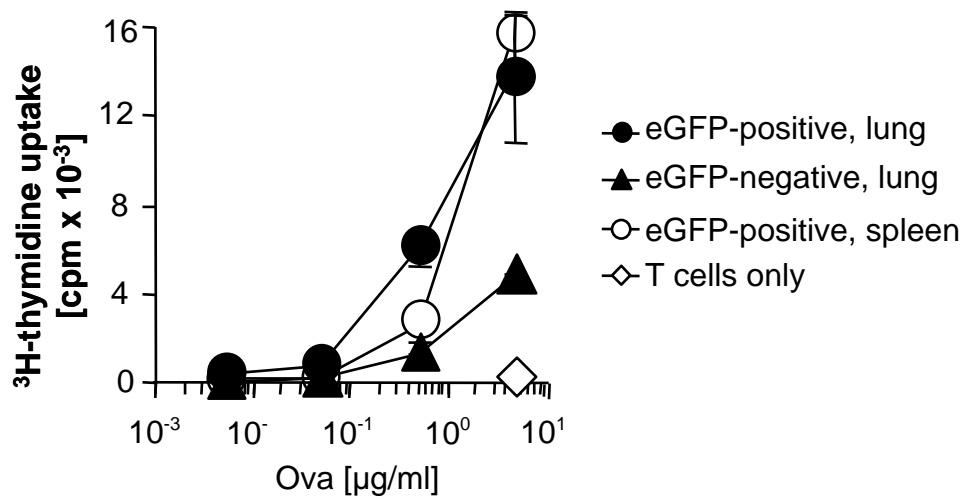
Fig. 3. 34. In contrast to their eGFP$^-$ counterparts, eGFP$^+$CD11c$^+$ lung cells are strong stimulators of Ova-specific T cell proliferation. eGFP$^+$CD11c$^+$ (full circles) and eGFP$^-$ CD11c$^+$ lung cells (full triangles) and, for comparison, eGFP$^+$CD11c$^+$ splenic DCs (open circles) were co-cultured with Ova-specific T cells (T cells alone: open diamonds) in the presence of graded concentrations of Ova (horizontal). ^{3}H-thymidine uptake of triplicate cultures was measured (mean cpm $\pm$ s.e.m.; vertical).
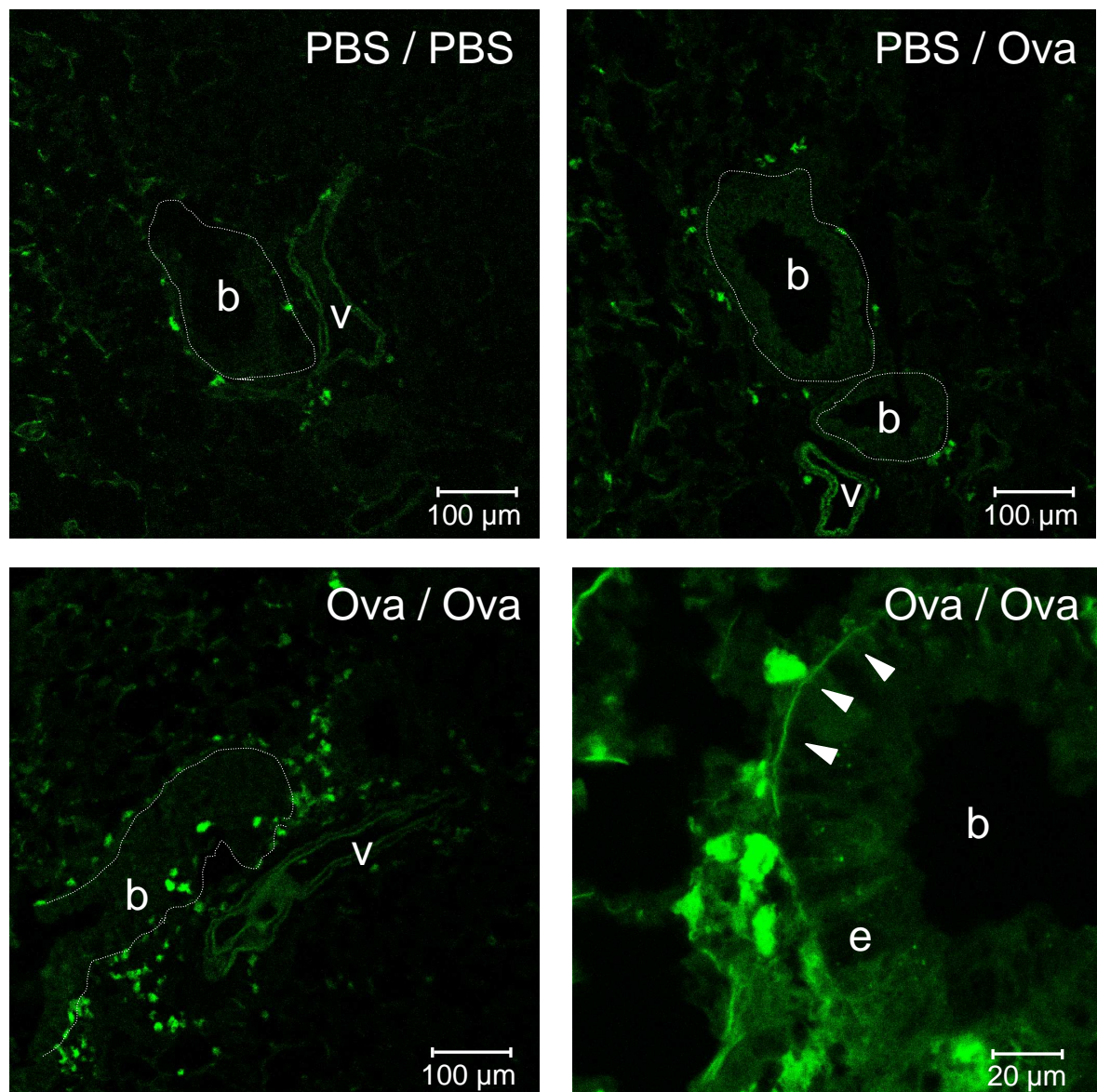
Fig. 3. 35. eGFP[+] DCs accumulate in Ova-dependent allergic lung inflammation. Lung sections from non-immunized α-DC TG mice (upper right panel: exposed to aerosolized Ova only (PBS/Ova); upper left panel: PBS inhalation only (PBS/PBS)) and Ova-immunized and Ova aerosol-challenged α-DC TG mice (Ova/Ova; lower left panel) were analyzed by confocal laser scanning microscopy. Higher magnification shows eGFP[+] DCs closely associated with bronchi and projecting dendrites into the bronchial basal lamina (arrowheads in lower right panel). Fluorescence light emission of 505-550 nm was recorded. b, bronchus/bronchiolus; v, blood vessel; e, bronchial epithelium.
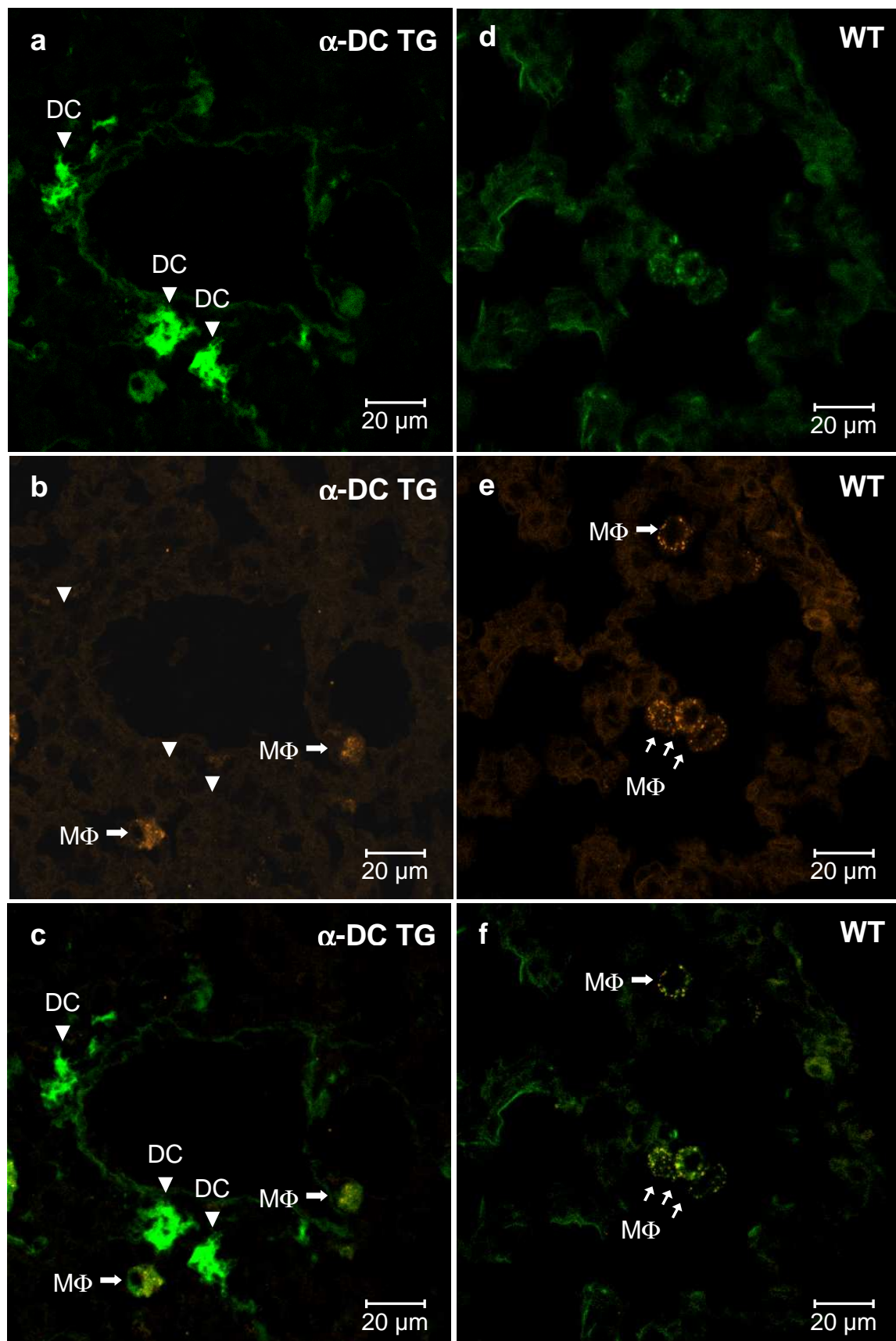
Fig. 3. 36 . Lung DCs but not macrophages (MΦs) express eGFP. Lung sections from Ova-immunized and Ova-challenged α-DC TG mice (left panels) were analyzed by confocal microscopy. Fluorescence light emission of 505-550 nm (green, upper left panel) and of 560-

615 (red, middle right panel) was recorded. Due to their broad autofluorescence, MΦs show equal light emission in both wavelength ranges. DCs, in contrast, emit light in the eGFP emission spectrum of 505-550 nm only (arrowheads). Lower left panel: merged image of the upper panels. As shown in the right panels, lung MΦs of WT mice display green (upper right panel) and red (middle right panel) autofluorescence equivalent to MΦs of α-DC TG mice. Lower right panel: merged image of the upper panels. In contrast to α-DC TG mice, cells with green but not red fluorescence cannot be discerned in WT mice. Arrows in the merged image (lower right panel) denote autofluorescent MΦs.

Lung recruitment of eGFP$^+$ DCs was also analyzed in IgE$^{-/-}$ α-DC TG mice. Expectedly, in IgE$^{-/-}$ α-DC mice no Ova-specific IgE was detectable after Ova immunization and lung challenge (Fig. 3.36).

In IgE$^{-/-}$ α-DC TG mice, the lung recruitment of eGFP$^+$ DCs was reduced (Fig. 3.37). Thus, the in vivo interaction of IgE with FcεRI on DCs also contributes to DC accumulation in the allergen-exposed lungs.
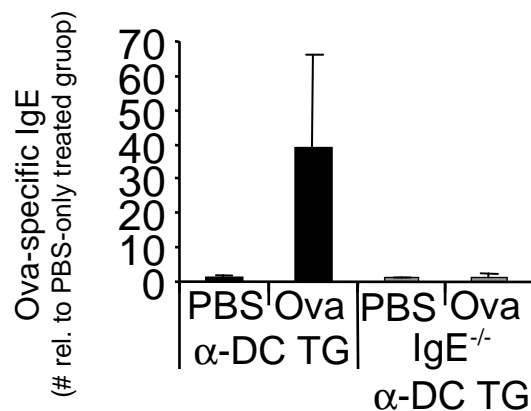
Fig. 3. 37. Antigen-specific serum IgE is not detectable in IgE$^{-/-}$ α-DC TG mice. Ova-specific serum IgE in Ova-immunized or non-immunized (PBS) α-DC TG mice (closed bars) and IgE$^{-/-}$ α-DC TG mice (grey bars). Results are presented as mean level of Ova-specific IgE relative to the PBS-treated control group as obtained with three mice per group.
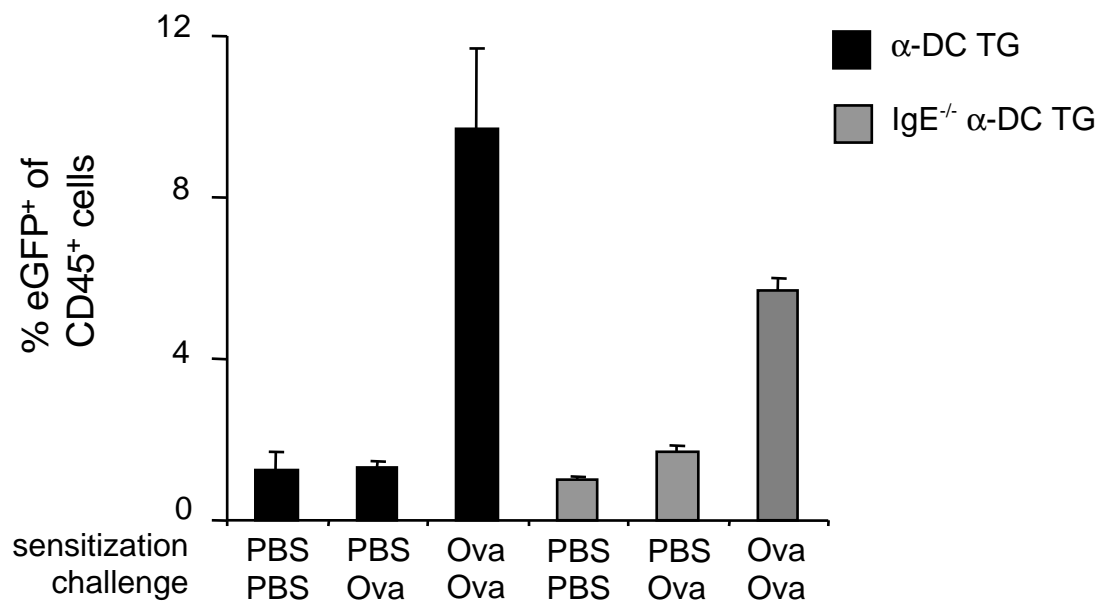
Fig. 3. 38. Inflammation-associated recruitment of FcεRI⁺ DCs depends, in part, on IgE.
The percentage of eGFP$^+$ DCs among all CD45$^+$ lung cells was determined by flow cytometry in naïve or Ova-treated α-DC TG (closed bars) and IgE$^{-/-}$ α-DC TG mice (gray bars). Results are presented as mean % (+s.e.m.; vertical) as obtained with three mice per group

3.6. FcεRI on DCs instigates IgE-dependent pulmonary Th2 activation and eosinophil chemoattraction to the lung

To see whether enhanced T cell activation indeed occurs in lungs of α-DC TG mice as compared to WT controls we performed adoptive in vivo transfer of CFSE-labelled Ova-specific T cells into Ova-immunized α-DC TG and WT control mice. Injected T cells homed to lung and the spleen in about the same frequency (Fig. 3.39).

By analyzing the CFSE-dependent fluorescence of Ova-specific T cells in lungs exposed to aerosolized Ova, we were able to monitor antigen-dependent T cell proliferation in situ (Fig. 3.40).

As shown in Fig. 3.41, Ova-specific lung T cells underwent, on average, 67% more cell divisions in α-DC TG mice than in WT controls (mean divisions in α-DC TG: 5.5; mean divisions in WT: 3.3). Thus, enhanced T cell activation in situ by FcεRI[+] lung DCs can contribute to the observed increased allergic late-phase-associated inflammatory cell infiltration in the lungs of α-DC TG mice.
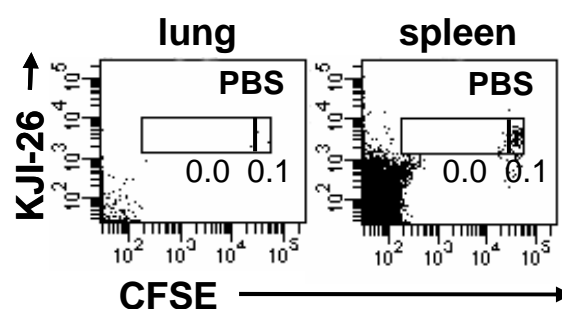
Fig. 3. 39. T cells home to the lung and the spleen at about the same frequency. Measurement of CFSE fluorescence of Ova-specific T cells in the lung (left panel) and spleen (right panel). CFSE-labelled DO11.10 T cells were transferred in Ova-immunized α-DC TG mice. From single cell lung suspensions, CD45^{+}CD3^{+}CD4^{+} T cells were gated and DO11.10 T cells identified by their reactivity with the clonotype TCR-specific mAb KJI-26 (vertical). DO11.10 T cells recovered from lungs of naïve control mice were used to define the CFSE fluorescence intensity gate of non-divided cells.
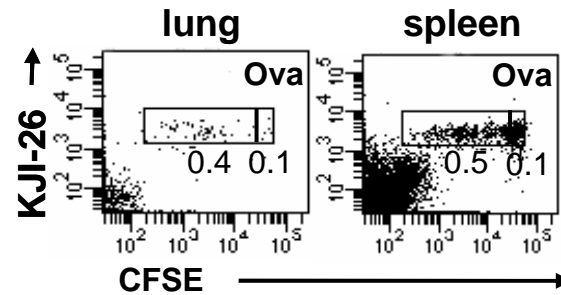
Fig. 3. 40. Activation of T cells occurs after allergen exposure. Measurement of in vivo proliferation of Ova-specific T cells in the lung (left panel) and the spleen (right panel). CFSE-labelled DO11.10 T cells were transferred in Ova-immunized α-DC TG mice and mice were exposed to aerosolized Ova. From single cell lung suspensions, CD45$^+$CD3$^+$CD4$^+$ T cells were gated and DO11.10 T cells identified by their reactivity with the clonotype TCR-specific mAb KJI-26 (vertical). DO11.10 T cells recovered from lungs and spleens of naïve control mice were used to define the CFSE fluorescence intensity gate of non-divided cells.
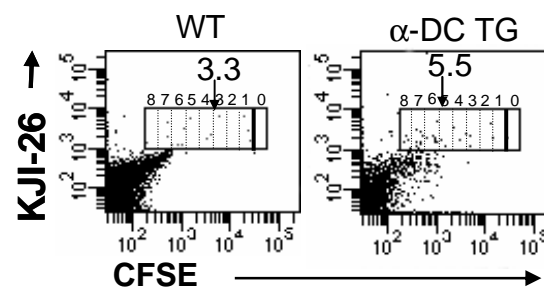
Fig. 3. 41. Measurement of in vivo proliferation of Ova-specific lung T cells. CFSE-labelled DO11.10 T cells were transferred in Ova-immunized WT (left panel) and α-DC TG mice (right panel) and mice were exposed to aerosolized Ova. From single cell lung suspensions, CD45$^+$CD3$^+$CD4$^+$ lung T cells were gated and DO11.10 T cells identified by their reactivity with the clonotype TCR-specific mAb KJI-26 (vertical). DO11.10 T cells recovered from lungs of naïve control mice were used to define the CFSE fluorescence intensity gate of non-divided cells (gate 0). CFSE dilution by a factor of two per cell division allows to track up to 8 cell divisions in Ova-specific lung T cells (gates 1-8). Mean cell division numbers are indicated.

Next we analyzed whether the enhanced lung T cell response in α-DC TG mice was Th2 dominated or not. As shown in Fig. 3.42, antigen-dependent IL-4 mRNA production was upregulated in lungs from immunized and Ova-challenged α-DC TG mice as compared to those from immunized and challenged WT mice. In immunized and challenged IgE$^{-/-}$ α-DC TG mice the increase in IL-4 mRNA was much less evident than in α-DC TG mice, particularly when considering the relative increase in CD3 mRNA in the IgE-deficient animals (Fig. 3.42). Thus, we conclude that IgE binding to FcεRI$^+$ lung DCs contributes to a strong allergen-specific Th2 response in the lung.

Eosinophils are not present in non-inflamed peripheral tissues. Thus eosinophils must be actively recruited to the site of allergic inflammation, the consequence of direct or indirect effects of Th2 cell activation in situ (121).
Among the Th2-related candidates of eosinophil chemoattractants, we found eotaxin upregulated in lungs of immunized and challenged α-DC TG mice, while RANTES was expressed equally in α-DC TG and WT mice (Fig. 3.42). The upregulated expression of eotaxin but not RANTES expression depended on IgE in lungs of α-DC TG mice.
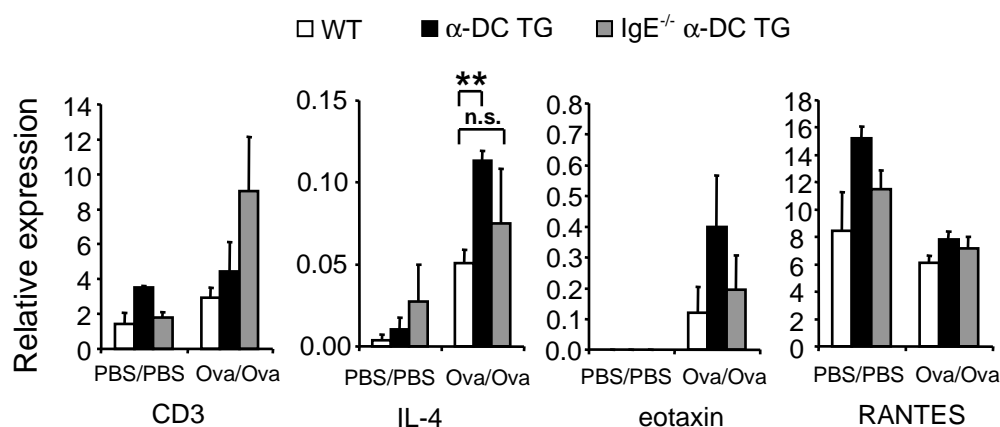
Fig. 3. 42. IL-4 and eotaxin mRNA production is upregulated in lungs of α-DC transgenic mice during allergic inflammation. Quantitative real-time PCR analysis of CD3, IL-4, eotaxin, and RANTES mRNA expression in lung cells of naïve and Ova-immunized and -challenged WT (open bars), α-DC TG (black bars), and IgE$^{-/-}$ α-DC TG mice (grey bars). Expression values

obtained were normalized to housekeeping gene expression and mean values (+ s.e.m., vertical) obtained with at least 3 mice per group are given. **, p<0.01. Experiment was performed in collaboration with U. Wiedermann-Schmidt.

Since α-DC TG mice mount an enhanced systemic Th2 cell response that depends on the presence of antigen-specific IgE, we asked whether the enhanced eosinophil recruitment in these mice is equally IgE-dependent. Thus, we compared eosinophil recruitment to antigen-exposed lungs of immunized WT, α-DC TG mice and α-DC TG mice with genetic ablation of IgE.

As shown in Fig. 3.43, the increased eosinophil recruitment to lungs of α-DC TG mice is completely lost in the IgE$^{-/-}$ α-DC TG background. Thus, IgE deficiency abolishes specifically the eosinophil recruitment-enhancing effect of DC-expressed FcεRI and leaves antigen-dependent eosinophil recruitment operative at the level seen in WT animals. Collectively, IgE interaction with FcεRI on lung DCs results in pulmonary Th2 activation, overproduction of eosinophil chemoattractants and IgE-dependent eosinophil recruitment what is not seen in WT animals.

As reported previously, we found that IgE deficiency does not alter the magnitude of lung eosinophilia in mice that do not express FcεRI on DCs but express FcεRI on their mast cells (124, Fig. 3.44). Thus, IgE-dependent lung eosinophil recruitment requires the expression of FcεRI on DCs but not FcεRI expression on mast cells.
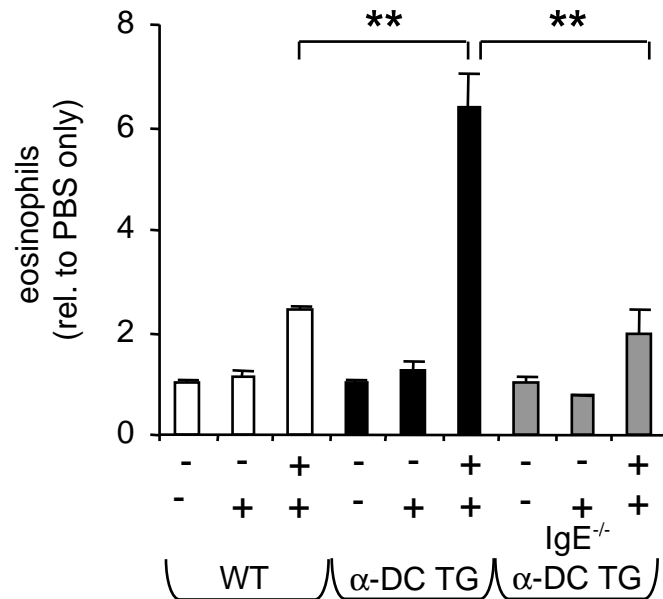
Fig. 3. 43. IgE-dependent eosinophil lung infiltration in α-DC TG mice but not in WT mice.
Lung eosinophils in naïve or Ova-immunized WT (open bars), α-DC TG (black bars), and IgE$^{-/-}$
α-DC TG mice (gray bars), after either PBS (-) or Ova (+) inhalation, were counted by flow
cytometry. Mean eosinophil counts (+s.e.m.) relative to the counts in the PBS only-treated
group as obtained with lungs from three mice per group are shown. **, p<0.01.
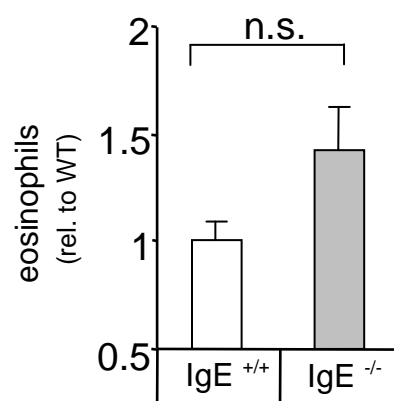
**Fig. 3. 44. IgE-deficiency in mice not expressing FcεRI on DCs does not negatively affect
eosinophil lung recruitment.** Lung eosinophils in Ova-immunized and Ova-challenged WT
(IgE$^{+/+}$, open bar) and IgE$^{-/-}$ mice (gray bar) were counted by flow cytometry. Mean eosinophil
counts (+ s.e.m.) relative to the counts in WT mice as obtained with lungs from three mice per
group are shown.

126

The enforced recruitment of tissue-destructing and remodelling eosinophils to lungs of α-DC TG may be solely due to facilitated Th2 cell activation in situ by IgE-loaded FcεRI⁺ DCs accumulating in the allergen-exposed tissue. This is supported by the strict dependence of FcεRI⁺ DC-mediated eosinophil recruitment on antigen priming and challenge. Besides, the mutually non-exclusive possibility exists that antigen/IgE binding to FcεRI⁺ tissue DCs, by itself, leads to eosinophil attraction in a rather T cell-independent fashion. To test this in vivo, human FcεRIα-specific mAbs with established FcεRI triggering capacity were injected into α-DC TG and control mice, both on the IgE-deficient background to retain FcεRI unoccupied.

As shown in Fig. 3.45, the systemic and selective engagement of DC-expressed FcεRI led to enhanced eosinophil migration to the spleen. We also noted increased numbers of eosinophils in the lungs of mAb-treated α-DC TG mice. The magnitude if this response was, however, somewhat smaller, possibly due to competition of the various organs for eosinophil recruitment in the setting of systemic FcεRI activation.
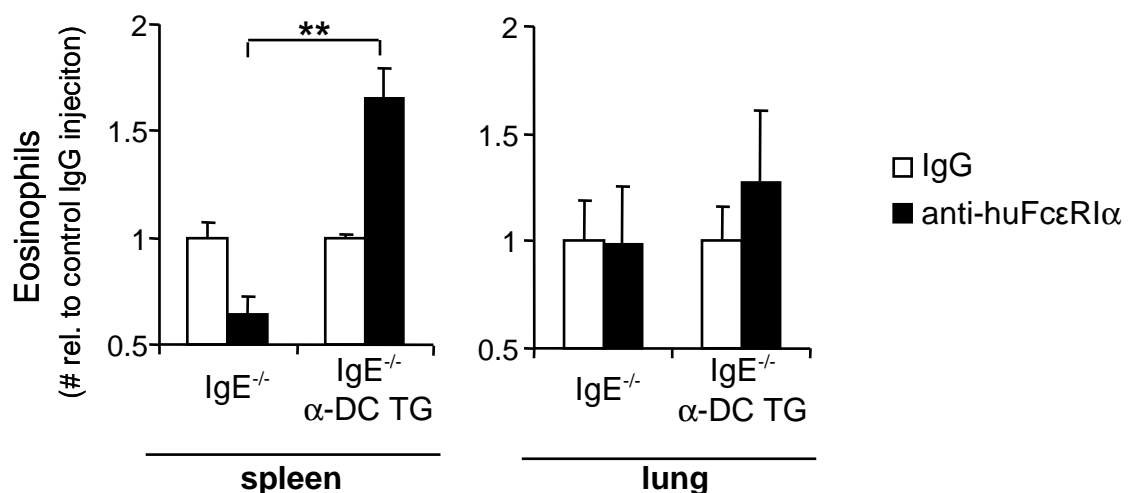
Fig. 3. 45. In vivo activation of FcεRI increases eosinophil recruitment independently of IgE and antigen. IgE$^{-/-}$ and IgE$^{-/-}$ α-DC TG mice injected with control antibody (open bars) or anti-huFcεRIα (15-1; black bars) antibody. Spleen (left) and lung (right) eosinophils in IgE$^{-/-}$ and IgE$^{-/-}$ α-DC TG were counted by flow cytometry. Mean eosinophil counts (+ s.e.m.) relative to the counts in the PBS only-treated group as obtained with lungs from three mice per group are shown **, p<0.01.

4. Discussion

The in vivo role of FcεRI expressed on mast cells in allergy is well known. Crosslinking of FcεRI by IgE-allergen-complexes leads to mast cell activation and subsequent release of preformed mediators which may result in an anaphylactic response in the worst case scenario (1, 7). The in vivo role of FcεRI expressed on mast cells was further demonstrated in studies using mice deficient in FcεRI or IgE (124).

Unlike in mice, in humans, FcεRI is expressed not only on mast cells and basophils but also on antigen-presenting DCs (10, 12, 13). However, the in vivo relevance of DC-expressed FcεRI and its contribution in IgE-dependent induction of allergic inflammation remained unknown. This is mainly due to the lack of a suitable mouse model to study the role of DC-expressed FcεRI in allergic reactions. To overcome this limitation, our laboratory generated α-DC TG that display a "humanized" FcεRI expression pattern.

α-DC TG mice express on their DCs FcεRI composed of a human FcεRI α-chain and the murine FcεRIγ-chain-dimer, which is expressed endogenously in murine DCs. Thus, α-DC TG mice, as humans, express FcεRI on DCs as trimer lacking the β-chain. In vivo, expression of huFcεRI is restricted to DCs. Other cell types like T cells, B cells and macrophages do not express huFcεRIα/muFcεRIγ₂ complexes. The restriction of huFcεRI-expression on DCs is the result of a constitutively active DC-specific promoter and the requirement of endogenous FcεRI γ-chain for surface expression of a functional FcεRI (27). As in humans, FcεRI is predominantly expressed on CD4$^+$ myeloid DCs and less on CD8$^+$ lymphoid DCs and plasmacytoid DCs. In addition, DCs from lymphoid organs like spleen and lymph nodes as well as from non-lymphoid organs like the lung express FcεRI. Functionality of FcεRI expressed on DCs was confirmed by its ability to bind both murine and human IgE in vivo and in vitro. Furthermore, we demonstrated that DCs from α-DC TG mice but not from

WT mice had the capacity of FcεRI-mediated and IgE-dependent antigen uptake und presentation.

The late-phase of allergic reaction (LAR) is characterized by chemokine- and cytokine-induced recruitment of leukocytes like DCs, T lymphocytes and eosinophils to sites of allergen exposure (1). LARs rather than the early-phase of allergic reaction (EAR) contribute to the morbidity and mortality in asthma. Eosinophils are a characteristic hallmark of the pathologic infiltrative process of asthma and are regarded as key effector cells of LARs. Eosinophils are bone marrow-derived granulocytes normally circulating in the blood. Th2 cell-released cytokines induce eosinophil maturation and their recruitment to LAR inflammatory sites (1, 120). Interestingly, Mehlhop et al. demonstrated that eosinophilic inflammation occurs even in IgE-deficient mice (124). The pulmonary histology was identical in IgE-deficient and WT mice concluding that IgE and, thus, FcεRI expressed on mast cells is not involved in the pathway of eosinophil recruitment to lungs of allergic WT mice. Furthermore, Takeda et al. showed in mast cell-deficient mice that even mast cells are not required for the development of eosinophilic inflammation (123). The fact that IgE, mast cells and, thus, mast cell-expressed FcεRI are not mandatory for eosinophil recruitment in the course of LARs permits a functional separation of the early and late-phase of allergic reaction. In human asthma, in contrast to mice, there is a correlation between antigen-specific IgE levels and eosinophil recruitment. As the consequence, increased antigen-specific IgE has a significant amplifying effect on the severity of the LAR in human asthma. This understanding originates from anti-IgE treatment studies in human asthmatics. For instance, Fahy et al. demonstrated that treatment with a humanized murine monoclonal antibody directed to the FcεRI-binding domain of IgE decreases serum IgE and drastically reduces the late-phase allergic response (125). Hence, besides the well-known role of IgE on mast cells, there has to be an additional function of IgE for the development of LARs in humans.

We compared eosinophil lung recruitment in response to aerosolized antigen in α-DC TG and WT mice. It must be pointed out that the only difference between

α-DC TG and WT mice is the expression of FcεRI on DCs and not on mast cells and basophils. In α-DC TG mice, we observed significantly increased and IgE-dependent LAR-associated eosinophil lung recruitment. Thus, we concluded that DCs through their in vivo expression of FcεRI are capable to increase lung eosinophilia in an IgE-dependent fashion.

In our studies, we could show that FcεRI-expressed on DCs can augment IgE-dependently antigen-specific T cell responses. This is due to a more efficient allergen-uptake, processing and allergen-derived peptide presentation to T cells mediated by FcεRI and IgE. Thus, targeting of allergen-IgE complexes to FcεRI expressed on DCs results in an amplified allergen-specific T cell response. Noteworthy, DCs in α-DC TG mice and humans express FcεRI. This fact corroborates the central role of IgE rather than of IgG in the modulation of antigen thresholds for DC-dependent T cell activation. Interestingly, our results also show that the proliferation-promoting function of IgE was stronger for naïve than for primed T cells. Thus, FcεRI-IgE mediated antigen-presentation may amplify T cell activation in vivo also by engaging the hitherto non-activated naïve T cell pool to participate in the allergic reaction.

In summary, FcεRI-facilitated antigen-presentation by DCs in vivo may be crucial for the expansion of memory T cells but may also boost the priming of naïve T cells which possibly will contribute to the diversity of the T cells response in terms of affinity and repertoire of recognized allergen peptides.

In α-DC TG mice, we found an augmented Th2 cell response not only in lymphoid organs, but also in non-lymphoid organs, such as the lung. After allergen-exposure, lung T cells expressing clonotypic T cell receptors underwent more cell division in sensitized α-DC TG mice than in WT controls. Furthermore, the absolute number of T cells was increased in lungs of allergen-sensitized and challenged α-DC TG mice compared to those from naïve α-DC TG mice which becomes evident taken into account the increase in total CD45^{+} lung cells in these animals. IgE-FcεRI-dependent T cell activation by DCs also induced Th2-cell polarization in vivo. Comparing the Th differentiation following

FcεRI-mediated and fluid-phase antigen uptake in DCs, we observed Th1 polarization in the case of conventional fluid-phase antigen uptake. In contrast, DCs which had taken up IgE-antigen complexes via FcεRI induced Th2 cell differentiation. Thus, it appears likely, that IgE-FcεRI-mediated antigen uptake results in FcεRI signaling eliciting a Th2-inducing program in DCs. Recent studies show such an enhanced Th2 response for rare basophils (129, 130, 131). Perrigoue et al. demonstrated a MHC class II-dependent activation of CD4^{+} T cells by basophils in helminth infection (130). Yoshimoto et al. showed that basophils loaded with IgE-antigen complexes acts as potent antigen-presenting cell in mice infected with Strongyloides venezuelensis (129) and Sokol et al. demonstrated that basophils function as APCs during a papain induced Th2 response (131). Thus, basophils and DCs play a pivotal role in the induction of Th2 responses. Basophils are normally located in the bone marrow and the blood and migrate rarely, and if so late into the inflamed tissues. In contrast to rare basophils, DCs are present in higher numbers in even non-inflamed lymphoid and non-lymphoid organs and further accumulate at sites of inflammation. Due to the preferential occurrence of DCs in terms of tissue location and quantity, we speculate, that FcεRI[+] DCs play the crucial role in the induction of Th2 responses, whereas basophils, which appear rarely and late in the course of allergic inflammation, may amplify DC-induced Th2 responses.

In our study, the in vivo relevance of this FcεRI-dependent Th2 promotion is directly shown by increased Th2 cytokine secretion in allergen stimulated splenocytes and in lungs from α-DC TG compared to WT mice. It is important to note that amplified IL-4 secretion in α-DC TG mice occurs independently of the route of sensitization, as similar results were obtained after intraperitoneal and epicutaneous sensitization. This is of particular medical importance since epicutaneous sensitization to antigen may be a key factor for the development of asthma-associated allergic disorders, such as atopic dermatitis (132).

Our studies suggest a central role of DCs and FcεRI on DCs in orchestrating inflammatory reactions resulting in an IgE-dependent amplification of lung

LARs. Sertl et al. was the first to illustrate the presence of DCs within the lungs of humans and mice (97). Their study demonstrated the presence of DCs within the airway epithelium, lung parenchyma and visceral pleura. Later studies from Tunon-De-Lara et al. demonstrated the presence of DCs in both normal and asthmatic human lungs within the bronchial epithelium and in the subepithelial tissue. Furthermore, these studies showed a significant increase of DCs in lungs of asthmatics compared to normal lungs. The majority of these lung DCs expressed FcεRI and displayed cell-bound IgE (102). α-DC TG mice fully recapitulate this DC and FcεRI representation seen in human lungs. In naïve α-DC TG mice, only few eGFP$^+$ cells were detected. These cells localize close to bronchioli but do not infiltrate the lung parenchyma. Aerosol-challenge with antigen in already sensitized α-DC TG mice lead to the increased recruitment of FcεRI$^+$ DCs resembling the situation in human asthmatic lungs. These newly recruited transgene-expressing DCs are found within and just beneath the bronchial epithelium as well as in the lung parenchyma. Their localization just beneath the bronchial epithelium also allows DCs extend their dendrites beneath and between epithelial cells. Our microscopic analyses indeed show that FcεRI$^+$ DCs extend elongated dendrites towards the alveolar lumen, most likely to probe for IgE-reactive inhaled allergen.

Our results allow the speculation that allergen binding by FcεRI-bearing DCs will drastically lower the critical antigen threshold required for T cell activation in the lung and the draining lymph nodes. This is also illustrated by the observation that IgE-dependent antigen presentation leads to an increased Th2-cell activation in the lungs of α-DC TG mice compared to WT controls. This initial event of IgE-dependent lung Th2 cell activation by FcεRI$^+$ DCs may provide the essential chemotactic signals for eosinophil lung recruitment and the function of accumulation of FcεRI$^+$ DCs which is, in part, also dependent on IgE-FcεRI interactions. Corroborating these novel observations, Djukanović et al. demonstrated in anti-IgE-treated (omalizumab) asthmatic patients a strong decrease in IgE$^+$ and FcεRI$^+$ cells in bronchial biopsy specimens (133).

Eosinophils are not present in non-inflamed peripheral tissues but recruited at the site of inflammation. Eosinophil recruitment to the lung occurs in response to the in situ activation of antigen-specific Th2 cells and is effectuated by the Th2 cytokine-induced production of eosinophil chemoattractants. Robinson et al. demonstrated a close correlation of eosinophil counts and activated CD4^{+} T cells producing IL-4 and IL-5 mRNA in human asthma (121). They concluded that cytokines produced by activated Th2 cells contribute to eosinophil recruitment and thus delayed-type lung inflammation. Our results also show this correlation of eosinophil counts and increased IL-4 and eotaxin. Furthermore, we provide an additional possibility of eosinophil recruitment. We have evidence that transgene-expressing DCs can recruit eosinophils to the lung in a T cell independent way by direct triggering of FcεRI. In α-DC TG mice, in vivo activation of FcεRI on DCs through systemic presence of human FcεRI agonistic mAbs enhance tissue eosinophilia. Thus, we conclude that FcεRI[+] DCs can exert at least three IgE-dependent synergistic activities for eosinophil recruitment: (i) augmentation of the systemic Th2 pool size, (ii) enhancement of T cell activation in the allergen-exposed organ and (iii) immediate attraction of inflammatory cells after triggering of their FcεRI by IgE-allergen complexes (Fig. 4.1).

Steroids are the first class therapy for asthma since they are still the only drug preventing mortality in human asthma (134). Inhaled corticosteroids reduce eosinophils LARs and its consequence, tissue damage, an irreversible lung function impairment. Besides the clinically benefit of corticosteroid treatment, this therapy has various adverse effects particularly during prolonged and high-dose application. Our finding that DCs in the lung and their trimeric FcεRI participate directly in the induction and severity of pulmonary LARs provides a new target for the development of novel therapies against allergic inflammation. For this pharmacological intervention, efficacious and persistent blockade of DC-expressed FcεRI is likely necessary to present the aggravation of LAR-associated tissue inflammation after allergen exposure as well as the IgE-FcεRI-dependent Th2 cell skewing. The use of our α-DC TG mouse model

which recapitulates the human situation of atopic inflammation in a fashion superior to WT mice will allow further investigations on novel therapies targeting FcεRI.
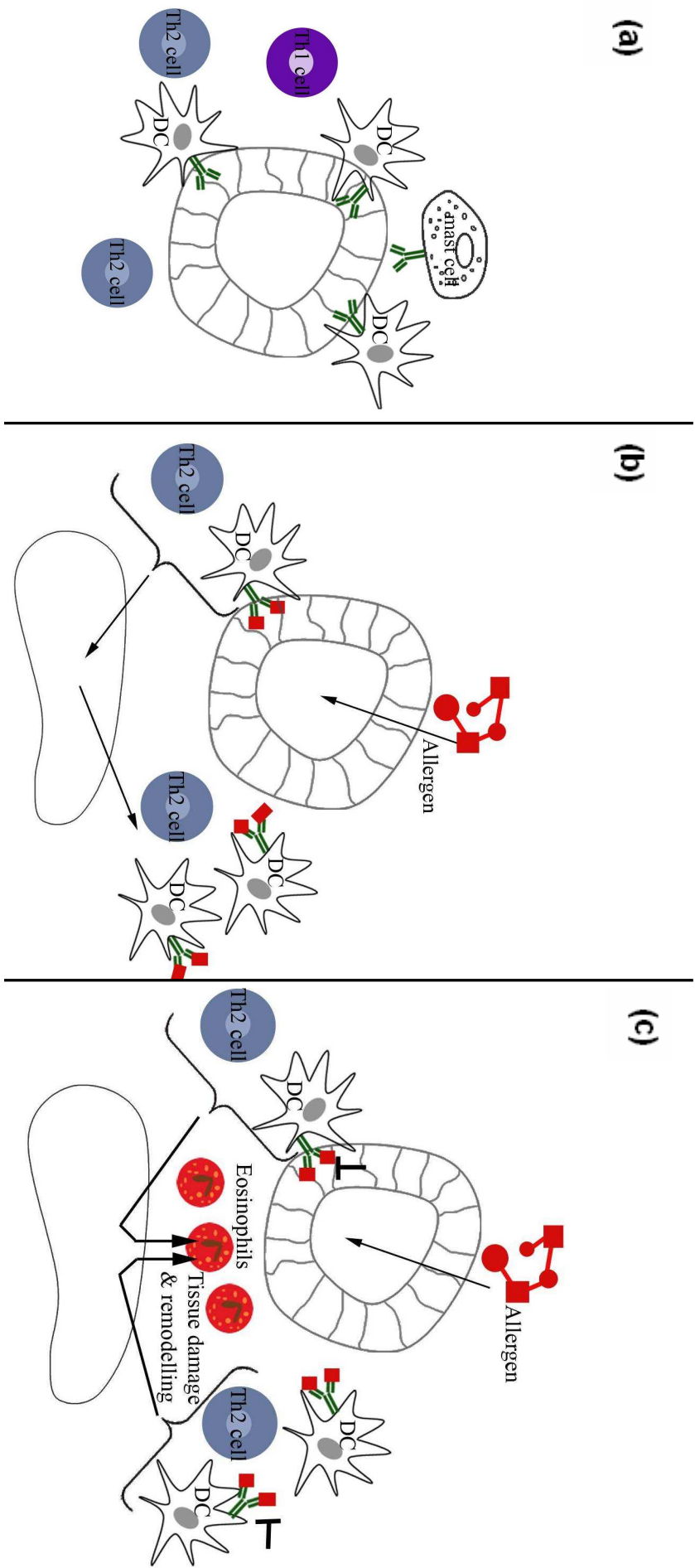
Fig. 4.1. Simplified scheme of events in FcεRI-mediated allergic tissue inflammation. (a) In normal lungs, FcεRI-expressing DCs, mast cells, Th1 and Th2 cells are present in the tissue. (b) Allergen-exposure leads to IgE-facilitated antigen-uptake, processing and presentation to T cells resulting in augmentation of the systemic Th2 cell pool size and enhanced T cell activation. Furthermore, FcεRI+ DCs are recruited into the lung where they assemble within and just beneath the bronchial epithelium as well as in the lung parenchyma. (c) Augmentation of the systemic Th2 cell pool size, enhanced T cell activation and triggering of DC-expressed FcεRI by IgE-allergen complexes results in increased eosinophil recruitment. Efficient and persistent blockade of DC-expressed FcεRI may prevent the induction of pulmonary LARs.

136

5. References

(1)   Gould HJ, Sutton BJ. IgE in allergy and asthma today. *Nat Rev Immunol.* **8**:205-17 (2008)

(2)   Mix E, Goertsches R, Zett UK. Immunoglobulins--basic considerations. *J Neurol.* **5**:9-17 (2006)

(3)   Nemazee D. Receptor editing in lymphocyte development and central tolerance*. Nat Rev Immunol.* **6**:728-40 (2006)

(4)   Abbas AK. *Cellular and molecular immunology*. 6th Edition. (2007)

(5)   Wilson DR et al. Increases in allergen-specific IgE in BAL after segmental allergen challenge in atopic asthmatics*. Am J Respir Crit Care Med.* **165**:22-6 (2002).

(6)   Tada T, Okumura K, Platteau B, Beckers A, Bazin H. Half-lives of two types of rat homocytotropic antibodies in circulation and in the skin. *Int Arch Allergy Appl Immunol.* **48**:116-31 (1975)

(7)   Galli SJ, Tsai M, Piliponsky AM. The development of allergic inflammation. *Nature.* **454**:445-54 (2008)

(8)   Ravetch JV, Kinet JP. Fc receptors. *Annu Rev Immunol.* **9**:457-92 (1991)

(9)   Metzger H. The high affinity receptor for IgE on mast cells. *Clin Exp Allergy.* **21**:269-79 (1991)

(10)   Bieber et al. Human epidermal Langerhans cells express the high affinity receptor for immunoglobulin E (Fc epsilon RI). *J Exp Med.* **175**:1285-90 (1992)

(11)   Wang et al. Epidermal Langerhans cells from normal human skin bind monomeric IgE via Fc epsilon RI. *J Exp Med.* **175**:1353-65 (1992)

(12)   Maurer et al. Peripheral blood dendritic cells express Fc epsilon RI as a complex composed of Fc epsilon RI alpha- and Fc epsilon RI gamma-chains and can use this receptor for IgE-mediated allergen presentation. *J Immunol.* **157**:607-16 (1996)

(13)   Osterhoff et al. Immunomorphologic characterization of Fc epsilon RI-bearing cells within the human dermis. *J Invest Dermatol.* **102**:315-20 (1994)

(14)   Maurer et al. Expression of functional high affinity immunoglobulin E receptors (Fc epsilon RI) on monocytes of atopic individuals. *J Exp Med.* **179**:745-50 (1994)

(15)   Gounni et al. High-affinity IgE receptor on eosinophils is involved in defence against parasites. *Nature.* **367**:183-6 (1994)

(16)   Joseph M et al. Expression and functions of the high-affinity IgE receptor on human platelets and megakaryocyte precursors. *Eur J Immunol.* **27**:2212-8 (1997)

(17)   Garman SC, Kinet JP, Jardetzky TS. Crystal structure of the human high affinity IgE receptor. *Cell.* **95**:951-61 (1998)

138

(18)   Shimizu et al. Human and rat mast cell high-affinity immunoglobulin E receptors: characterization of putative alpha-chain gene products. *Proc Natl Acad Sci U S A.* **85**:1907-11 (1988)

(19)   Kinet JP, Metzger H, Hakimi J, Kochan J. A cDNA presumptively coding for the alpha subunit of the receptor with high affinity for immunoglobulin E. *Biochemistry.* **26**:4605-10 (1987)

(20)   Garman SC, Wurzburg BA, Tarchevskaya SS, Kinet JP, Jardetzky TS. Structure of the Fc fragment of human IgE bound to its high-affinity receptor Fc epsilonRI alpha. *Nature.* **406**:259-66 (2000)

(21)   Kinet et al. Isolation and characterization of cDNAs coding for the beta subunit of the high-affinity receptor for immunoglobulin E. *Proc Natl Acad Sci U S A.* **85**:6483-7 (1988)

(22)   Lin S, Cicala C, Scharenberg AM, Kinet JP. The Fc(epsilon)RIbeta subunit functions as an amplifier of Fc(epsilon)RIgamma-mediated cell activation signals. *Cell.* **85**:985-95 (1996)

(23)   Jouvin et al. Differential control of the tyrosine kinases Lyn and Syk by the two signaling chains of the high affinity immunoglobulin E receptor. *J Biol Chem.* **269**:5918-25 (1994)

(24)   Donnadieu E, Jouvin MH, Kinet JP. A second amplifier function for the allergy-associated Fc(epsilon)RI-beta subunit. *Immunity.* **12**:515-23.9 (2000)

(25)   Küster H, Thompson H, Kinet JP. Characterization and expression of the gene for the human Fc receptor gamma subunit. Definition of a new gene family. *J Biol Chem.* **265**:6448-52 (1990)

(26)   Ra C, Jouvin MH, Blank U, Kinet JP. A macrophage Fc gamma receptor and he mast cell receptor for IgE share an identical subunit. *Nature.* **341**:752-4 (1989)

(27)   Metzger H, Kinet JP, Blank U, Miller L, Ra C. The receptor with high affinity for IgE. *Ciba Found Symp.* **147**:93-101 (1989)

(28)   Malveaux FJ, Conroy MC, Adkinson NF Jr, Lichtenstein LM. IgE receptors on human basophils. Relationship to serum IgE concentration. *J Clin Invest.* **62**:176-81 (1978)

(29)   MacGlashan et al. Down-regulation of Fc(epsilon)RI expression on human basophils during in vivo treatment of atopic patients with anti-IgE antibody. *J Immunol.* **158**:1438-45 (1997)

(30)   MacGlashan D Jr, Xia HZ, Schwartz LB, Gong J. IgE-regulated loss, not IgE regulated synthesis, controls expression of FcepsilonRI in human basophils. *J Leukoc Biol.* **70**:207-18 (2001)

(31)   MacGlashan et al. Upregulation of FcepsilonRI on human basophils by IgE antibody is mediated by interaction of IgE with FcepsilonRI. *J Allergy Clin Immunol.* **104**:492-8 (1999)

(32)   MacGlashan et al. In vitro regulation of FcepsilonRIalpha expression on human basophils by IgE antibody. *Blood.* **91**:1633-43 (1998)

(33)   Borkowski TA, Jouvin MH, Lin SY, Kinet JP. Minimal requirements for IgE mediated regulation of surface Fc epsilon RI. *J Immunol.* **167**:1290-6 (2001)

(34)   Jouvin MH, Numerof RP, Kinet JP. Signal transduction through the conserved motifs of the high affinity IgE receptor Fc epsilon RI. *Semin Immunol.* **7**:29-35 (1995)

(35)   Pribluda VS, Pribluda C, Metzger H Transphosphorylation as the mechanism by which the high-affinity receptor for IgE is phosphorylated upon aggregation. *Proc Natl Acad Sci U S A*. **91**:11246-50 (1994)

(36)   Kalesnikoff J, Galli SJ. New developments in mast cell biology. *Nat Immunol.* **9**:1215-23 (2008)

(37)   Gilfillan AM, Tkaczyk C. Integrated signaling pathways for mast-cell activation. *Nat Rev Immunol.* **6**:218-30 (2006)

(38)   Saitoh et al. LAT is essential for Fc(epsilon)RI-mediated mast cell activation. *Immunity*. **12**:525-35 (2000)

(39)   Parravicini et al. Fyn kinase initiates complementary signals required for IgE-dependent mast cell degranulation. *Nat Immunol.* **3**:741-8 (2002)

(40)   Alber G, Miller L, Jelsema CL, Varin-Blank N, Metzger H. Structure-function relationships in the mast cell high affinity receptor for IgE. Role of the cytoplasmic domains and of the beta subunit. *J Biol Chem*. **266**:22613-20 (1991)

(41)   Bieber et al. New insights in the structure and biology of the high affinity receptor for IgE (Fc epsilon RI) on human epidermal Langerhans cells. *J Dermatol Sci*. **13**:71-5 (1996)

(42)   Asai et al. Regulation of mast cell survival by IgE. *Immunity*. **14**:791-800 (2001)

(43)   Maurer et al. Fc epsilon receptor I on dendritic cells delivers IgE-bound multivalent antigens into a cathepsin S-dependent pathway of MHC class II presentation. *J Immunol.* **161**:2731-9 (1998)

(44)   Jürgens M, Wollenberg A, Hanau D, de la Salle H, Bieber T. Activation of human epidermal Langerhans cells by engagement of the high affinity receptor for IgE, Fc epsilon RI. *J Immunol.* **155**:5184-9 (1995)

(45)   Kraft et al. Enhanced expression and activity of protein-tyrosine kinases establishes a functional signaling pathway only in FcepsilonRIhigh Langerhans cells from atopic individuals. *J Invest Dermatol.* **119**:804-11 (2002)

(46)   Kraft S, Novak N, Katoh N, Bieber T, Rupec RA. Aggregation of the high affinity IgE receptor Fc(epsilon)RI on human monocytes and dendritic cells induces NF-kappaB activation. *J Invest Dermatol.* **118**:830-7 (2002)

(47)   Steinman RM, Cohn ZA. Identification of a novel cell type in peripheral lymphoid organs of mice. I. Morphology, quantitation, tissue distribution. *J Exp Med.* **137**:1142-62 (1973)

(48)   Reis e Sousa C. Dendritic cells in a mature age. *Nat Rev Immunol.* **6**:476-83 (2006)

(49)   De Smedt et al. Regulation of dendritic cell numbers and maturation by lipopolysaccharide in vivo. *J Exp Med.* **184**:1413-24 (1996)

(50)   Langenkamp A, Messi M, Lanzavecchia A, Sallusto F. Kinetics of dendritic cell activation: impact on priming of TH1, TH2 and nonpolarized T cells. *Nat Immunol.* **1**:311-6 (2000)

(51)   Sallusto F et al. Rapid and coordinated switch in chemokine receptor expression during dendritic cell maturation. *Eur J Immunol.* **28**:2760-9 (1998)

(52)   Lanzavecchia A, Sallusto F. Dynamics of T lymphocyte responses: intermediates, effectors, and memory cells. *Science.* **290**:92-7 (2000)

(53)   de Jong EC, Smits HH, Kapsenberg ML. Dendritic cell-mediated T cell polarization. *Springer Semin Immunopathol.* **26**:289-307 (2005)

(54)   Gately MK et al. The interleukin-12/interleukin-12-receptor system: role in normal and pathologic immune responses*. Annu Rev Immunol.* **16**:495-521 (1998)

(55)   Kaplan MH, Sun YL, Hoey T, Grusby MJ. Impaired IL-12 responses and enhanced development of Th2 cells in Stat4-deficient mice. *Nature.* **382**:174-7 (1996)

(56)   Wenner CA, Güler ML, Macatonia SE, O'Garra A, Murphy KM. Roles of IFN-gamma and IFN-alpha in IL-12-induced T helper cell-1 development. *J Immunol.* **156**:1442-7 (1996)

(57)   Zhou M, Ouyang W. The function role of GATA-3 in Th1 and Th2 differentiation*. Immunol Res.* **28**:25-37 (2003)

(58)   Ouyang W. et al. Stat6-independent GATA-3 autoactivation directs IL-4-independent Th2 development and commitment. *Immunity.* **12**:27-37 (2000)

(59)   Ouyang W. et al. Inhibition of Th1 development mediated by GATA-3 through an IL-4-independent mechanism. *Immunity.* **9**:745-55 (1998)

(60) Kelleher P, Maroof A, Knight SC. Retrovirally induced switch from production of IL-12 to IL-4 in dendritic cells. *Eur J Immunol.* **29**:2309-18 (1999)

(61) Plaut M. et al. Mast cell lines produce lymphokines in response to cross-linkage of Fc epsilon RI or to calcium ionophores. *Nature.* **339**:64-7 (1989)

(62) Bradding P et al. Interleukin 4 is localized to and released by human mast cells. *J Exp Med.* **176**:1381-6 (1992)

(63) Brunner T, Heusser CH, Dahinden CA. Human peripheral blood basophils primed by interleukin 3 (IL-3) produce IL-4 in response to immunoglobulin E receptor stimulation. *J Exp Med.* **177**:605-11 (1993)

(64) MacGlashan D Jr et al. Secretion of IL-4 from human basophils. The relationship between IL-4 mRNA and protein in resting and stimulated basophils*. J Immunol.* **152**:3006-16 (1994)

(65) Kolls JK, Lindén A. Interleukin-17 family members and inflammation. *Immunity.* **21**:467-76 (2004)

(66) Harrington LE et al. Interleukin 17-producing CD4+ effector T cells develop via a lineage distinct from the T helper type 1 and 2 lineages. *Nat Immunol.* **6**:1123-32 (2005)

(67) Veldhoen M, Hocking RJ, Atkins CJ, Locksley RM, Stockinger B. TGFbeta in the context of an inflammatory cytokine milieu supports de novo differentiation of IL-17-producing T cells. *Immunity.* **24**:179-89 (2006)

(68)   Bettelli E, Korn T, Kuchroo VK. Th17: the third member of the effector T cell trilogy. *Curr Opin Immunol.* **19**:652-7. (2007)

(69)   Jonuleit H, Schmitt E, Schuler G, Knop J, Enk AH. Induction of interleukin 10-producing, nonproliferating CD4(+) T cells with regulatory properties by repetitive stimulation with allogeneic immature human dendritic cells. *J Exp Med.* **192**:1213-22 (2000)

(70)   McGuirk P, McCann C, Mills KH. Pathogen-specific T regulatory 1 cells induced in the respiratory tract by a bacterial molecule that stimulates interleukin 10 production by dendritic cells: a novel strategy for evasion of protective T helper type 1 responses by Bordetella pertussis. *J Exp Med.* **195**:221-31 (2002)

(71)   Levings MK et al. IFN-alpha and IL-10 induce the differentiation of human type 1 T regulatory cells. *J Immunol.* **166**:5530-9 (2001)

(72)   Steinbrink K, Wölfl M, Jonuleit H, Knop J, Enk AH. Induction of tolerance by IL-10-treated dendritic cells. *J Immunol.* **159**:4772-80 (1997)

(73)   Heath WR et al. Cross-presentation, dendritic cell subsets, and the generation of immunity to cellular antigens. *Immunol Rev.* **199**:9-26 (2004)

(74)   Trombetta ES, Mellman I. Cell biology of antigen processing in vitro and in vivo. *Annu Rev Immunol.* **23**:975-1028 (2005)

(75)   Bakke O, Dobberstein B. MHC class II-associated invariant chain contains a sorting signal for endosomal compartments. *Cell.* **63**:707-16 (1990)

(76) Riese et al. Essential role for cathepsin S in MHC class II-associated invariant chain processing and peptide loading. *Immunity*. **4**:357-66 (1996)

(77) Weber DA, Evavold BD, Jensen PE. Enhanced dissociation of HLA-DR bound peptides in the presence of HLA-DM. *Science*. **274**:618-20 (1996)

(78) Guermonprez et al. ER-phagosome fusion defines an MHC class I cross-presentation compartment in dendritic cells. *Nature*. **425**:397-402 (2003)

(79) Colonna M. TLR pathways and IFN-regulatory factors: to each its own. Eur *J Immunol*. **37**:306-9. (2007)

(80) Taniguchi, T., Ogasawara, K., Takaoka, A., Tanaka, N. IRF family of transcription factors as regulators of host defense. *Annu. Rev. Immunol.* **19**:623–655 (2001)

(81) Nakano H, Yanagita M, Gunn MD. CD11c(+)B220(+)Gr-1(+) cells in mouse lymph nodes and spleen display characteristics of plasmacytoid dendritic cells. *J Exp Med*. **194**:1171-8 (2001)

(82) Honda K et al. IRF-7 is the master regulator of type-I interferon-dependent immune responses. *Nature*. **434**:772-7 (2005)

(83) Schindler C, Darnell JE Jr. Transcriptional responses to polypeptide ligands: the JAK-STAT pathway. *Annu Rev Biochem*. **64**:621-51 (1995)

(84) Bluyssen AR, Durbin JE, Levy DE. ISGF3 gamma p48, a specificity switch for interferon activated transcription factors. *Cytokine Growth Factor Rev*. **7**:11-7 (1996)

(85) Vremec D, Pooley J, Hochrein H, Wu L, Shortman K. CD4 and CD8 expression by dendritic cell subtypes in mouse thymus and spleen. *J Immunol*. **164**:2978-86 (2000)

(86) Henri et al. The dendritic cell populations of mouse lymph nodes. *J Immunol*. **167**:741-8 (2001)

(87) Valladeau et al. Langerin, a novel C-type lectin specific to Langerhans cells, is an endocytic receptor that induces the formation of Birbeck granules. *Immunity*. **12**:71-81 (2000)

(88) Bursch LS et al. Identification of a novel population of Langerin+ dendritic cells. *J Exp Med.* **204**:3147–3156. (2007)

(89) Nagao K et al. Murine epidermal Langerhans cells and langerin-expressing dermal dendritic cells are unrelated and exhibit distinct functions*. Proc Natl Acad Sci U S A*. **106**:3312-7 (2009)

(90) Merad M. et al. Langerhans cells renew in the skin throughout life under steady-state conditions. *Nat Immunol*. **3**:1135-41. (2002)

(91) Merad M et al. Depletion of host Langerhans cells before transplantation of donor alloreactive T cells prevents skin graft-versus-host disease. *Nat Med*. **10**:510-7 (2004)

(92) Romani N, Holzmann S, Tripp CH, Koch F, Stoitzner P. Langerhans cells – dendritic cells of the epidermis. *APMIS*. **111**:725-40 (2003)

(93) Itano et al. Distinct dendritic cell populations sequentially present antigen to CD4 T cells and stimulate different aspects of cell-mediated immunity. *Immunity*. **19**:47-57 (2003)

(94)   Klechevsky E. et al. Functional specializations of human epidermal Langerhans cells and CD14+ dermal dendritic cells. *Immunity*. **29**:497-510 (2008)

(95)   Van Voorhis WC, Hair LS, Steinman RM, Kaplan G. Human dendritic cells. Enrichment and characterization from peripheral blood. *J Exp Med*. **155**:1172-87 (1982)

(96)   Egner W, McKenzie JL, Smith SM, Beard ME, Hart DN. Identification of potent mixed leukocyte reaction-stimulatory cells in human bone marrow. Putative differentiation stage of human blood dendritic cells. *J Immunol*. **150**:3043-53 (1993)

(97)   Sertl et al. Dendritic cells with antigen-presenting capability reside in airway epithelium, lung parenchyma, and visceral pleura. *J Exp Med*. **163**:436-51 (1986)

(98)   Vermaelen K, Pauwels R. Accurate and simple discrimination of mouse pulmonary dendritic cell and macrophage populations by flow cytometry: methodology and new insights. *Cytometry A*. **61**:170-77 (2004)

(99)   Havenith et al. Separation of alveolar macrophages and dendritic cells via autofluorescence: phenotypical and functional characterization. *J Leukoc Biol*. **53**:504-10 (1993)

(100) Schon-Hegrad MA, Oliver J, McMenamin PG, Holt PG. Studies on the density, distribution, and surface phenotype of intraepithelial class II major histocompatibility complex antigen (Ia)-bearing dendritic cells (DC) in the conducting airways. *J Exp Med*. **173**:1345-56 (1991)

(101) Lambrecht BN, Salomon B, Klatzmann D, Pauwels RA. Dendritic cells are required for the development of chronic eosinophilic airway

inflammation in response to inhaled antigen in sensitized mice. *J Immunol.* **160**:4090-7 (1998)

(102) Tunon-De-Lara JM et al. Dendritic cells in normal and asthmatic airways: expression of the alpha subunit of the high affinity immunoglobulin E receptor (Fc epsilon RI -alpha). *Clin Exp Allergy.* **26**:648-55 (1996)

(103) von Pirquet C., Allergie. *Munch. Med. Wochenschr.* **53**, 1457 (1906)

(104) Coombs RRA, Gell PGH The classification of allergic reactions underlying disease. *Clinical aspects of immunology.* pp 317–337 (1963)

(105) Kay AB. Overview of 'allergy and allergic diseases: with a view to the future'. *Br Med Bull.* **56**:843-64 (2000)

(106) De Swert LF. Risk factors for allergy. *Eur J Pediatr.* **158**:89-94 (1999)

(107) Hopp RJ, Bewtra AK, Watt GD, Nair NM, Townley RG. Genetic analysis of allergic disease in twins. *J Allergy Clin Immunol.* **73**:265-70 (1984)

(108) Cookson WO et al. Maternal inheritance of atopic IgE responsiveness on chromosome 11q. *Lancet.* **340**:381-4 (1992)

(109) Hill MR, Cookson WO. A new variant of the beta subunit of the high-affinity receptor for immunoglobulin E (Fc epsilon RI-beta E237G): associations with measures of atopy and bronchial hyper-responsiveness. *Hum Mol Genet.* **5**:959-62 (1996)

(110) Marsh DG et al. Linkage analysis of IL4 and other chromosome 5q31.1 markers and total serum immunoglobulin E concentrations. *Science.* **264**:1152-6 (1994)

(111) Holt PG et al. Genetic 'risk' for atopy is associated with delayed postnatal maturation of T-cell competence. *Clin Exp Allergy*. **22**:1093-9 (1992)

(112) Strachan DP. Hay fever, hygiene, and household size. *BMJ*. **299**:1259-60. (1989)

(113) Matricardi PM et al. Exposure to foodborne and orofecal microbes versus airborne viruses in relation to atopy and allergic asthma: epidemiological study. *BMJ*. **320**:412-7 (2000)

(114) Benn CS, Melbye M, Wohlfahrt J, Björkstén B, Aaby P. Cohort study of sibling effect, infectious diseases, and risk of atopic dermatitis during first 18 months of life. *BMJ*. **328**:1223 (2004)

(115) Akdis M et al. Immune responses in healthy and allergic individuals are characterized by a fine balance between allergen-specific T regulatory 1 and T helper 2 cells. *J Exp Med*. **199**:1567-75 (2004)

(116) Hart PH. Regulation of the inflammatory response in asthma by mast cell products. *Immunol Cell Biol*. **79**:149-53 (2001)

(117) Dombrowicz D, Flamand V, Brigman KK, Koller BH, Kinet JP. Abolition of anaphylaxis by targeted disruption of the high affinity immunoglobulin E receptor alpha chain gene. *Cell*. **75**:969-76 (1993)

(118) Till et al. IL-13 production by allergen-stimulated T cells is increased in allergic disease and associated with IL-5 but not IFN-gamma expression. *Immunology*. **91**:53-7 (1997)

(119) Cohn L, Whittaker L, Niu N, Homer RJ. Cytokine regulation of mucus production in a model of allergic asthma. *Novartis Found Symp*. **248**:201-13 (2002)

(120) Sanderson CJ. Interleukin-5: an eosinophil growth and activation factor. *Dev Biol Stand.* **69**:23-9 (1988)

(121) Robinson et al. Activation of CD4+ T cells, increased TH2-type cytokine mRNA expression, and eosinophil recruitment in bronchoalveolar lavage after allergen inhalation challenge in patients with atopic asthma. *J Allergy Clin Immunol.* **92**:313-24 (1993)

(122) Coyle AJ et al. Interleukin-4 is required for the induction of lung Th2 mucosal immunity. *Am J Respir Cell Mol Biol.* **13**:54–59 (1995)

(123) Takeda K et al. Development of eosinophilic airway inflammation and airway hyperresponsiveness in mast cell-deficient mice. *J Exp Med.* **186**:449-54 (1997)

(124) Mehlhop et al. Allergen-induced bronchial hyperreactivity and eosinophilic inflammation occur in the absence of IgE in a mouse model of asthma. *Proc Natl Acad Sci U S A.* **94**:1344-9 (1997)

(125) Fahy JV. The effect of an anti-IgE monoclonal antibody on the early- and late-phase responses to allergen inhalation in asthmatic subjects. *Am J Respir Crit Care Med.* **155**:1828-34 (1997)

(126) Charlesworth EN. Late-phase inflammation: influence on morbidity. *J Allergy Clin Immunol.* **98**:291-7 (1996)

(127) Prussin C et al. Omalizumab treatment downregulates dendritic cell FcepsilonRI expression. *J Allergy Clin Immunol.* **112**:1147-54 (2003)

(128) Bruynzeel-Koomen C, van Wichen DF, Toonstra J, Berrens L, Bruynzeel PL. The presence of IgE molecules on epidermal Langerhans cells in patients with atopic dermatitis. *Arch Dermatol Res.* **278**:199-205 (1986)

(129) Yoshimoto T. et al. Basophils contribute to T(H)2-IgE responses in vivo via IL-4 production and presentation of peptide-MHC class II complexes to CD4(+) T cells. *Nat Immunol*. (published online: May, 2009); **doi:10.1038/ni.1737**

(130) Perrigoue JG. et al. MHC class II-dependent basophil-CD4(+) T cell interactions promote T(H)2 cytokine-dependent immunity. *Nat Immunol*. (published online: May, 2009); **doi:10.1038/ni.1740**

(131) Sokol CL et al. Basophils function as antigen-presenting cells for an allergen-induced T helper type 2 response. *Nat Immunol*. (published online: May, 2009); **doi:10.1038/ni.1738**

(132) Beck LA, Leung DY Allergen sensitization through the skin induces systemic allergic responses. *J Allergy Clin Immunol*. **106**:S258-63 (2000)

(133) Djukanović R Effects of treatment with anti-immunoglobulin E antibody omalizumab on airway inflammation in allergic asthma. *Am J Respir Crit Care Med*. **15**;170:583-93 (2004)

(134) Suissa S, Ernst P. Inhaled corticosteroids: impact on asthma morbidity and mortality. *J Allergy Clin Immunol*. **107**:937-44 (2001)

6. Curriculum Vitae

Personal Data:

Name: Mitterhumer Eva
Nationality: Österreich
Date of birth: may, 28th 1980
Place of birth: Linz
Sex: female
Address: Bräuhausgasse 48/9; 1050 Wien

Education:

Elementary school:	1986 – 1990	Volksschule Lenzing
Secondary school:	1990 – 1994	Private Mädchenhauptschule der Schulschwestern, Vöcklabruck
Grammar school:	1994 – 1998	Privates Oberstufenrealgymnasium der Schulschwestern, Vöcklabruck School leaving examination: 26th June, 1998
University:	1998 – 2004	Study of Biology/Genetics, Paris Lodron University of Salzburg
	2003 – 2004	Diploma work at the Department of Cell Biology, University of Salzburg Title: *Ribosomal Protein S15 functional analysis in the eukaryotic model system Saccharomyces cerevisiae* final examination: 17th December 2004
	since 2005	PhD thesis at the department of dermatology, division of immunology, allergy and infectious diseases, Vienna Medical University

Paper submitted:

Eva Mitterhumer, Bärbel Reininger, Sabine Brandt, Nikolaus Duschek, Elisabeth Hoflehner, Erika Garner-Spitzer, Eleonora Dehlink, Barbara Platzer, Martina Hammer, Martin Holcmann, Hans C. Oettgen, Ursula Wiedermann, Maria Sibilia, Edda Fiebiger, Antal Rot, Dieter Maurer. The expression of high-affinity IgE receptors on dendritic cells biases immune responses towards Th2 and exacerbates allergic tissue inflammation.

7. Acknowledgement

Als erstes möchte ich Univ. Prof. Dr. Dieter Maurer anführen. Er hat es mir ermöglicht, meine Dissertation in seiner Gruppe zu absolvieren. Weiters möchte ich mich für seine hervorragende Betreuung, Ideen und Verbesserungs-vorschläge bedanken.

Bedanken möchte ich mich bei meinem Arbeitskollegen Ernst Kriehuber für seine technischen Einweisungen und Hilfestellungen.
Bedanken möchte ich mich bei meinem Arbeitskollegen Stefan Amatschek für eine freundschaftliche und angenehme Arbeitsatmosphäre. Ein besonderer Dank gilt Wolfgang Bauer und Frieder Koszik, die ich mit unendlich vielen Fragen nerven durfte.
Der größte Dank allerdings gilt Bärbel Reininger, die mir immer wieder Mut gemacht hat, wenn ich ihn schon fast verloren hätte. Sie hat mit mir die langen Nächte im Labor und zahlreichen Stunden vor dem Sorter verbracht.

Bedanken möchte ich mich auch bei Martina Hammer, die mir im Maushaus immer tatkräftig zur Seite gestanden ist.

Ganz besonders möchte ich mich bei meinen Eltern bedanken, nicht nur für ihre finanzielle Unterstützung, sondern vor allem für ihr Vertrauen.

Ich bedanke mich ganz herzlich bei meiner Schwester Birgit für ihren Zuspruch und ihre guten Ratschläge während meiner Dissertation.

Meinem Freund Clemens bin ich für seine Unterstützung, seine Hilfe (meistens erwartet mich am Abend ein ausgezeichnetes Essen) und seine Liebe dankbar.